

**UNIVERSITÉ DU QUÉBEC À CHICOUTIMI**

**MÉMOIRE PRÉSENTÉ À  
L'UNIVERSITÉ DU QUÉBEC À CHICOUTIMI  
COMME EXIGENCE PARTIELLE  
DE LA MAÎTRISE EN INGÉNIERIE**

**BY  
BEHNAM GOLBAHAR**

**EFFECT OF GRAIN REFINER-MODIFIER INTERACTION  
ON THE PERFORMANCE OF A356.2 ALLOY**

**WINTER 2008**



### **Mise en garde/Advice**

Afin de rendre accessible au plus grand nombre le résultat des travaux de recherche menés par ses étudiants gradués et dans l'esprit des règles qui régissent le dépôt et la diffusion des mémoires et thèses produits dans cette Institution, **l'Université du Québec à Chicoutimi (UQAC)** est fière de rendre accessible une version complète et gratuite de cette œuvre.

Motivated by a desire to make the results of its graduate students' research accessible to all, and in accordance with the rules governing the acceptance and diffusion of dissertations and theses in this Institution, the **Université du Québec à Chicoutimi (UQAC)** is proud to make a complete version of this work available at no cost to the reader.

L'auteur conserve néanmoins la propriété du droit d'auteur qui protège ce mémoire ou cette thèse. Ni le mémoire ou la thèse ni des extraits substantiels de ceux-ci ne peuvent être imprimés ou autrement reproduits sans son autorisation.

The author retains ownership of the copyright of this dissertation or thesis. Neither the dissertation or thesis, nor substantial extracts from it, may be printed or otherwise reproduced without the author's permission.

**UNIVERSITÉ DU QUÉBEC À CHICOUTIMI**

**MÉMOIRE PRÉSENTÉ À  
L'UNIVERSITÉ DU QUÉBEC À CHICOUTIMI  
COMME EXIGENCE PARTIELLE  
DE LA MAÎTRISE EN INGÉNIERIE**

**PAR  
BEHNAM GOLBAHAR**

**EFFET DE L'INTERACTION AFFINEUR DE GRAIN-  
MODIFICATEUR SUR LA PERFORMANCE DE L'ALLIAGE A356.2**

**HIVER 2008**

***Dedicated to my patient family***

XXXXXXXXXXXXXXXXXXXX



## RÉSUMÉ

L'affinage de grain et la modification sont deux traitements communs du métal liquide appliqués aux alliages de fonderie Al-Si. La modification est effectuée au moyen d'additions d'éléments tels que le Na, le Sr ou le Sb dans le but de changer la morphologie du silicium eutectique d'aciculaire à la forme fine et fibreuse, et améliorer de ce fait la ductilité de l'alliage. Une structure de grain fine et équiaxe améliorera également les propriétés mécaniques; ceci est réalisé par le processus de l'affinement de grain, où l'addition d'éléments tels que le Ti et le B à l'aluminium liquide - habituellement présentés sous forme d'alliage mère d'aluminium - fournissent des noyaux nécessaires pour la formation d'un grand nombre de grains, et par conséquent une structure de grain fine est réalisée. L'utilisation d'une combinaison d'un affineur de grain et d'un modificateur pour certains alliages hypoeutectiques de fonderie Al-Si a démontrée qu'il causait un certain degré d'empoisonnement en termes de réduction du niveau de la modification des particules de silicium et de l'affinage de grain.

Le présent travail vise l'étude de l'influence de l'addition du Ti et du B sous forme de cinq alliages mères différents (affineurs de grain), à savoir, Al-10%Ti, Al-5%Ti-1 %B, Al-2.5%Ti-2.5%B, Al-1.7%Ti-1.4%B et Al-4%B en combinaison avec le Sr comme modificateur sous forme d'Al-10%Sr dans l'alliage A356.2. L'affinement de grain de l'alliage A356.2 avec des additions de Ti et de B dans des gammes allant de 0.02 à 0.5% et 0.01 à 0.5%, respectivement, a été examiné en utilisant ces différents types d'affineurs de grain. Des additions de strontium ont été réalisées à deux niveaux de 30 et 200 ppm. L'occurrence de toutes les interactions probables de Sr-Ti et/ou de B-Sr a été étudiée en utilisant l'analyse par la microsonde et les techniques métallographiques. Tous les alliages ont subi un traitement thermique de type T6 avant l'essai mécanique. Des essais de traction et de résilience ont été effectués pour évaluer l'influence de l'interaction entre l'affineur de grain et le modificateur sur les propriétés mécaniques. Les propriétés ont été déterminées pour les alliages tels que coulés et pour ceux traités thermiquement. Des techniques thermiques d'analyse ont également été employées pour évaluer les interactions entre le Sr et le B, aussi bien que celles entre le Sr et le Ti.

L'analyse à l'aide de la microsonde électronique a indiqué que l'ajout de B > 0.1% à l'alliage A356.2 peut mener à la formation des particules contenant principalement le B et Sr, avec une composition approchant  $\text{SrB}_6$ . Aucune interaction significative entre le Sr et le Ti n'a été observée dans le contexte de l'effet sur les caractéristiques eutectiques des particules de silicium. Les mesures quantitatives des microstructures prouvent que la morphologie des particules eutectiques de silicium est soumise à un retour important à une forme brute et aciculaire. La recherche a également montré que l'interaction B-Sr peut retarder l'affinement des grains de l'alliage A356.2 contenant 0.02-0.1%B. Cette interaction peut diminuer considérablement les propriétés mécaniques de l'alliage, en particulier, dans

la condition telle que coulée. Ainsi, le contenu en B de l'alliage devrait être considéré en tant qu'un des paramètres qui affectent l'affinement de grain et la modification des alliages A356.2.

## ABSTRACT

Grain refining and modification are two common melt treatments applied to Al-Si casting alloys. Modification is carried out by means of the addition of such elements as Na, Sr or Sb in order to change the morphology of the eutectic Si from acicular to a fine and fibrous form and thereby improve the alloy ductility. A fine equiaxed grain structure will also improve the mechanical properties; this is achieved through the process of grain refining, where the addition of such elements as Ti and B to the melt - usually introduced in the form of an aluminium master alloy - provide the necessary nuclei for the formation of a large number of grains and hence a fine grain structure. The use of a combination of grain refiner and modifier for certain hypoeutectic Al-Si foundry alloys has been shown to cause a certain degree of "poisoning" in terms of reduction in the level of silicon particle modification and grain refining achieved for the amount of grain refiner and modifier added to the alloy.

The present study aims at investigating the influence of the addition of Ti and B in the form of five different grain refiners/aluminium master alloys (Al-10%Ti, Al-5%Ti-1%B, Al-2.5%Ti-2.5%B, Al-1.7%Ti-1.4%B and Al-4%B) in conjunction with that of Sr (as modifier) added in the form of Al-10%Sr master alloy to A356.2 alloy. Grain refinement of A356.2 alloy with Ti and B additions in the ranges of 0.02 – 0.5% and 0.01-0.5%, respectively, was examined using these different types of grain refiners. Strontium additions were made at two levels of 30 and 200 ppm each. The occurrence of any probable Sr-Ti and/or Sr-B interactions was investigated using electron microprobe analysis and metallographic techniques. All alloys were T6-heat treated before mechanical testing. Tensile and impact tests were conducted to evaluate the influence of the interaction between grain refiner and modifier on the mechanical properties. The properties were determined for both the as-cast and heat-treated conditions. Thermal analysis techniques were also used to evaluate the interactions between Sr and B, as well as that between Sr and Ti.

The EPMA analysis revealed that adding  $> 0.1\%B$  to the A356.2 alloy may lead to formation of particles containing predominantly B and Sr, with a composition approaching  $SrB_6$ . No significant sign of interaction between Sr and Ti was observed in the context of the effect on the eutectic Si particle characteristics. The quantitative measurements of the microstructures show that the morphology of the eutectic silicon particles is subjected to a major reversion to a coarse, acicular form. The investigation also showed the Sr-B interaction may postpone grain refinement of A356.2 alloy containing 0.02-0.1%B. This interaction may diminish the mechanical properties of the alloy considerably, in particular, in the as-cast condition. Thus, the boron-content of the alloy should be considered as one of the parameters which affect successful grain refinement and modification of A356.2 castings.

## ACKNOWLEDGEMENTS

I am grateful to Professor Fawzy H. Samuel for giving me an opportunity to work with him on this project. The motivation and sound advice he provides have been major contributing factors in bringing this work to a successful conclusion. Professor Agnes M. Samuel's guidance and thoughtful suggestions throughout the duration of the project were particularly helpful, and her technical editing of this thesis is greatly appreciated.

I wish to acknowledge the financial assistance received in the form of scholarships from the Natural Sciences and Engineering Research Council of Canada (NSERC), General Motors Powertrain Group (USA), and the Fondation de l'Université du Québec à Chicoutimi (FUQAC).

I would also like to thank my colleagues, particularly Alain Bérubé and Mathieu Paradis for helping me at various stages of my experimental work, and to acknowledge Madame M. Sinclair for proofreading the manuscript.

Last, but not least, I would like to thank my family for their patience and unfailing support. This thesis is dedicated to them.

## TABLE OF CONTENTS

<b>RÉSUMÉ .....</b>	<b>i</b>
<b>ABSTRACT.....</b>	<b>iii</b>
<b>ACKNOWLEDGEMENTS .....</b>	<b>iv</b>
<b>TABLE OF CONTENTS .....</b>	<b>v</b>
<b>LIST OF FIGURES .....</b>	<b>vii</b>
<b>LIST OF TABLES .....</b>	<b>xii</b>
<b>CHAPTER 1 DEFINING THE PROBLEM .....</b>	<b>1</b>
1.1    INTRODUCTION .....	2
1.2    OBJECTIVES OF THE STUDY.....	5
<b>CHAPTER 2 REVIEW OF THE LITERATURE.....</b>	<b>6</b>
2.1    INTRODUCTION .....	7
2.2    SOLIDIFICATION OF Al-Si ALLOYS .....	8
2.3    EUTECTIC SILICON MODIFICATION .....	11
2.4    RELEVANT NUCLEANTS IN GRAIN REFINERS.....	17
2.5    COMMON GRAIN REFINERS USED FOR Al-Si-Mg ALLOYS.....	21
2.6    POROSITY IN A356 CASTINGS .....	26
2.7    INTERACTION OF GRAIN REFINERS AND MODIFYING AGENTS .....	29
<b>CHAPTER 3 EXPERIMENTAL PROCEDURES.....</b>	<b>35</b>
3.1    INTRODUCTION .....	36
3.2    MATERIALS, MELTING AND MELT TREATMENT PROCEDURES.....	37
3.3    THERMAL ANALYSIS .....	40
3.4    HEAT TREATMENT PROCEDURE.....	42
3.5    MECHANICAL TESTING.....	42
3.6    METALLOGRAPHY .....	44
<b>CHAPTER 4 ASPECTS OF MICROSTRUCTURE AND MACROSTRUCTURE ...</b>	<b>46</b>
4.1    MICROSTRUCTURAL FEATURES.....	47
4.1.1    INTRODUCTION .....	47
4.1.2    ADDITION OF 200 ppm STRONTIUM .....	47
4.1.3    ADDITION OF 30 ppm STRONTIUM .....	59
4.2    ELECTRON PROBE MICROANALYSIS.....	65
4.2.1    INTRODUCTION .....	65

4.2.2	UNREACTED PARTICLES .....	65
4.2.3	INTERACTION OF GRAIN REFINER AND MODIFIER .....	66
4.2.4	THERMAL ANALYSIS .....	77
4.3	CHARACTERIZATION OF MACROSTRUCTURE.....	81
4.3.1	INTRODUCTION .....	81
4.3.2	EFFECTS OF ADDITION LEVEL OF GRAIN REFINERS.....	81
4.3.3	EFFECTS OF ADDING LOWER LEVELS OF MODIFIER .....	89
<b>CHAPTER 5 MECHANICAL PROPERTIES .....</b>		<b>94</b>
5.1	INTRODUCTION .....	95
5.2	TENSILE PROPERTIES.....	95
5.2.1	AS-CAST CONDITION.....	95
5.2.2	T6-TEMPERED CONDITION .....	113
5.3	IMPACT PROPERTIES.....	130
5.3.1	AS-CAST CONDITION.....	130
5.3.2	T6-TEMPERED CONDITION .....	136
5.4	OPTIMUM GRAIN REFINING CONDITIONS.....	141
<b>CHAPTER 6 CONCLUSIONS.....</b>		<b>144</b>
<b>RECOMMENDATIONS FOR FUTURE RESEARCH .....</b>		<b>148</b>
<b>REFERENCES.....</b>		<b>149</b>

## LIST OF FIGURES

Figure 2.1	Schematic of Al-Si Phase Diagram. <sup>1</sup> .....	8
Figure 2.2	Variation of the amount of dendritic $\alpha$ -Al phase with Sr in an Al-11.6% Si-0.4%Mg alloy. <sup>22</sup> .....	13
Figure 2.3	Modification level versus holding time for Al-7%Si alloy. <sup>19</sup> .....	15
Figure 2.4	The Al-rich side of the Al-B phase diagram. ....	19
Figure 2.5	Grain refinement of A356 alloy using Al-Ti, Al-Ti-B and Al-B master alloys. <sup>38</sup> .....	24
Figure 2.6	Sr concentrations, as a function of time after Al-Ti-B grain refiners were added to obtain 0.15% Ti in the melts (solid lines). The dotted line refers to the case of Sr modification without addition of any grain refiner. <sup>50</sup> .....	32
Figure 2.7	Grain size analysis of grain-refined Al-7%Si alloy with different sequences of grain refiner and modifier addition (1.0% of Al-1%Ti-3%B and 0.02% Sr). <sup>63</sup> .....	33
Figure 2.8	The relationship between eutectic undercooling, silicon morphology and the Sr:B ratio. <sup>66</sup> .....	34
Figure 3.1	(a) ASTM B108 permanent mold used for preparing tensile test bars; .....	38
Figure 3.2	Schematic diagram of graphite mold used for thermal analysis. ....	41
Figure 3.3	Blue M forced air furnace used for heat treatment. ....	42
Figure 3.4	(a) Instron Universal Mechanical Testing machine, (b) Instron SI-1 Impact Testing machine. ....	43
Figure 3.5	(a) Optical microscope-image analyzer system, and (b) Electron probe microanalyzer used in the present study. ....	45
Figure 4.1	Optical micrograph showing the microstructures of as-cast A356.2 alloy modified by addition of 200 ppm Sr. ....	48
Figure 4.2	Optical micrographs of microstructures in as-cast 200 ppm Sr-modified A356.2 alloy after refining by addition of (a) 0.02%Ti, and (b) 0.08% Ti as Al-10%Ti. ....	48

Figure 4.3	Optical micrographs of the microstructures of 200 ppm Sr-modified A356.2 as-cast alloy grain-refined with additions of: .....50
Figure 4.4	Optical micrographs of the microstructures of 200 ppm Sr-modified A356.2 as-cast alloy refined by the addition of Al-10%Ti and Al-4%B: (a) 0.1%Ti, (b) 0.5% Ti, (c) 0.01% B, and (d) 0.05% B. ....51
Figure 4.5	Optical micrograph of microstructures of 200 ppm Sr-modified A356.2 as-cast alloy refined by addition of : (a,b) Al-5%Ti-1%B, (c,d) Al-2.5%Ti-2.5%B, and (e,f) Al-1.7%Ti-1.4%B master alloys; (a,c,e) 0.1% Ti addition; (b,d,f) 0.5% Ti addition. ....53
Figure 4.6	Variation of eutectic Si particle length in 200 ppm Sr-modified as-cast A356.2 alloy grain refined with different types and amounts of master alloy: (a) lower addition levels, and (b) higher addition levels. ....57
Figure 4.7	Optical micrograph showing the microstructure of as-cast A356.2 alloy modified by addition of 30 ppm Sr.....59
Figure 4.8	Optical micrographs of the microstructures of 30 ppm Sr-modified as-cast A356.2 alloy refined using addition of Al-10%Ti and Al-4%B, (a) 0.1%Ti, (b) 0.5% Ti, (c) 0.01% B, and (d) 0.05% B. ....60
Figure 4.9	Microstructures of the 30 ppm Sr-modified as-cast A356.2 alloy refined by addition of master alloys: (a,b) Al-5%Ti-1%B; (c,d) Al-2.5%Ti-2.5%B; (e,f) Al-1.7%Ti-1.4%B; (a,c,e) 0.1% Ti addition; (b,d,f) 0.5% Ti addition.....62
Figure 4.10	Variation in the length of eutectic Si for the 30ppm Sr-modified as-cast A356.2 alloy samples, after grain refinement using various types and amounts of master alloys. ....64
Figure 4.11	Backscattered images of titanium aluminide particles observed in 200 ppm Sr-modified A356.2 alloy at two addition levels of Al-10%Ti: (a) 0.1% Ti, and (b) 0.5% Ti. ....66
Figure 4.12	Backscattered images of TiB <sub>2</sub> particles observed at two Al-5%Ti-1%B addition levels in A356.2 alloy: (a) 0.1% Ti, and (b) 0.5% Ti. ....67
Figure 4.13	Backscattered image of different particle types observed in the sample refined with Al-5%Ti-1%B master alloy (0.5% Ti), and corresponding EDS spectrum.....67
Figure 4.14	(a) Backscattered image of tiny, bright particles in the sample refined with Al-2.5%Ti-2.5%B master alloy (0.5% Ti), and (b) X-ray image of Sr. ....68



Figure 4.15	Proximity of $\text{Al}_3\text{Ti}$ particle with Sr-rich particle in 200 ppm Sr-modified alloy refined with addition of 0.5%Ti in the form of Al-10%Ti: (a) backscattered image; (b) X-ray image of Ti distribution; and (c) X-ray image of Sr distribution. ....	69
Figure 4.16	(a) Backscattered electron image showing intermetallic particles found in 200 ppm Sr-modified as-cast A356.2 alloy refined by addition of 0.01 %B using Al-4%B, and corresponding X-ray images of (b) B, (c) Sr, and (d) Ti. ....	71
Figure 4.17	(a) Backscattered electron image showing intermetallic particles found in 200 ppm Sr-modified as-cast A356.2 alloy refined by addition of 0.05% B using Al-4%B, and corresponding X-ray images of (b) B, (c) Sr, and (d) Ti. ....	72
Figure 4.18	Backscattered electron image of intermetallic particles found in the same sample as the one shown in Figure 4.17. ....	73
Figure 4.19	Backscattered image of a region which includes Sr-rich particles in as-cast 200 ppm Sr-modified A356.2 alloy refined with 0.5% B using Al-4%B.....	75
Figure 4.20	X-ray images corresponding to the backscattered image of Figure 4.19 (a) Al; (b) B; (c) Sr; and (d) Ti.....	76
Figure 4.21	Cooling curves for thermal analysis of 200 ppm Sr-modified A356.2 alloy with different Ti additions using Al-10%Ti. ....	79
Figure 4.22	Cooling curves for thermal analysis of 200 ppm Sr-modified A356.2 alloy with different B additions using Al-4%B. ....	80
Figure 4.23	Macrostructures of 200 ppm Sr-modified A356.2 alloy refined with: (a, b) 0.1% Ti and 0.5% Ti, using Al-10%Ti; (c, d) 0.01% B and 0.05% B, using Al-4%B; and (e) without any grain refiner addition.....	83
Figure 4.24	Macrostructures of 200 ppm Sr-modified A356.2 alloy refined with: (a, b) 0.1% and 0.5% Ti, using Al-5%Ti-1%B; (c, d) 0.1% and 0.5% Ti, using Al-2.5%Ti-2.5%B; and (e, f) 0.1% and 0.5% Ti, using Al-1.7%Ti-1.4%B master alloys, respectively. ....	84
Figure 4.25	Graph showing average measured grain sizes in 200 ppm Sr-modified A356.2 alloy as a function of boron addition levels using different grain refiners. Corresponding data for Ti additions using Al-10%Ti are also shown (see individual squares). ....	85

Figure 4.26	Macrostructures of 200 ppm Sr-modified A356.2 refined with: (a) 0.02% Ti, and (b) 0.08% Ti, using Al-10%Ti master alloy.....	86
Figure 4.27	Macrostructures of 200 ppm Sr-modified A356.2 refined with: (a, b) 0.02% and 0.08% Ti, using Al-5%Ti-1%B; (c, d) 0.02% and 0.08% Ti, using Al-2.5%Ti-2.5%B; and (e, f) 0.02% and 0.08% Ti, using Al-1.7%Ti-1.4%B master alloys, respectively.....	88
Figure 4.28	Macrostructures of 30 ppm Sr-modified A356.2 alloy refined with: (a, b) 0.1% and 0.5% Ti, using Al-10%Ti; (c, d) 0.01% and 0.05% B, using Al-4%B; and (e) without any grain refiner addition.....	91
Figure 4.29	Macrostructures of 30 ppm Sr-modified A356.2 alloy refined with: (a, b) 0.1% and 0.5% Ti, using Al-5%Ti-1%B; (c, d) 0.1% and 0.5% Ti, using Al-2.5%Ti-2.5%B; and (e, f) 0.1% and 0.5% Ti, using Al-1.7%Ti-1.4%B master alloys, respectively.....	92
Figure 4.30	Graph showing average grain sizes measured in 30 ppm Sr-modified A356.2 alloys as a function of boron addition level using different grain refiners. Corresponding data for Ti additions using Al-10%Ti are also shown (see individual squares).....	93
Figure 5.1	Percentage elongation as a function of Ti or B content in Sr-modified grain-refined as-cast A356.2 alloy: (a) modified with addition of 30 ppm Sr; (b, c) modified with addition of 200 ppm Sr. Note the low and high Ti/B addition ranges in (b) and (c). .....	101
Figure 5.2	Variation of tensile strength as a function of Ti or B content in the Sr-modified grain-refined as-cast A356.2 alloy:(a) modified with addition of 30 ppm Sr; (b, c) modified with addition of 200 ppm Sr. ....	106
Figure 5.3	Variation of yield strength as a function of Ti or B content in the Sr-modified grain-refined as-cast A356.2 alloy: (a) modified with addition of 30 ppm Sr; (b, c) modified with addition of 200 ppm Sr. ....	112
Figure 5.4	Variation of percentage elongation as a function of Ti or B content in T6-tempered Sr-modified grain-refined A356.2 alloy: (a) modified with 30 ppm Sr addition; (b, c) modified with 200 ppm Sr addition.....	118
Figure 5.5	Variation of tensile strength as a function of Ti or B content in T6-tempered Sr- modified grain-refined A356.2 alloy: (a) modified with 30 ppm Sr addition; (b, c) modified with 200 ppm Sr addition. ....	122

Figure 5.6	Variation of yield strength as a function of Ti or B content in T6 tempered, Sr-modified, grain-refined A356.2 alloy: (a) modified with 30 ppm Sr addition; (b, c) modified with 200 ppm Sr addition. ....	129
Figure 5.7	Variation of total absorbed energy as a function of Ti or B content in as cast, Sr-modified, A356.2 alloy, (a) modified with 30 ppm Sr addition (b, c) modified with 200 ppm Sr addition. ....	135
Figure 5.8	Variation of total absorbed energy as a function of Ti or B content in T6-tempered, Sr-modified A356.2 alloy, (a) modified with 30 ppm Sr addition (b, c) modified with 200 ppm Sr addition.....	140

## LIST OF TABLES

Table 2.1	General composition of A356.2 alloy (wt %) <sup>1</sup> .....	8
Table 3.1	Range of strontium, titanium, and boron addition levels used in A356.2 alloy melts .....	37
Table 3.2	Composition (wt %) of the A356.2 base alloy used in this study .....	37
Table 3.3	Details of grain refiner and modifier additions made to A356.2 alloy melts ...	39
Table 3.4	A356.2 alloy melts used for thermal analysis experiments .....	40
Table 4.1	Silicon particle characteristics of 200 ppm Sr-modified, grain refined as-cast A356.2 alloys .....	55
Table 4.2	Particle characteristics of the 30 ppm Sr-modified as-cast A356.2 alloy. ....	63
Table 4.3	Average chemical composition of particles observed in as-cast A356.2 alloy (200 ppm Sr-modified, refined with 0.05% B using Al-4%B). ....	73
Table 4.4	Chemical composition of particles observed in Figure 4.19 as obtained from WDS analysis.....	75
Table 5.1	Grain refiner addition for achieving optimum properties for Sr-modified A356.2 alloy in the as-cast condition.....	142
Table 5.2	Grain refiner addition for achieving optimum properties for Sr-modified A356.2 alloy in the T6-tempered condition.....	143

## **CHAPTER 1**

### **DEFINING THE PROBLEM**

# CHAPTER 1

## DEFINING THE PROBLEM

### 1.1 INTRODUCTION

Aluminum-Silicon (Al-Si) alloys constitute an important class of alloys used in aluminum foundries, in large part because of their excellent casting characteristics. The properties displayed by these alloys make them popular for the various applications required by such fields as the automotive, aerospace and defence industries.

Based on the Al-Si binary phase diagram, the volume fraction of Al-Si eutectic in commonly used hypoeutectic Al-Si alloys may be over 50%. The mechanical properties of these alloys are strongly influenced by the way in which the formation of Al-Si binary eutectic occurs, and which determines the amount, size and morphology of the eutectic phase, as well as the distribution of the eutectic silicon particles and the level of microporosity in the microstructure. The mode of nucleation and growth of the eutectic phase within the dendritic network will influence the specific surface area of the solid network significantly, and this, in turn, will affect feeding during the last stages of solidification.

With regard to grain refining in hypoeutectic Al-Si alloys, it is taken as a matter of course that the pre-eutectic  $\alpha$ -Al is to be refined by the addition of a grain refiner. A fine

equiaxed grain structure will then result in a number of benefits including such characteristics as high yield strength, greater toughness values, improved machinability, and excellent deep drawability in the cast products under discussion.<sup>1, 2, 3</sup> Grain refiners are generally added in the form of master alloys of the type Al-Ti, Al-Ti-B or Al-B. Aluminum-Titanium-Boron master alloys, such as Al-5%Ti-1%B contain two active intermetallic phases, namely,  $\text{Al}_3\text{Ti}$  and  $\text{TiB}_2$ , while Al-Ti types contain  $\text{Al}_3\text{Ti}$  particles only. The  $\text{TiB}_2$  and  $\text{Al}_3\text{Ti}$  particles provide heterogeneous nucleation sites for  $\alpha\text{-Al}$  during solidification, at which time  $\text{TiB}_2$  particles show evidence of a stronger effect than do the  $\text{Al}_3\text{Ti}$  particles.<sup>4</sup> Based on this finding, it may be concluded that ternary Al-Ti-B master alloys have better grain refining efficiency than binary Al-Ti types.<sup>5</sup> Sigworth and Guzowski<sup>3</sup> also reported that, when using an Al-4%B master alloy, it is possible to obtain satisfactory grain refinement in the A356.2 alloy, which is even better than that obtained using the Al-5%Ti-1%B master alloy.

Researchers also report that optimum percentages of Ti and B for the A356 alloy lie approximately between 0.06% Ti - 0.01% B and 0.08% Ti - 0.02% B.<sup>6</sup> Higher additions of Ti and B, however, cause the formation of Ti-based intermetallic compounds within the eutectic region.<sup>7</sup> Furthermore, the eutectic silicon-particle characteristics of size and morphology have a significant influence on the mechanical properties of Al-Si-Mg alloys. With a view to improving the corresponding mechanical properties, elements such as strontium, sodium and antimony may be added to the melt so as to modify the morphology of the eutectic silicon from a coarse and plate-like form to one which is fine and fibrous.

The effects of the modifiers have already been well-established by research.<sup>8</sup> By altering the nucleation and growth of eutectic Si, the constituents of the microstructure are capable of assuming a variety of morphologies depending on the level or degree of modification desired. The various eutectic Al-Si structures observed have been grouped into six categories which include plate-like, acicular Si, a lamellar or partially modified structure, and a fine, fibrous network. For Al-Si-Mg alloys, modification of eutectic silicon usually involves the addition of strontium to the molten metal.<sup>9</sup> A significant improvement in tensile strength may be observed with the addition of 0.01% Sr.<sup>10</sup> Further improvements in modification at higher Sr levels yield only slight increases in tensile strength, although elongation continues to rise.

The combined use of grain refiner and modifier in certain hypoeutectic Al-Si casting alloys has been shown to result in “poisoning” in terms of a reduction in the amount of silicon particle modification and grain refining expected in the alloy. In the case of Sr, the poisoning effect was thought to result from the formation of a strontium bromide compound.<sup>11</sup>

Furthermore, with the addition of the Al-5%Ti-1%B master alloy to near-eutectic Al-Si alloys already modified with Sr, the effectiveness of Sr in the melt decreases with increasing additions of Al-5%Ti-1%B. It has been suggested that the poisoning effect which the Al-5%Ti-1%B master alloy has on Sr modification is due to the interaction between Sr and Ti.<sup>12</sup> The amount of porosity in the Al-Si alloy subjected to a combined grain refining and modification treatment may also be affected.<sup>13</sup>



## 1.2 OBJECTIVES OF THE STUDY

The present study aimed at investigating the effects of Ti and B additions on probable interactions with Sr used as a modifier in A356.2 alloy. These additions were made at different concentrations using various master alloys. Techniques such as electron probe microanalysis (EPMA) and metallography were used to investigate the microstructures of the alloy under the different conditions studied. The effects of the grain refiner-modifier interactions on the tensile and impact properties of the alloy were also examined.

The main goals of the study are as follows:

1. To determine the effects of Ti and B, acting singly or in combination, on the tensile and impact properties of a fully-modified A356.2 alloy in both the as-cast and T6-tempered conditions.
2. To determine the effects of the interaction between grain-refiner and modifier on both the performance of the grain refiner and the shape of the silicon particles.
3. To draw comparisons among the various types and amounts of grain-refiner to be added to the Sr-modified A356.2 alloy from the standpoint of improving the mechanical properties.

## **CHAPTER 2**

### **REVIEW OF THE LITERATURE**

## **CHAPTER 2**

### **REVIEW OF THE LITERATURE**

#### **2.1 INTRODUCTION**

Al-Si alloys have the potential for excellent castability, good weldability, good thermal conductivity, high strength at elevated temperatures and excellent corrosion resistance. The hypoeutectic A356.2 alloy is a popular commercial alloy used widely in industry, while its structure and mechanical properties are dependent to a high degree upon the chemical composition, the modification and grain refinement treatment applied to the alloy melt, the cooling rate used during casting, and the heat treatment operations applied to the alloy casting.

With the addition of certain elements to Al-Si alloys, a wide range of physical and mechanical properties may be obtained, including high corrosion resistance, good weldability, low shrinkage, low thermal expansion and high tensile properties. Magnesium and copper are two of the most important alloying additions, so that within Al-Si alloys, Al-Si-Mg, Al-Si-Cu and Al-Si-Cu-Mg are the three main alloying systems, for which A356, A319 and B319 alloys are typical examples.

## 2.2 SOLIDIFICATION OF Al-Si ALLOYS

Aluminum-Silicon casting alloys fall into three main groups, depending on their silicon content. As shown in the phase diagram in Figure 2.1, the Al-Si eutectic occurs at 577°C, at ~12% Si and alloys containing Si levels below and above the eutectic level are termed hypoeutectic and hypereutectic Al-Si alloys, respectively.

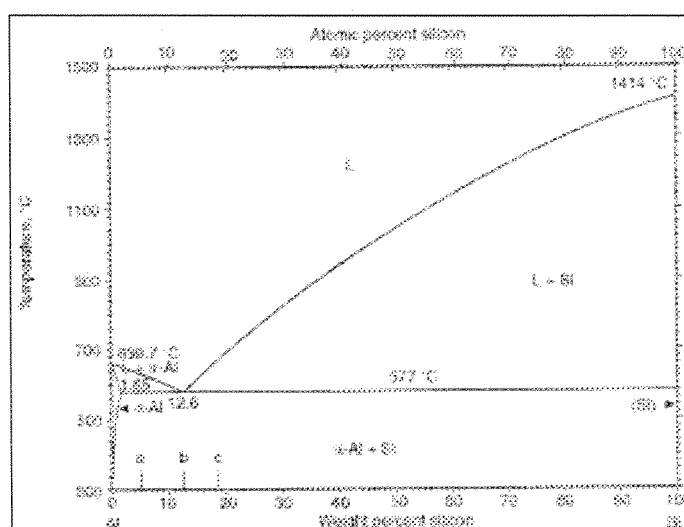


**Figure 2.1** Schematic of Al-Si Phase Diagram. <sup>1</sup>

Hypoeutectic A356.2 alloy (Al-7%Si-0.4%Mg) is a commercial alloy which is frequently used in the industry, since it provides optimal castability and corrosion resistance. The excellent mechanical properties of this alloy are attributed to the effects of Si and Mg after the application of heat treatment to the alloy. The chemical composition of this alloy is provided in Table 2.1.

**Table 2.1** General composition of A356.2 alloy (wt %) <sup>1</sup>

Si	Cu	Fe	Mg	Mn	Ti
6.5-7.5	≤0.10	≤0.12	0.30-0.45	≤0.05	≤0.20

During the solidification of Al-Si-Mg alloys, the main phases which appear in the microstructure precipitate in the following sequence:

1. Formation of a network of  $\alpha$ -aluminum dendrites which enriches the solute silicon-content of the remaining liquid until the eutectic composition is reached;
2. Precipitation of the aluminum-silicon eutectic in areas between the  $\alpha$ -aluminum dendrites; and
3. Precipitation of secondary eutectic phases such as  $\text{Mg}_2\text{Si}$  and of ternary phases such as  $\beta\text{-AlFeSi}$ .

Although the  $\alpha$ -Al dendrites in an Al alloy are expected to form at the equilibrium freezing point, in practice, cooling below the equilibrium freezing point is required in order to cause the first dendrites to nucleate. Secondary dendrite arm spacing (SDAS) is a microstructural feature of dendritic  $\alpha$ -Al which is determined by alloy composition, cooling rate, local solidification time and temperature gradient. As these dendrites grow, heat is liberated and the temperature begins to rise. The required temperature drop is termed “undercooling”, and is a measure of the difficulty in nucleating the first aluminum dendrites. Following the temperature rise or “recalescence”, the temperature begins to fall again as heat is extracted, until the eutectic temperature is reached when it stabilizes while solidification of the Al-Si eutectic reaction is completed.

Cooling rate plays an important role in determining the microstructure of the casting. In Al-Si alloys the volume fraction of aluminum dendrites increases at higher cooling rates, possibly related to a shift in the eutectic point towards a higher silicon content.<sup>14</sup> Polyhedral Si crystals also precipitate at low cooling rates, a fact which may be

related to the corresponding changes occurring in the liquidus lines with the cooling rate, since the composition of the Al-Si eutectic ranges from 11.7 to 12.7 mass% Si.<sup>15</sup>

In the as-cast condition, the eutectic Si particles may be observed in the form of brittle acicular plates which are detrimental to tensile and impact properties. Studies by Meyers<sup>16</sup> suggest that the ductility of unmodified alloys is controlled by the mean size of the silicon particles, whilst that of modified alloys is determined by their distribution. Two possible explanations exist for the nucleation mechanism of the eutectic Si in the unmodified Al-Si alloys: (a) Si nucleation on the primary dendrites; and (b) Si nucleation on substrate particles in the melt.

A two-dimensional examination has led to the impression that eutectic Si is needle-like in form; a three-dimensional SEM observation of deeply etched specimens, however, reveals that it is of a plate-like nature.<sup>17</sup> The rapid cooling rate, as occurs in a metallic mold, appears to scale down the dimensions of Si particles rather than their shape and arrangement. A fast cooling rate also reduces the amount of primary Si and leads to an increase in the amount of Al dendrites present.<sup>17</sup>

The A356.2 alloy has a freezing range of almost 70°C, causing the extension of the solidification time available at the solidification front of the alloy. Thus, more time is available at this front for the diffusion of dissolved atoms which become depleted at this site, resulting in a phenomenon known as constitutional undercooling.

Aluminum-Silicon-Magnesium alloys, such as the A356 alloy, are heat-treatable due to the presence of magnesium. The main function of Mg is to aid in Mg<sub>2</sub>Si precipitation, which improves the alloy properties upon age-hardening.<sup>18</sup> In samples with a

magnesium content of more than 0.2%, the  $\text{Mg}_2\text{Si}$  phase may be expected to precipitate at a temperature of  $\sim 540^\circ\text{C}$ , *i.e.*  $30\text{--}40^\circ\text{C}$  below the start of the main eutectic.

More complex phases with low melting points usually develop in the region of  $500\text{--}480^\circ\text{C}$  during solidification of the final amount of liquid left, at which point the remaining Si, Fe, Mg, Mn, Cu and Zn may participate. Two of the most commonly observed iron intermetallics are the  $\beta\text{-Al}_5\text{FeSi}$  and  $\alpha\text{-Al}_{15}(\text{Fe,Mn})_3\text{Si}_2$  phases.

### 2.3 EUTECTIC SILICON MODIFICATION

In addition to the abovementioned parameters, which include SDAS and grain size, other parameters such as the size and morphology of eutectic silicon particles also influence the relevant mechanical properties of Al-Si alloys to a noticeable extent. Through the application of a melt treatment known as modification, the morphology of the eutectic Si particles may be altered or modified to a fine fibrous form, thereby improving alloy ductility significantly, as well as strength to some extent. The treatment is carried out through the addition of certain elements to the melt, generally in the form of master alloys and in the appropriate amounts for obtaining a well-modified eutectic structure; such elements would include Na, Sr, and Sb.

In the case of Al-Si-Mg alloys, eutectic silicon modification usually involves the addition of strontium to the molten metal. In general, modifiers have the capacity to:

- increase inclusion content in the melt;
- decrease hydrogen solubility in solid metal;
- alter the morphology of the solid-liquid interface;

- reduce surface tension of the liquid metal; and
- increase volumetric shrinkage.

As regards A356 alloy, with an increase of Sr content of up to 56 ppm, the eutectic silicon changes from a coarse lamellar structure to a fully-modified fibrous one. There is little shape change with a strontium content of over 56 ppm.<sup>9,19</sup> Apelian and Cheng<sup>20</sup> carried out a study on the A356.2 alloy and found that the depression in the eutectic temperature increased until Sr levels in the melt reached 100 ppm. With further Sr additions, the eutectic temperature depression began to decrease up to 150 ppm. Beyond that, the depression remained invariable up to the limit of 300 ppm set for the study.<sup>20</sup>

Clapham and Smith<sup>21</sup> studied the mechanism of the partial modification of the Al-Si eutectic alloy and they discovered that the alloy does not alter its growth behavior gradually; instead, the change from flakelike to fibrous morphology occurs almost instantaneously, but only in distinct regions of the structure. As modification becomes more complete, the number of acicular areas decreases until, finally, all of the eutectic silicon particles become fibrous.

Liao *et al.*<sup>22,23</sup> reported that the addition of Sr to Al-11.6%Si alloys promotes the columnar growth of primary Al dendrites, a condition which is deleterious to the mechanical properties of alloys. Thus, subsequent grain refinement of primary Al dendrites becomes a necessary step to further materialize the beneficial effects of eutectic modification on properties. These researchers<sup>22</sup> also reported that Sr addition affects the amount of dendritic  $\alpha$ -Al phase. They suggest that the effect is related to the depression of the eutectic temperature due to the addition of strontium. The statistical results<sup>22</sup> show that



the amount of dendritic  $\alpha$ -Al phase increases with the addition of Sr, as may be seen in Figure 2.2.

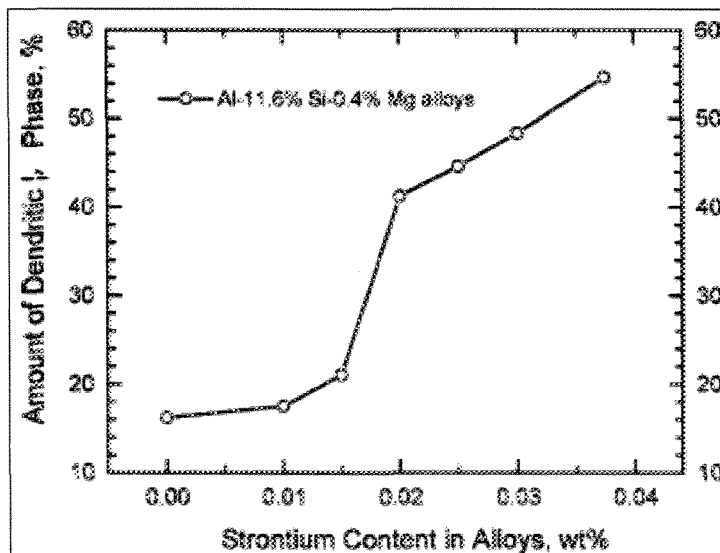


**Figure 2.2** Variation of the amount of dendritic  $\alpha$ -Al phase with Sr in an Al-11.6% Si-0.4%Mg alloy.<sup>22</sup>

For silicon modification assessment, the eutectic growth temperature difference between modified and unmodified melts is used to indicate the modification level.<sup>24</sup> The larger the magnitude of this difference, the higher the level of modification. Based on the American Foundry Society (AFS) Chart, the modification level in Al-7%Si increases rapidly at a low Sr addition level, and then reaches a maximum modification level of 6 when the Sr content is 70 ppm. After that, upon further increasing the Sr content, the modification level of eutectic silicon remains constant at level 6.

Eutectic arrest is used to determine the presence or absence of modification, since the detailed shape of this feature of the cooling curve has been shown to depend on the presence or absence of modifiers.<sup>25</sup> When a modifier is added to the melt, the eutectic temperature is depressed by up to 10°C, and thus the temperature of the eutectic plateau is

most often used as the basis for modification control. Other aspects of eutectic arrest which depend on modifier level include the magnitude of the apparent undercooling associated with the eutectic transformation and the duration of this undercooling. These criteria are not used to any great extent in assessment of modification, simply because they are more difficult to measure than is the eutectic temperature.

The eutectic parameters of the A356.2 alloy are a function of strontium level and degree of modification if the thermal analysis is conducted at slow cooling rates of 0.1 and 0.8°C/s.<sup>26</sup> Any one of these parameters may be used for evaluation of microstructures, but it is suggested that a time difference parameter calculated from the eutectic plateau is preferable to the commonly used depression of the eutectic temperature.<sup>27</sup> Thermal analysis is much less effective for microstructure control if the cooling rate of the thermal analysis sample is high. The eutectic reaction time in A356.2 alloy is lengthened considerably by strontium treatment. This is generally true for a number of Al-Si alloys at the lowest cooling rate. At a rate of 3.5°C/s the eutectic reaction in the A356.2 alloy exhibits no plateau and is obscured by other reactions which occur simultaneously in the sample.<sup>26</sup>

In their research investigations, Tenekedjiev *et al.*,<sup>27</sup> Rauta<sup>28</sup> and Apelian and Cheng<sup>20</sup> found that a possible method for quantifying the effect of chemical modification was to use the time duration between the thermal events associated with the Al-Si eutectic reaction of the 319, 355, 356, 357, 380 and 413 alloys used in their studies. It was found that the time duration of the undercooling effect and the whole duration of the Al-Si eutectic thermal signature increases with an increase in Sr content.

Apelian and Cheng<sup>20</sup> specifically studied the time duration involved in the Al-Si eutectic undercooling and the associated plateau. These parameters indicate that as Sr levels increase by up to 80 ppm, the duration of the undercooling event reaches a maximum, while the duration of the plateau drops to a minimum. Tenekedjiev *et al.*<sup>27</sup> and Rauta,<sup>28</sup> on the other hand, combined both parameters and revealed the existence of a continuous increase in time duration as Sr levels and modification levels went up.

The fading of modification is closely related to the Sr-content in the melt. With a given Sr-content, the intensity of the modification decreases as the holding time increases. As shown in Figure 2.3, the modification level decreases as the holding time increases after only a small amount of master alloy has been added. When the Sr addition is at a higher level, however, the degree of modification remains constant at the initial period, and then decreases with the holding time.<sup>19</sup>

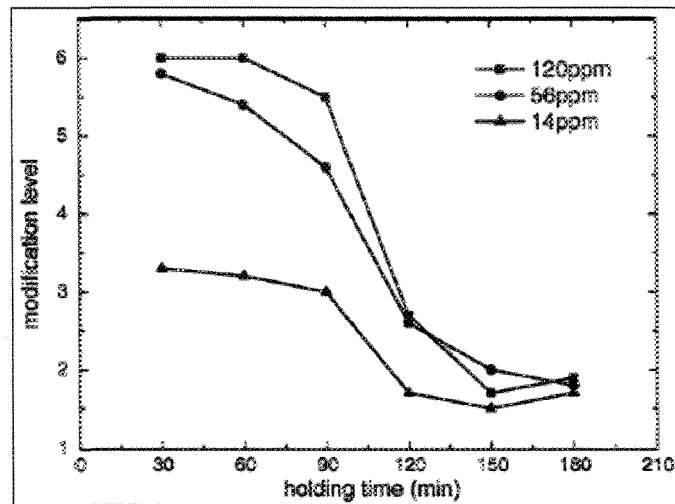


**Figure 2.3** Modification level versus holding time for Al-7%Si alloy.<sup>19</sup>

Although the knowledge of the Sr levels in Al-Si alloy melts provides an indication of the degree of Si modification possible, it is a fact that Sr has been shown to react with alloying elements and impurities in the A356.2 alloy, thereby reducing the quantity of Sr capable of modifying the eutectic silicon. The dissolution of strontium and the associated binding into compounds has the potential for affecting the amount of active Sr available for modifying silicon.

Strontium fading in the A356.2 alloy has an obvious influence on the mechanical properties of this alloy. The literature suggests that Sr fading may occur in three different ways.<sup>3</sup> The modifier may thus:

- vaporize due to the high vapor pressure at the melt temperature;
- oxidize due to a high affinity for oxygen; or
- react with other elements which have a high affinity for it.

It should be noted that intermetallic particles of the  $\text{Al}_2\text{SrSi}_2$  type will form in samples with a high Sr-content of 500 ppm, thereby reducing the amount of strontium in solution and consequently its modifying effect as well.<sup>29</sup> Meanwhile, Joenoes and Gruzleski<sup>30</sup> found that higher Mg-content changes the eutectic silicon from acicular to lamellar in Al-Si alloys. According to their study, Mg additions of up to 1% were found to decrease the eutectic temperature by 17.6°C. This drop was accompanied by an increase in the undercooling of about 1.5°C. Both the morphology of the silicon phase and the depression of the eutectic temperature, as well as the increased undercooling, suggest that high levels of Mg act to modify the silicon phase slightly in the high purity Al-7%Si alloy. The reason that Mg is capable of affecting the silicon growth mechanism could be related

to the fact that the ratio of its atomic radius to that of silicon approaches 1.65, which is a value where modification is thought to be the most effective. Moreover, it was reported by Grand <sup>12</sup> that eutectic silicon may also be modified to some extent by the addition of boron and titanium to Al-Si alloys.

Enhancement of the characteristics of eutectic Si particles may also be obtained through the use of a suitable heat treatment process which would comprises the three stages of solutionizing, quenching and aging, during which fragmentation of the Si particles takes place, followed by spheroidization leading to the fibrous form; longer treatment times, on the other hand, would lead to coarsening of the Si particles. Such modification is referred to as thermal modification as opposed to the chemical modification obtained through the addition of Sr or other modifying elements. In view of the fact that the eutectic Si particles are already fine in the as-cast condition of such chemically modified alloys, however, the spheroidization rate will be higher than that of non-modified alloys, and they will thus require a shorter solution treatment time to achieve optimum eutectic structure.

## **2.4 RELEVANT NUCLEANTS IN GRAIN REFINERS**

Grain refinement may also be obtained by the addition of various ratios of Ti and B to the melt, usually introduced in the form of an aluminium master alloy. A key criterion for particles to be effective nucleating substrates is their ability to be wetted by the  $\alpha$ -Al. Ideally, the refiner particles should be evenly distributed throughout the melt so that when solidification begins, there are a significant number of nucleation events which are triggered on these particles.

Titanium produces a grain refining effect by promoting the release of intermetallic  $\text{Al}_3\text{Ti}$  particles from the master alloy; these particles have a melting point of approximately  $1340^\circ\text{C}$ ,<sup>31</sup> and act as nucleants for  $\alpha\text{-Al}$  dendrites. According to Johnsson,<sup>32</sup>  $\text{Al}_3\text{Ti}$  particles in master alloys usually appear in block form with particle sizes between 5 to  $15\mu\text{m}$ , some of which may even go as high as  $50\mu\text{m}$ . The size of the  $\text{Al}_3\text{Ti}$  particles and the value of the target concentration are of considerable importance since they determine the time required for full dissolution.

Excess B in the master alloy can react with Ti in the melt to form  $\text{TiB}_2$ , thus providing additional potential nucleating particles. The process of grain refinement appears to be inefficient, with  $<1\%$  of the  $\text{TiB}_2$  particles acting as nucleants.<sup>33</sup> Lee *et al.*<sup>34</sup> report that the  $\text{TiB}_2$  particles are rendered less potent in Al–Si foundry alloys due to the formation of such Ti–Si compounds as  $\text{Ti}_5\text{Si}_3$ , on the surface of  $\text{TiB}_2$  particles in the presence of high Si in the melts.

When both Ti and B are available in molten aluminium, the percentage of titanium determines the solubility of the boron. Thus, if this percentage is reduced, the solubility of boron increases correspondingly.<sup>35</sup> Boron does not reduce the  $\text{Al}_3\text{Ti}$  dissolution rate by reducing the solubility of Ti; instead, the dissolution rate of  $\text{Al}_3\text{Ti}$  determines the dissolution rate of  $\text{TiB}_2$ .

An inherent feature of  $\text{TiB}_2$  particles when present in molten aluminium appears to be their tendency to form agglomerations, thus any small particulates will tend to cluster together and reduce the surface energy. Agglomerations of  $\text{TiB}_2$  can cause end product quality problems in certain applications because  $\text{TiB}_2$  particles are much harder than

aluminium. Individually, they are generally sub-micron in size, and, when examined metallographically in the grain refiner, their size is rarely observed to be above  $\sim 2 \mu\text{m}$ . It is also possible that the agglomerations formed may be one order of magnitude, or more, greater than the individual particles.

According to the Al-B phase diagram shown in Figure 2.4,  $\text{AlB}_{12}$  is a high temperature phase, whereas  $\text{AlB}_2$  is stable at room temperature when the boron content is less than 44.5 wt%. Particles of  $\text{AlB}_2$  are much less stable than  $\text{TiB}_2$  particles in the aluminum melt. There is a eutectic reaction in the pure Al-B binary system which occurs at  $659.7^\circ\text{C}$  for a boron-content of 0.022% B.<sup>36,37</sup> Below this concentration,  $\text{AlB}_2$  is not in equilibrium with liquid aluminum. The eutectic reaction, however, occurs at lower boron levels in hypoeutectic Al-Si alloys,<sup>37</sup> this implies that  $\text{AlB}_2$  stability is greater in these alloys than it is in the pure Al-B system.

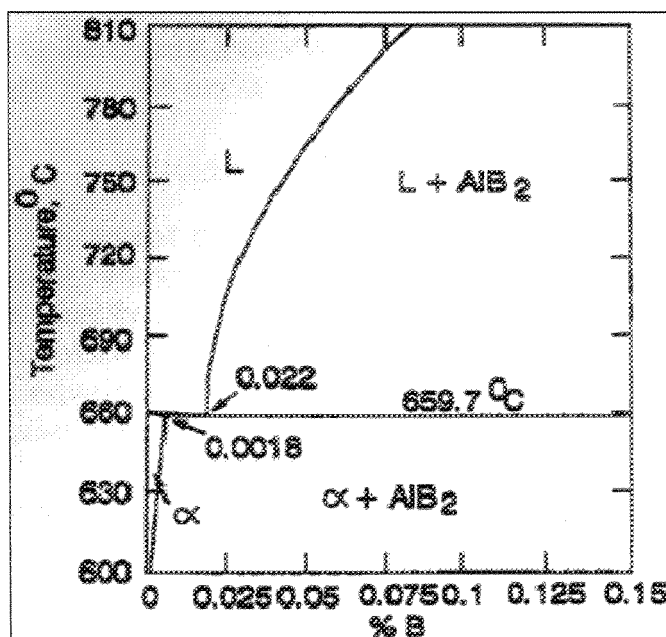


Figure 2.4 The Al-rich side of the Al-B phase diagram.<sup>38</sup>

According to the Al-B phase diagram, the following peritectic reaction takes place at 975°C:



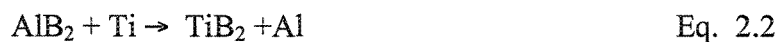
Thus,  $\text{AlB}_2$  is the only stable phase at temperatures lower than 975 °C. Although the  $\text{AlB}_{12}$  phase is only stable at temperatures above 975 °C, its presence at low concentration was reported in Al–B alloys.<sup>6,39</sup> A possible explanation for the coexistence of  $\text{AlB}_2$  and  $\text{AlB}_{12}$  in Al-B master alloys is the growth of  $\text{AlB}_2$  on the facets of  $\text{AlB}_{12}$ ; it is also direct proof of the existence of a slow peritectic reaction between  $\text{AlB}_{12}$  and Al.

Different Ti compounds, such as  $\text{TiB}_2$  and  $\text{Al}_3\text{Ti}$ , have a higher density than that of pure aluminum (4.5 and 3.35 g/cm<sup>3</sup>, respectively) although this is not the case for  $\text{AlB}_2$  and  $\text{AlB}_{12}$  compounds (3.1 and 2.55 g/cm<sup>3</sup>, respectively). Hence, in grain refined Al–Si alloys,  $\text{TiB}_2$  particles settle during melt holding. A large fraction of these settled  $\text{TiB}_2$  particles appear in interdendritic regions because of extensive particle pushing during growth of the  $\alpha$ -Al grains,<sup>40</sup> as a result of which the majority of particles in the settled layer are found at the grain boundaries. Pushing of  $\text{TiB}_2$  particles to  $\alpha$ -Al grain boundaries has been reported to occur in Al-5%Ti-1%B master alloys.<sup>10</sup> Moreover, in Al-Si alloys, the segregated  $\text{TiB}_2$  particles cause modification of the Al-Si eutectic, *i.e.* the morphology of the eutectic Si particles is altered to a fine fibrous form. This type of modification is a result of the segregation of  $\text{TiB}_2$  particles to the eutectic Al-Si phase boundaries, where they obstruct solute redistribution and refine the eutectic Si.<sup>40</sup> A  $\text{TiB}_2$ -containing grain-refiner has been reported to facilitate removing inclusions through settling in molten aluminum alloys.<sup>41</sup>



## 2.5 COMMON GRAIN REFINERS USED FOR Al-Si-Mg ALLOYS

Grain refiners are generally added in the form of master alloys of the type Al-Ti, Al-Ti-B or Al-B, so as to provide an enhanced number of nuclei for the nucleation of new  $\alpha$ -Al crystals. These are produced commercially with a wide range of Ti-to-B ratios, and include the Al-(3 or 5)%Ti-1%B grain refiners belonging to the Al-Ti-B system. It has been reported at various instances in the literature that the Ti-to-B ratio of the master alloy is an important contributing factor in the grain refinement process, with the best grain refining effects being obtained with a Ti-to-B ratio of 5:1 in weight percentage.<sup>7</sup> For many years the range of grain refiners available was limited mostly to three compositions, all based on the Al-Ti-B system, namely, Al-5%Ti-1%B, Al-3%Ti-1%B and Al-5%Ti-0.2%B. The Al-5%Ti-1%B was, and remains, the most popular composition because of its high refining potency. The refining ability of Al-B and Al-Ti-B master alloys is dependent to a high degree on the prevailing processing conditions such as holding time, residual Ti-content in the melt, melt temperature, temperature gradients during casting, and possible reactions of the following type:



The Al-3%Ti-1%B refiner containing a lower Ti-content was developed to meet the requirements of an efficacious refiner without exceeding Ti melt specifications, a situation which may occur frequently especially in plants with a high level of commitment to recycling. The lower boron-content refiners are used specifically for the production of surface critical products, and to help reduce or eliminate the number of boride defects in the end product through the simple expedient of introducing fewer boride particles.<sup>8</sup>

A significant improvement in the mechanical properties of aluminum alloys may be obtained by means of the addition of small amounts of Al-Ti-B master alloys which contain microscopic  $\text{TiB}_2$  and  $\text{Al}_3\text{Ti}$  nucleating particles.<sup>42</sup> When an Al-Ti-B grain refiner is stirred into the melt, the  $\text{Al}_3\text{Ti}$  particles dissolve rapidly and introduce solute titanium into the melt to assist growth restriction after the nucleation event. The  $\text{TiB}_2$  particles remain stable in the aluminum melt and provide sites for heterogeneous nucleation. That is why these particles act as the nucleating substrates. These master alloys are effective grain refiners whereas those containing only  $\text{TiB}_2$  and  $\text{Al}_3\text{Ti}$  particles are much less effective. Various theories regarding the grain refining mechanism of Al-Ti-B refiners have been proposed, including the particle theory, the phase diagram theory, the duplex nucleation theory, and the peritectic hulk theory.<sup>17</sup>

In the case of the Al-Ti type grain-refiners containing only  $\text{Al}_3\text{Ti}$  particles, these particles must act as the nucleating substrates; their effectiveness, however, is relatively poor when compared with that of Al-Ti-B type grain-refiners.<sup>8</sup> Al-Si alloys may also be efficiently grain refined by Al-4%B master alloys. It has been suggested<sup>36</sup> that the grain refinement mechanism for this master alloy is the heterogeneous nucleation of aluminum crystals on intermetallic  $\text{AlB}_2$  particles, combined with a more common growth restriction process resulting from the segregation of silicon during solidification. As regards the Al-B type grain refiner, Sigworth and Guzowski<sup>36</sup> proposed that  $\text{TiB}_2$  particles act as nucleants, and the presence of Si enhances their nucleating potential.

In the Al-5%Ti-1%B master alloy where the ratio of Ti-to-B is  $> 2.22$ , Ti in excess of  $\text{TiB}_2$  stoichiometry goes into solution and is expected to behave in a similar fashion to

that of Al-Ti master alloys. Although the nominal Ti addition levels for the Al-5%Ti-1%B and Al-6%Ti grain refiners would be the same in a melt, they represent different Ti solute levels. All of the Ti in Al-6%Ti forms a solute after the  $\text{Al}_3\text{Ti}$  intermetallic particles dissolve, whereas only about 56% of the Ti from the Al-5%Ti-1%B forms a solute, the remainder being tied up in the  $\text{TiB}_2$  particles.<sup>43</sup>

Based on the observation of the grain refinement of Al-Si alloys using Al-B master alloys, Sigworth and Guzowski<sup>36</sup> suggested that the mixed boride structure  $(\text{Al,Ti})\text{B}_2$  is close enough to the  $\text{AlB}_2$  phase to produce the grain refinement of Al-Si casting alloys in a similar manner. Researchers<sup>20, 36</sup> believe that the presence of the metastable boride nucleus  $(\text{Al,Ti})\text{B}_2$  and a Ti-to-B ratio of  $<2.22$  are responsible for the improved performance of 2.5%Ti-2.5%B master alloys over that of Al-5%Ti-1%B in Al-Si alloys. On the other hand, the enhanced performance of Al-2.5%Ti-2.5%B master alloys is thought to be due to heterogeneous nucleation of the  $(\text{Al,Ti})\text{B}_2$  phase as compared to Al-B master alloys in the relevant study by Sigworth and Guzowski.<sup>36</sup>

When Al-2.5%Ti-2.5%B master alloy is added, the boron in excess of the  $\text{TiB}_2$  stoichiometry will remain as solute boron. In the presence of  $\text{TiB}_2$  particles, the excess boron will segregate at the  $\text{TiB}_2$ /melt interface. As a result, the effective boron concentration at the interface will increase significantly. The interfacial boron-rich layer is expected to undergo a eutectic reaction upon cooling, thus nucleating  $\alpha$ -Al well above the liquidus temperature of an Al-7%Si alloy. It is interesting to note that this process will not produce the grain-refinement of pure aluminum, since the eutectic reaction occurs below the melting point of this element, a fact which has been well demonstrated by both

laboratory and industrial tests.<sup>29</sup> Figure 2.5 compares the performance of different types of grain refiners for the case of the A356 aluminum alloy.

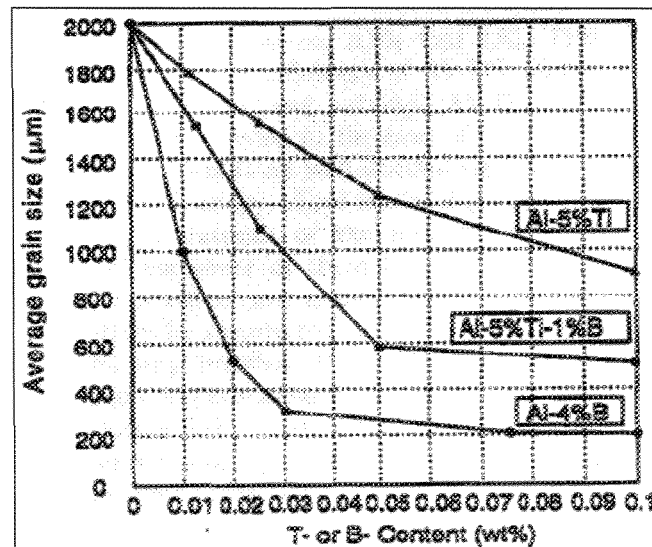


**Figure 2.5** Grain refinement of A356 alloy using Al-Ti, Al-Ti-B and Al-B master alloys.<sup>38</sup>

Spittle<sup>44</sup> studied several refiner systems and found that near-stoichiometric ratios of Ti/B did not refine as well as when either excess titanium or significant amounts of excess boron were present. The refinement was not reliable in the vicinity of the stoichiometric ratio, and since fade occurs rapidly, the result was often a larger grain size. Industrial practice has suggested that 0.1% excess titanium is required to ensure satisfactory performance from sub-stoichiometric refiners.<sup>45, 46</sup>

Other studies have suggested that the addition of excess titanium has no effect on grain size in Al-Si casting alloys. Easton and St-John<sup>47</sup> tested the effects of increasing titanium levels while at the same time maintaining  $\text{TiB}_2$  additions at a constant level, and found that the change in grain size was negligible. This result was attributed to the fact that Al-Si alloys already have a high growth-restriction factor (GRF), and the effect of solute

titanium on refinement should therefore be negligible. Sigworth and Guzowski<sup>36,48</sup> also suggested that only the particle component of a master alloy, in this case the boride, is required to obtain effective grain refinement in Al-Si casting alloys.

Easton and St-John<sup>47</sup> proposed that, in order to produce effective grain refinement, the optimum chemical grain refiner needs to include both solute titanium, with its very high growth restriction factor, and nucleating particles including  $\text{TiB}_2$  or  $\text{Al}_3\text{Ti}$ . For this reason, the Al-5%Ti-1%B type of refiner is extremely effective. The GRF of any solute element may be expressed by the factor  $mC_o(k-1)$ , where  $m$  is the gradient of the liquidus line in the binary alloy phase diagram,  $C_o$  is the concentration of the solute in the alloy, and  $k$  is the partition coefficient. It is generally assumed that individual GRFs are additive in multi-component alloy systems; this method, however, has the potential for grossly overestimating the value of the GRF.<sup>47</sup>

The beneficial effect of boron in conjunction with titanium for grain-refining aluminum alloys was also explored by others<sup>48,49</sup> who proposed alternative mechanisms. Such mechanisms involve various permutations of mixed (Al,Ti) $\text{B}_2$  borides and  $\text{Al}_3\text{Ti}$  which become stabilized at sub-peritectic compositions. Easton and St John<sup>47</sup> also suggested that, because such aluminum casting alloys as A356 already contain high solute levels and have a high GRF (the GRF of 7%Si being equivalent to that of 0.17% Ti), the optimum grain-refiner, in fact, need only contain nucleating particles. This observation indicates that such master alloys as Al-2.2%Ti-1%B (containing  $\text{TiB}_2$  particles with no extra solute Ti) or Al-4%B (containing  $\text{AlB}_2$  and/or  $\text{AlB}_{12}$  particles) are wholly suitable as grain refiners for foundry alloys.<sup>36</sup> It has been reported that optimum percentages of Ti and B for

A356 alloys are found to be approximately between 0.06% Ti - 0.01% B and 0.08% Ti - 0.02% B. Higher additions of Ti and B appear to cause the undesirable formation of Ti-based intermetallic compounds within the eutectic region.<sup>9</sup>

After the addition of Al-Ti-B master alloy to the unmodified melts, the Ti and B concentrations show that fading of both elements occurs to some extent as a function of time for both Al-5%Ti-1%B and Al-1.5%Ti-1.5%B master alloys.<sup>50,51</sup> It is believed that TiB<sub>2</sub> particles, with a theoretical density of 4.495 g/cm<sup>3</sup> as introduced by the master alloys, tend to settle, leading to a consequent decrease of Ti and B in the melt.<sup>52</sup> In addition to settling, agglomeration also plays an important role in the loss of grain refinement.<sup>45</sup>

Grain-coarsening is known to occur when chemical grain refiners become poisoned by other elements present in the melt in the form of alloying elements or impurities.<sup>53</sup> For instance, the effectiveness of Ti-based grain refiners is known to be severely diminished in the presence of Zr, which is another grain-refining element in its own right. Grain-coarsening may also result from “fade” associated with extended holding times.<sup>44</sup> Such fade may occur because the nucleating particles either settle, agglomerate or undergo some chemical transformation into another compound.

## 2.6 POROSITY IN A356 CASTINGS

The formation of porosity during solidification is one of the features of the microstructure which causes costly scrap loss and limits the use of castings in critical, high-strength applications. The solidification range has always been correlated with castability and feedability. Ratings of these generalized characteristics, by practical experience as well

as from what is available in theoretical treatments, confirm this direct correlation. At any particular location in the casting, the local solidification time determines secondary dendrite arm spacing (SDAS) and, hence, the mechanical properties.<sup>54</sup> The SDAS controls the size and the distribution of porosity and intermetallic particles in the casting. As it becomes smaller, porosity and second phase constituents are dispersed more finely and evenly. Wang and Cáceres<sup>55</sup> observed that in Al-Si-Mg alloys with large SDAS values, fracture occurs along the dendritic cell boundaries, while for alloys exhibiting small SDAS values, the final fracture tends to occur along the grain boundaries.

In alloys 319, 332 and 355, rapid cooling leads to the distribution of voids in the grain boundaries while slow cooling results in interdendritically distributed shrinkage.<sup>56</sup> Shrinkage in the 443 and 356 alloys, characterized by narrower solidification ranges, is found to be more localized at both solidification rates than in the 319, 332 and 355 alloys. In all cases, voids first begin to form at temperatures corresponding to 65-75% solid. Typical microstructures of A356 alloy, produced under laboratory conditions, contain a wide variety of pores. As SDAS or the hydrogen concentration increases in the alloy, the pores become larger and more spherical.<sup>56</sup> When either the hydrogen content or the local solidification time is increased, the pore distribution is skewed towards large pore sizes. Under most conditions, unmodified A356 alloys contain minimal amounts of irregular, (generally interdendritic) porosity, occupying less than 5% by area.

Grain refinement through the addition of titanium may alter the amount and morphology of the pores in the casting. The presence of the grain refiner leads to a redistribution of porosity. In many cases, there is also an overall reduction in the amount of

porosity upon grain refinement.<sup>57, 58</sup> It has been reported that a greater quantity of interdendritic liquid feeds through a partially solidified network when grain refined to an extent even beyond the coherency point.<sup>8</sup> Nonetheless, it was thought that burst feeding was the predominant mechanism of feeding in grain-refined castings, while interdendritic feeding was predominant in unrefined castings. The formation of pores in a casting occurs on heterogeneous nucleation sites, considering that homogenous nucleation of pores would require very high gas content and shrinkage pressure.<sup>2</sup> Researchers have proposed that nucleation occurs on oxide films<sup>59</sup> and particles.<sup>46</sup> Also,  $\text{TiB}_2$  particles, especially  $\text{TiB}_2$  clusters, have been found to nucleate porosity.<sup>11, 60</sup>

Unfortunately, the addition of strontium is associated with an increase in the amount of microporosity found within castings. More specifically, the addition of strontium to Al-Si alloys tends to increase the percentage porosity as a result of the difficulty of dissolution, as well as a depression in the eutectic transformation temperature.<sup>61</sup> Anson *et al.*<sup>62</sup> reported that the addition of strontium has a significant effect on the overall properties of microporosity by facilitating the formation of gas porosity to the detriment of shrinkage porosity.

In addition to the above drawbacks, bad foundry practice can lead to the occurrence of gross defects such as shrinkage and gas porosity or to entrapped dross and oxide films. Hydrogen is the only gas with significant solubility in molten aluminum. This gas is known to play a major role in the incident of unsoundness resulting from porosity in castings. Hence, degassing is a basic step in the aluminum casting process.



## 2.7 INTERACTION OF GRAIN REFINERS AND MODIFYING AGENTS

In view of the fact that  $\text{TiB}_2$  and Sr are commonly used in combination for commercial castings, possible interactions between boron and eutectic modifier elements such as strontium have been the subject of many recent studies. Modification and grain refinement used in conjunction will combine the negative effects of these two processes. The mushy zone will be longer and the radius of liquid channels smaller while the number of flow channels will increase. It is thus reasonable to expect that there should be more porosity in this case. Studies reporting on the effect of these two melt treatments when applied in combination are relatively scarce to date. Shivkumar *et al.*<sup>2</sup> studied this effect and found that the amount of porosity in the alloy treated to a combined grain refinement and modification treatment is lower than it is in a modified alloy but higher than in a grain refined alloy.

In the A356 alloy, individual additions of the grain refiner raise the primary  $\alpha\text{-Al}$  nucleation temperature by as much as  $4\text{-}5^\circ\text{C}$ , while additions solely of the Sr-modifier will depress the eutectic temperature by almost  $7\text{-}8^\circ\text{C}$ . In other words, if both additives perform in the same manner when combined, the solidification range, or the temperature difference from  $\alpha\text{-Al}$  nucleation temperature to eutectic temperature, should increase by  $11\text{-}13^\circ\text{C}$ .<sup>9</sup>

The addition of small amounts of Ti and B will cause shifts in the cooling curves upwards as the magnitude of recalescence decreases. The addition of grain refiners accelerates the nucleation of primary  $\alpha\text{-Al}$ , because of the presence of a greater number of nuclei in the melt. Both the nucleation and growth temperatures of the  $\alpha\text{-Al}$  particles increase although this increase is greater in the case of nucleation. This indicates that there

are more nuclei with a lower chance of growth at any given time during the nucleation and early growth of the  $\alpha$ -Al phase. The changes in eutectic temperature parameters are the same whether for the individual or the combined treatments, which may indicate that the grain refiner and the modifier act independently during solidification.

Liao and Sun<sup>22</sup> concluded that in near-eutectic alloys, the refining effect of boron is weakened due to an increase in the addition of strontium, in other words, the refining ability of boron is poisoned by strontium. A mutual poisoning effect was to be observed when the contents of Sr and B exceeded a certain limit, *i.e.* the refining effect of boron and the modifying effect of Sr are weakened. This interaction may be attributed to the formation of  $\text{SrB}_6$  compound. Moreover, Rao *et al.*<sup>39</sup> used the Al-5%Ti-2%C-15%Sr master alloy for the LM25 alloy, which is equivalent to A356 alloy. They believe that, under these conditions, the strong affinity of B for Ti leading to the formation of  $\text{TiB}_2$  nucleants, tends to impede any reaction between Sr and B causing the formation of  $\text{SrB}_6$ ; this would then have an adverse effect on grain refinement and modification, thereby deactivating Sr as a modifier. Adequate modification results when the addition level of the Al-Ti-B grain refiner in the Al-10%Si-0.35%Mg alloy, represented by combined additions of Sr and Al-Ti-B, reaches low levels of 1.4 and 2.8 kg/tonne, respectively.<sup>50</sup>

Similar mutual poisoning was also reported for Al-Si alloys as a result of the addition of Al-Ti-B and Al-Sr master alloys in combination.<sup>39</sup> Furthermore, the effectiveness of Sr in the melt decreases with increasing additions of the Al-5%Ti-1%B master alloy made to near-eutectic Al-Si alloys which have been modified with Sr. It was

observed by Liao and Sun <sup>23</sup> that the poisoning effect operated by the Al-5%Ti-1%B master alloy on Sr modification results from interaction between Sr and Ti.

Lu and Dahle <sup>50</sup> reported that the A356 melt treated with Al-1.5%Ti-1.5%B loses its Sr rapidly, particularly in the initial stages after addition has been made, compared to the melt which was treated with Al-5%Ti-1%B (see Figure 2.6). This fact may explain the quick loss of eutectic modification in the Al-1.5%Ti-1.5%B treated melt, indicating that there is insufficient free Sr in the melt to modify all of the eutectic Si.

Whichever mechanism may be in operation, however, the Sr concentration in the melt is expected to decrease gradually over time. Results from the experiment where the melt was treated only with Sr are also included in Figure 2.6 and are indicated by a dotted line. It is readily apparent that both the Sr-only treated melt and the melt treated with Sr plus Al-5%Ti-1%B behave in a similar manner, showing a slow and almost linear loss of Sr over time. Molten Al-Si alloys are known to lose their Sr through surface oxidation and vaporization.<sup>3</sup> The addition of the Al-5%Ti-1%B grain refiner does not significantly accelerate the loss of Sr in the melt. In this regard, Lu and Dahle <sup>50</sup> also concluded that, while a slight coarsening of eutectic Si occurs over time for the modified Al-10%Si-0.35%Mg melt treated with the Al-5%Ti-1%B grain refiner, this last has a strong poisoning effect on the Sr modification. It was also shown that the sequence of the addition of the grain refiner and modifier significantly influences the grain size of  $\alpha$ -Al, as may be seen in Figure 2.7 compared to the results for their combined additions.<sup>63</sup>

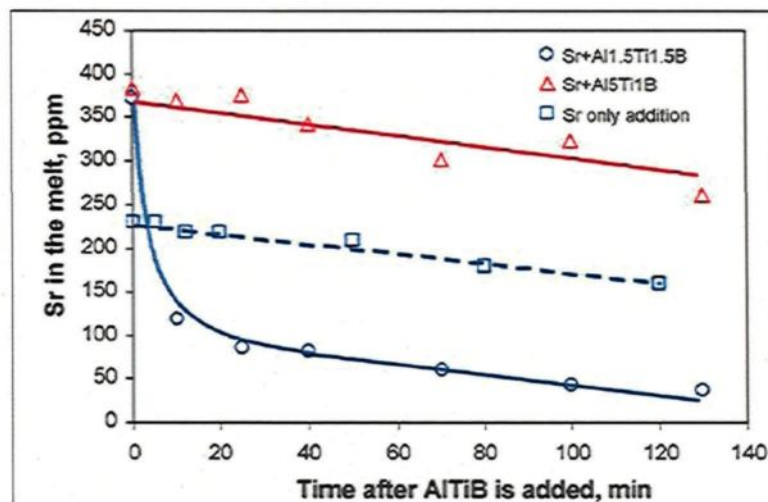


**Figure 2.6** Sr concentrations, as a function of time after Al-Ti-B grain refiners were added to obtain 0.15% Ti in the melts (solid lines). The dotted line refers to the case of Sr modification without addition of any grain refiner.<sup>50</sup>

The master alloy Al-10%Sr also appears to have a certain amount of grain refining effect on Al-Si-Cu alloys.<sup>64</sup> According to the refinement mechanism in the Al-B system proposed by Mohanty and Gruzleski,<sup>38</sup> the grain-refining effect of Al-10wt% Sr on Al-Si-Cu alloys may also be explained by the occurrence of the eutectic reaction in the Al-Sr system at a temperature of 654°C, which is higher than the liquidus of the Al-Si-Cu alloys. Through this mechanism, some of the Sr may also refine the grains of hypoeutectic Al-Si alloys.

Nogita and Dahle,<sup>65</sup> however, reported that boron itself has no influence on the structure of the eutectic Si which remains unaltered or undergoes only a very slight change in morphology. The same group of researchers showed that the addition of boron has no effect on the eutectic growth temperature which usually decreases with modification,<sup>66</sup> where they showed that the recovered Sr levels were similar to the nominal addition levels in strontium-added samples in the absence of boron.

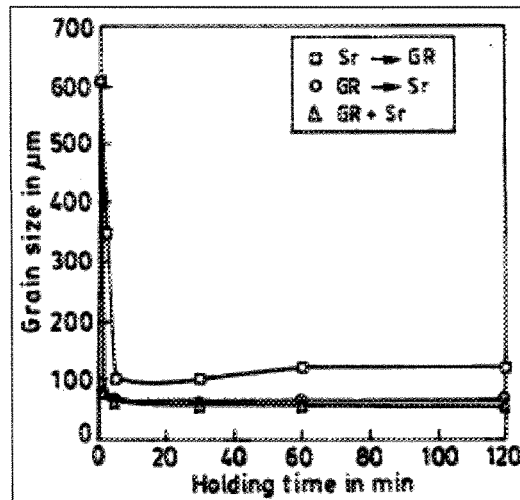


**Figure 2.7** Grain size analysis of grain-refined Al-7%Si alloy with different sequences of grain refiner and modifier addition (1.0% of Al-1%Ti-3%B and 0.02% Sr).<sup>63</sup>

This fact might tend to indicate that Sr was a stable element in that melt, resulting in very high recovery of the addition, whereas boron-added samples, without injecting additional strontium, showed boron recoveries of less than 50%. Furthermore, the amount of recovered Sr drops exponentially with increasing B addition when both Sr and B are added to the melt, thus suggesting a strong interaction between them.

Figure 2.8 shows the relationship between eutectic undercooling, the Sr-to-B ratio, and the microstructure observed by means of optical microscopy. According to Nogita *et al.*,<sup>66</sup> the eutectic growth temperature drops with increasing Sr-to-B ratio. They found fibrous eutectic silicon in all samples where eutectic undercooling was greater than 2°C. Thus, significant modification is only obtained at Sr-to-B ratios exceeding 0.4.

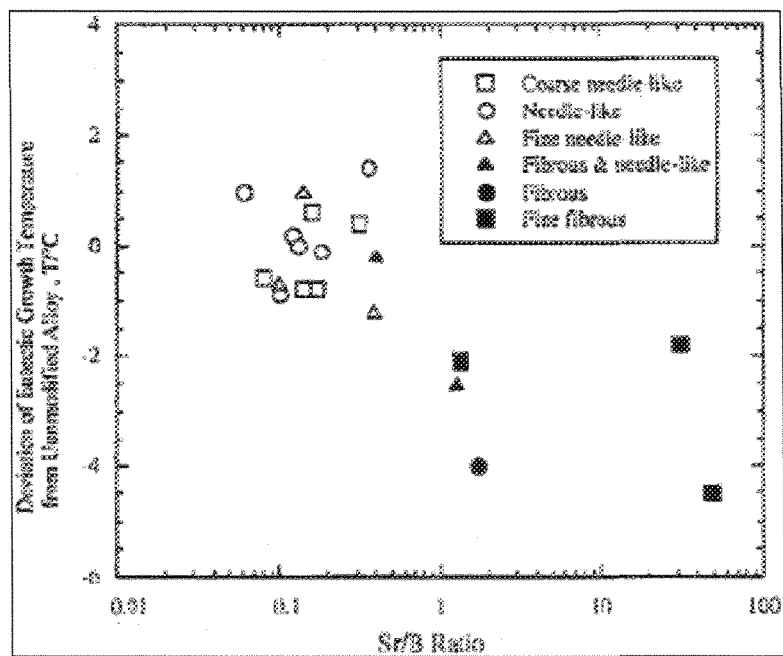


**Figure 2.8** The relationship between eutectic undercooling, silicon morphology and the Sr:B ratio.<sup>66</sup>

**CHAPTER 3**

**EXPERIMENTAL PROCEDURES**

## **CHAPTER 3**

### **EXPERIMENTAL PROCEDURES**

#### **3.1 INTRODUCTION**

This chapter will discuss the various experiments designed and conducted in order to study the interactions taking place between Ti/B and Sr in modified Al-Si alloys, with particular reference to A356.2 alloy. The various A356.2 alloy melts prepared in relation to these experiments and the master alloys and addition levels used will also be discussed. There will follow a step-by-step description of the melting, casting and heat treatment procedures used, the thermal analysis experiments conducted for each melt composition, the preparation of samples for metallographic examination and tensile and impact testing, and the methods used for carrying out the microstructure analysis and the tensile and impact tests.

The experiments were conducted in three different stages or groups, corresponding to specific Ti, Ti and B, and Sr additions made to the A356.2 alloy melts, and covering various ranges for each additive as shown in Table 3.1. It should be noted that all Ti and B additions are in weight percent while the Sr additions are given in ppm levels.



**Table 3.1** Range of strontium, titanium, and boron addition levels used in A356.2 alloy melts

Step No.	Grain refiner addition range (wt%)	Sr addition	Mold type
1	0.1% Ti - 0.5% Ti	200 ppm	Metallic
2	0.02% Ti - 0.08% Ti 0.01% B - 0.05% B	200 ppm	Metallic
3	0.1% Ti and 0.5% Ti 0.01% B and 0.05% B	30 ppm	Metallic

### 3.2 MATERIALS, MELTING AND MELT TREATMENT PROCEDURES

The A356.2 alloy used in this study was received in the form of 12.5 kg-ingots. Table 3.2 shows the composition of the as-received base alloy, which was taken into consideration for material balancing during the addition of master alloys.

The ingots were first cut into smaller pieces, then cleaned, dried and melted in a 40-kg capacity SiC crucible using an electrical resistance furnace. The molten metal was maintained at a temperature of  $750 \pm 5^\circ\text{C}$ .

**Table 3.2** Composition (wt %) of the A356.2 base alloy used in this study

Al	Si	Mg	Cu	Ti	Mn	Zn	Fe
Bal.	7.21	0.41	< 0.01	0.11	< 0.01	< 0.01	0.08

Addition of Sr was made using Al-10%Sr master alloy and two strontium levels of 30 ppm and 200 ppm each. Grain-refiner additions were then made to the Sr-modified A356.2 alloy melts in various concentrations and using different types of grain refiner. The amounts of the grain-refiner master alloy additions were calculated in terms of the weight percent of Ti or B required for obtaining the targeted concentrations in the melt. All master

alloys used were manufactured by KB Alloys Inc. Table 3.3 summarizes the details of the grain refiner additions which were made for the purpose of the present research.

The master alloys were added to the melt using a perforated graphite bell which was immersed into the melt for about 2-3 minutes. The melt was stirred, and then degassed for 15 minutes using pure, dry argon introduced into the melt through a graphite rotary impeller operating at a speed of 150 rpm. Following degassing, the melt was poured at  $735 \pm 5^\circ\text{C}$  into coated metallic molds preheated at  $440 \pm 10^\circ\text{C}$ , in order to produce impact and tensile test bars. Samplings for chemical analyses were also simultaneously taken for each of the melt compositions prepared.

Castings were made using the two metallic molds shown in Figure 3.1. The ASTM B-108 type metallic mold shown in Figure 3.1(a) was used to prepare tensile test bar castings, each casting providing two test bars. The impact test bars were prepared using the mold shown in Figure 3.1(b), where each casting provided ten impact test bars.

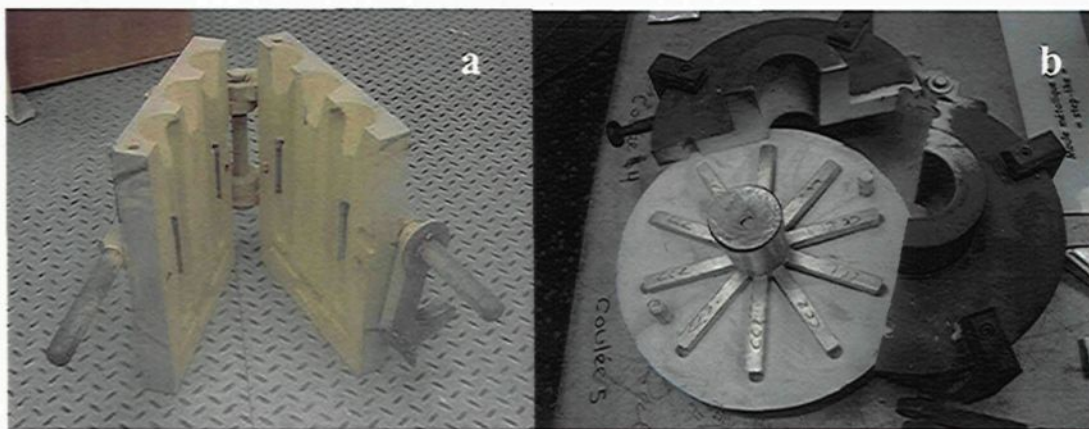


**Figure 3.1** (a) ASTM B108 permanent mold used for preparing tensile test bars; (b) Impact test specimen casting and mold.

**Table 3.3** Details of grain refiner and modifier additions made to A356.2 alloy melts

Group	Strontium Addition (ppm)	Grain Refiner Type and Addition Level (wt %)					Number of Specimens* and Condition			
		Al-10Ti	Al-5 Ti-1B	Al-2.5 Ti-2.5B	Al-1.7 Ti-1.4B	Al- 4B	As-cast		T6	
							Tensile	Impact	Tensile	Impact
1	200	0.1%Ti	0.1%Ti	0.1%Ti	0.1%Ti	0.01%B	125 (130)	125 (130)	125 (130)	125 (130)
		0.2%Ti	0.2%Ti	0.2%Ti	0.2%Ti	0.02%B				
		0.3%Ti	0.3%Ti	0.3%Ti	0.3%Ti	0.03%B				
		0.4%Ti	0.4%Ti	0.4%Ti	0.4%Ti	0.04%B				
		0.5%Ti	0.5%Ti	0.5%Ti	0.5%Ti	0.05%B				
2	200	0.02%Ti	0.02%Ti	0.02%Ti	0.02%Ti	—	80	80	80	80
		0.04%Ti	0.04%Ti	0.04%Ti	0.04%Ti					
		0.06%Ti	0.06%Ti	0.06%Ti	0.06%Ti					
		0.08%Ti	0.08%Ti	0.08%Ti	0.08%Ti					
3	30	0.1%Ti	0.1%Ti	0.1%Ti	0.1%Ti	0.01%B	50 (55)	50 (55)	50 (55)	50 (55)
		0.5%Ti	0.5%Ti	0.5%Ti	0.5%Ti	0.05%B				

\*The numbers in parentheses refer to the total number of specimens, including specimens with no grain refiner addition

### 3.3 THERMAL ANALYSIS

Thermal analysis was used to examine the combined interaction between strontium and boron, as well as the likely effect of boron on the partial modification of the eutectic silicon particles, through a study of the cooling curves obtained upon solidification of the corresponding melts. Table 3.4 shows the alloy melts for which thermal analysis was carried out.

**Table 3.4** A356.2 alloy melts used for thermal analysis experiments

Group	Al-4%B or Al-10%Ti addition (ppm)	Sr addition (ppm)
1	-	200 ppm
2	500-5000 ppm Boron	200 ppm
3	500-5000 ppm Titanium	200 ppm

The melts were prepared in a 1.5-kg capacity SiC crucible, using a small electric resistance furnace. The melting temperature was kept at  $750^{\circ} \pm 5^{\circ}\text{C}$ . The required amounts of Al-10%Sr and the other master alloys were added to the melt. The melt was degassed and stirred for ~10 min to ensure homogeneous mixing.

The molten metal was then poured into a cylindrical graphite mold (of 10 cm length and 6 cm diameter) preheated at  $600^{\circ}\text{C}$  to obtain close-to-equilibrium cooling conditions (approximately 855 g of metal, poured at a temperature of  $735^{\circ}\text{C} \pm 5^{\circ}\text{C}$ ). Thermal analysis was performed by attaching a high sensitivity thermocouple (chromel-alumel, type K) to the mold system, passing through the bottom of the mold and reaching halfway up into the mold cavity. The parts of the thermocouple within the mold was protected using double-

walled ceramic tubing. The temperature-time data was collected using a high-speed data acquisition system (DASYLab) linked to a computer with an acquisition rate of 5 readings/sec. From the thermal analysis data, the cooling curves were plotted in each case. Figure 3.2 shows a schematic diagram of the graphite mold used for thermal analysis.

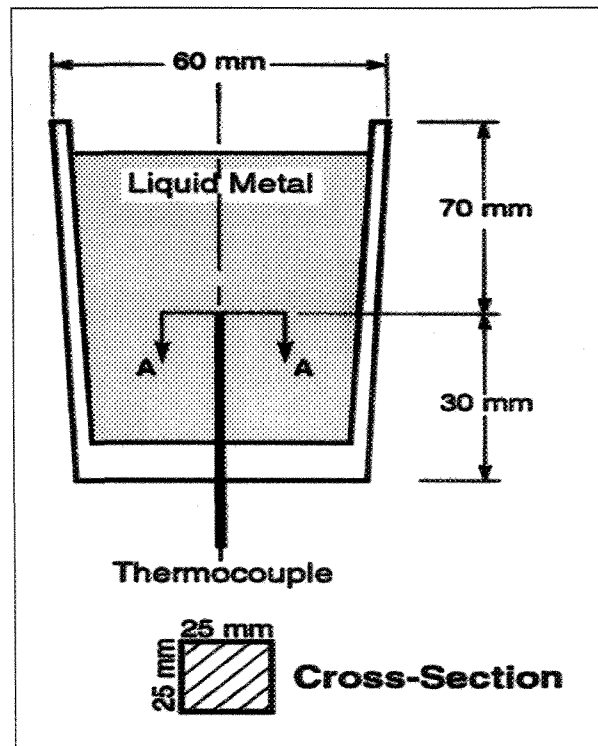


**Figure 3.2** Schematic diagram of graphite mold used for thermal analysis.

Samples were sectioned from the graphite mold castings as shown Figure 3.2 (A-A section), with dimensions of 2.5 x 2.5 cm. These samples were mounted in bakelite and polished to a fine finish for purposes of metallographic examination.

### 3.4 HEAT TREATMENT PROCEDURE

The tensile and impact samples were heat-treated following the T6 temper which comprises solution heat treatment at 540°C for 8 hours, followed by quenching in warm water at 60°C. The samples were then aged at room temperature for 24 hours, followed by artificial aging at 155°C for 5 hours, then air cooled. The heat treatment was carried out in a Blue M forced air furnace, as shown in Figure 3.3. The furnace is fully programmable with a temperature control of  $\pm 2^{\circ}\text{C}$ .



**Figure 3.3** Blue M forced air furnace used for heat treatment.

### 3.5 MECHANICAL TESTING

Tensile and impact tests were conducted to evaluate the mechanical properties. Tensile testing was carried out on as-cast and T6 heat-treated test bars of the various alloys prepared, using an Instron Universal Mechanical Testing machine, as shown in Figure 3.4.



The tests were conducted at room temperature at a strain rate of  $2 \times 10^{-4} \text{ s}^{-1}$ , cross-head speed of 0.02 in/min (or 0.51 mm/min). Tensile properties measured included ultimate tensile strength (UTS), the 0.2% offset yield strength (YS), and percentage elongation (%El). Five tests bars were used per alloy composition/condition. The average of the five values was taken to represent the tensile properties for that specific alloy condition.

The impact tests were carried out on unnotched samples obtained in both the as-cast and heat-treated conditions, using an Instron SI-1 Impact Testing machine to measure the traditional impact strength, or total absorbed energy, as shown in Figure 3.4(b). Whenever a specimen showed porosity or oxide defects, the results were rejected. At sufficiently low levels of porosity, microstructural features other than the pores tend, primarily, to govern the mechanical properties.

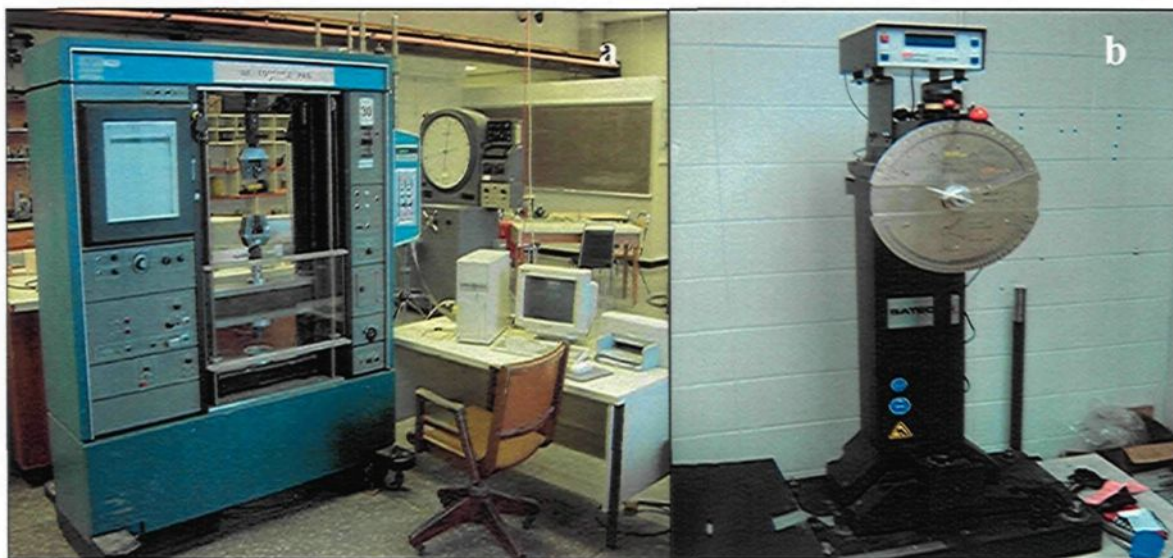


**Figure 3.4** (a) Instron Universal Mechanical Testing machine, (b) Instron SI-1 Impact Testing machine.

### 3.6 METALLOGRAPHY

A number of samples were chosen for metallographic inspection. Metallography samples were sectioned from the as-cast tensile tested specimens, about 3 mm below the fracture surface. These sections were mounted in bakelite and then polished to a fine finish (1  $\mu\text{m}$  diamond suspension), to facilitate the examination of the corresponding microstructures. The grain sizes of the specimens were measured by the linear intercept method after etching the polished surface with Keller's reagent (comprising 66 vol.%  $\text{HNO}_3$ , 33 vol.%  $\text{HCl}$ , and 1 vol.%  $\text{HF}$ ). Each grain size reported in this thesis is an average of 80 readings (with a standard deviation of  $\sim 20 \mu\text{m}$ ).

The metallographic samples were examined using optical microscopy and electron probe microanalysis (EPMA) associated with energy dispersive X-ray (EDX) and wavelength dispersion spectroscopic (WDS) analyses. Eutectic silicon particle characteristics and grain size were measured using a Clemex image analysis system in conjunction with the optical microscope. Identification of a number of the intermetallic phases formed by the addition of different grain refiners was carried out using EPMA. The WDS analysis provided the means for determining the chemical composition and formulae for these phases. Figure 3.5 shows the optical microscope-image analyzer system and the electron probe microanalyzer used for this purpose.



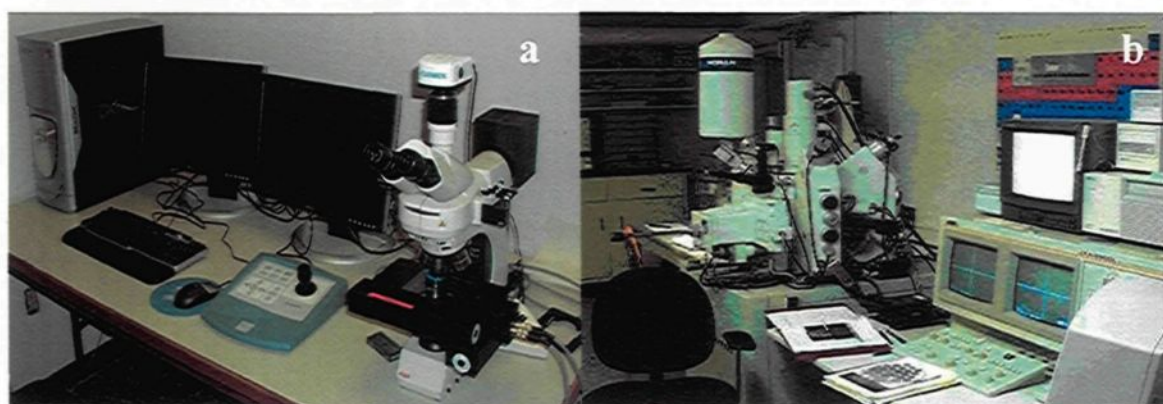


**Figure 3.5** (a) Optical microscope-image analyzer system, and (b) Electron probe microanalyzer used in the present study.

**CHAPTER 4**

**ASPECTS OF MICROSTRUCTURE AND**

**MACROSTRUCTURE**

## **CHAPTER 4**

### **ASPECTS OF MICROSTRUCTURE AND MACROSTRUCTURE**

#### **4.1 MICROSTRUCTURAL FEATURES**

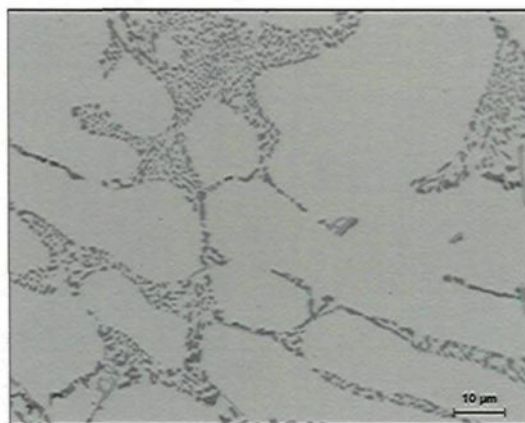
##### **4.1.1 INTRODUCTION**

The significant features of the microstructure of any given alloy, by their very nature, tend to regulate the inherent properties of that alloy. In the case of Al-Si alloys, the characteristics of the eutectic silicon particles, including their size and morphology, influence the relevant mechanical properties to a noticeable degree. This section will thus describe in detail the microstructures of the A356.2 alloy after it has been exposed to a variety of different master alloy types and addition levels. The aim of such an approach is to examine the interactions occurring between Sr, Ti, and B, in themselves, and at the same time to investigate the outcome of their action upon the modification of eutectic silicon.

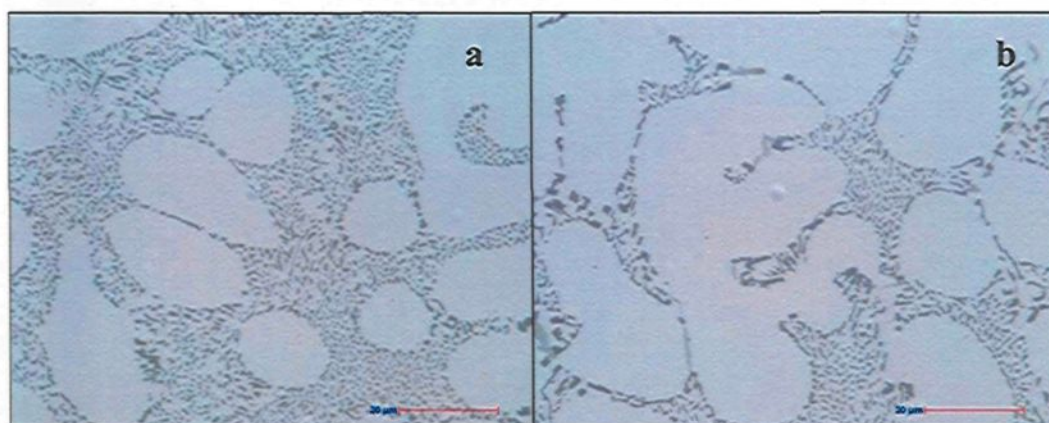
##### **4.1.2 ADDITION OF 200 ppm STRONTIUM**

Figure 4.1 shows the microstructure of the 200 ppm Sr-modified as-cast alloy without any addition of grain refiner. This type of microstructure generally contains primary  $\alpha$ -aluminum dendrites, eutectic silicon, magnesium silicide precipitates ( $\text{Mg}_2\text{Si}$ ),

and iron intermetallics, all of which undergo refinement with the increasing cooling rate of the alloy as a result of the metallic mold casting process.



**Figure 4.1** Optical micrograph showing the microstructures of as-cast A356.2 alloy modified by addition of 200 ppm Sr.



**Figure 4.2** Optical micrographs of microstructures in as-cast 200 ppm Sr-modified A356.2 alloy after refining by addition of (a) 0.02%Ti, and (b) 0.08% Ti as Al-10%Ti.

Figures 4.2 (a) and (b) illustrate the microstructures to be observed in the A356.2 alloy, after it has been refined with the binary master alloy Al-10% Ti at addition levels of 0.02% and 0.08% Ti, respectively. A comparison of these two figures reveals no significant difference in the morphology of the silicon. It is thus clear that the morphology of eutectic

silicon particles remains almost unchanged when the Al-10% Ti grain refiner is added to the 200 ppm Sr-modified as-cast A356.2 alloy.

Figures 4.3 (a) to (f) show the corresponding microstructures for low addition levels of Al-Ti-B in the form of master alloys combined with 200 ppm Sr. A comparison of Figures 4.3 (a) and (b) indicates that there is no major change to be observed in the morphology of the silicon particles; in this case, a boron-content of 0.004 and 0.016 %, respectively, also becomes available in addition to the same content in Ti, as shown earlier in Figure 4.2. A similar comparison between Figures 4.3 (c) and (d), and another between Figures 4.3 (e) and (f), illustrate the effects of the master alloy type and the change in boron-content. With reference to Figures 4.3 (c) and (d), grain refining was applied using the Al-2.5%Ti-2.5%B master alloy; the corresponding boron-content for these figures is 0.02 and 0.08 %, respectively, while for Figures 4.3 (e) and (f), where the Al-1.7%Ti-1.4%B master alloy was used, the boron-content is 0.016 and 0.066 %, respectively. In Figure 4.3 (d) some evidence of coarsening appears, while in Figure 4.3 (f) the shape and size of the silicon particles resemble those shown in Figure 4.3 (b). It is clear that by gradually increasing the boron-content, a number of changes may occur in the shape and size of these particles; thus, for the Al-2.5%Ti-2.5%B master alloy, the addition of 0.08%Ti may be considered the threshold level for affecting silicon morphology by using boron. From a comparison of the microstructures shown in Figures 4.2 and 4.3, it may be concluded that there is no significant interaction between strontium and boron, or between strontium and titanium, at low addition levels of Ti and B.



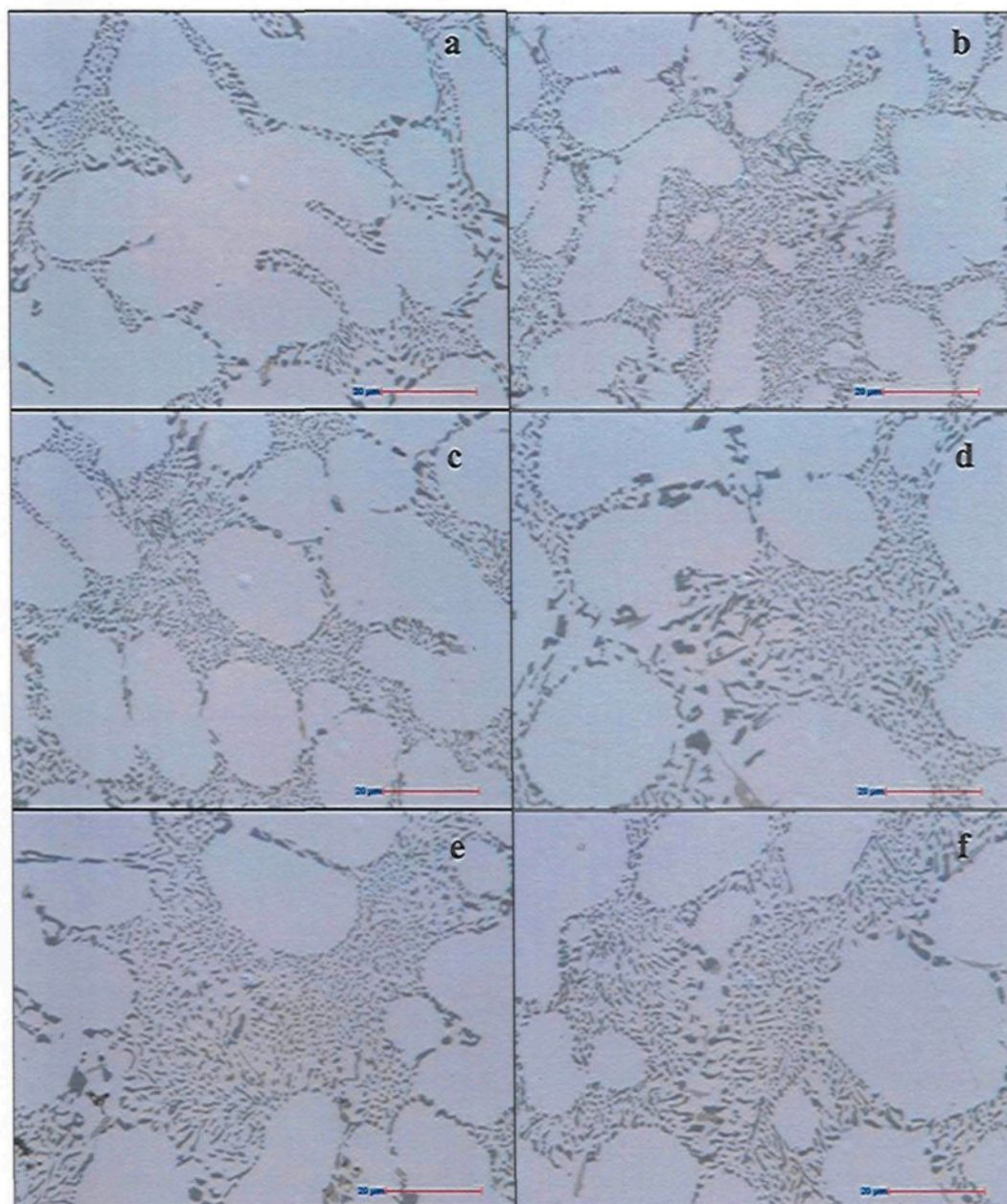


**Figure 4.3** Optical micrographs of the microstructures of 200 ppm Sr-modified A356.2 as-cast alloy grain-refined with additions of:  
 (a) 0.02%Ti and (b) 0.08% Ti using Al-5%Ti -1%B;  
 (c) 0.02%Ti and (d) 0.08% Ti using Al-2.5%Ti -2.5%B;  
 (e) 0.02%Ti and (f) 0.08% Ti using Al-1.7%Ti-1.4%B.

Figures 4.4 (a, b) and 4.4 (c, d) represent the microstructures of the A356.2 alloy refined with two individual binary master alloys, Al-10%Ti and Al-4%B, at addition levels

of 0.1 and 0.5%Ti, and 0.01 and 0.05%B, respectively. Such additions make it possible to distinguish the individual effects of adding Ti and B. A comparison of Figures 4.4 (a) and (b), corresponding to additions of Al-10%Ti, does not show any significant difference in the morphology of the silicon particles. The same may be said for the microstructures shown in Figures 4.4 (c) and (d), representing additions of Al-4%B. It may thus reasonably be concluded that individual additions of Ti and B, up to 0.5% Ti and 0.05% B, do not appear to influence the morphology of eutectic silicon particles in modified A356.2 alloys.

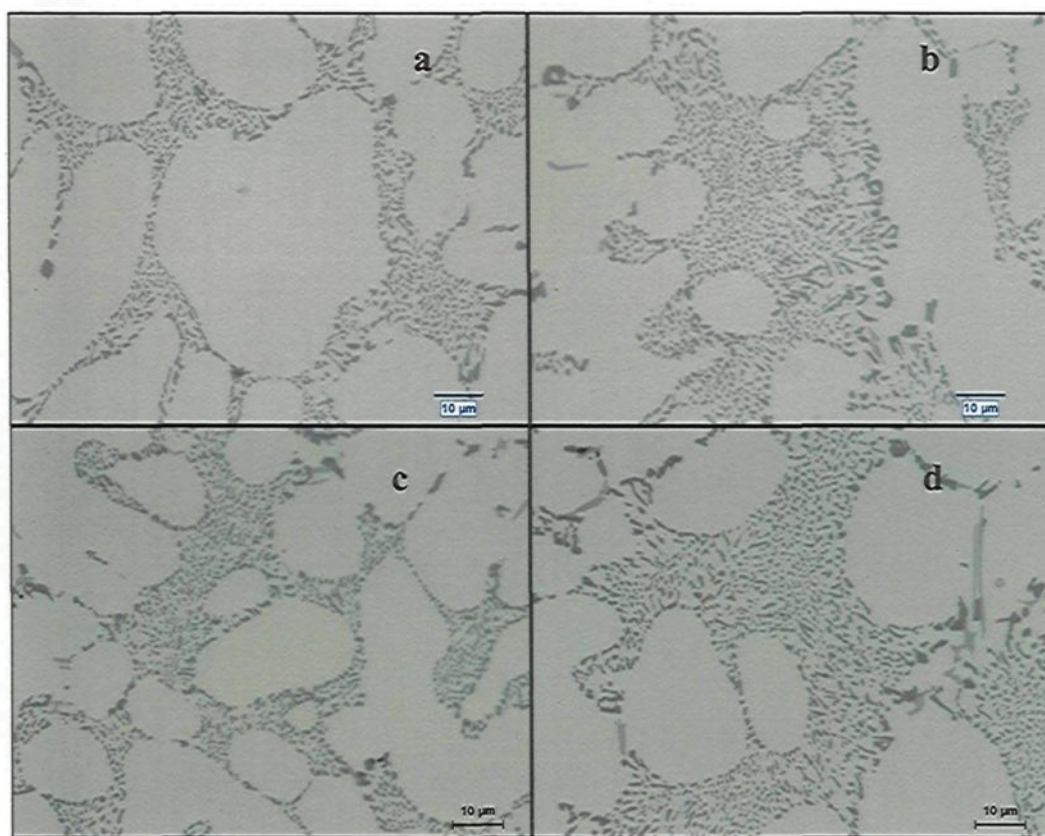


**Figure 4.4** Optical micrographs of the microstructures of 200 ppm Sr-modified A356.2 as-cast alloy refined by the addition of Al-10%Ti and Al-4%B: (a) 0.1%Ti, (b) 0.5% Ti, (c) 0.01% B, and (d) 0.05% B.

Figures 4.5 (a) to (f) illustrate the microstructures of the 200 ppm Sr-modified A356.2 alloy refined by adding three types of Al-Ti-B master alloys at two levels of Ti addition: 0.1% and 0.5 %. Only when using the Al-2.5%Ti-2.5%B and Al-1.7%Ti-1.4%B master alloys does the amount of boron addition exceed 0.1%B, as shown in Figures 4.5 (d) and (f).

Bearing in mind which of the Al-Ti-B master alloy types is in question, and what the percentage of titanium and boron addition is in each case, then the existence of some coarser and larger Si particles would indicate that 0.1% B is the starting point at which eutectic Si particles begin to revert to coarse flakes, as shown in Figures 4.5 (b), (c), and (e); in other words, the modification effect of Sr begins to be poisoned by the presence of B at this threshold level. The size of the eutectic Si particles does not show any significant increase with a boron-content of between 0.004 and 0.1%. The presence of some coarse Si particles may be attributed to the gradual nature of silicon modification, as well as to the probable interaction between strontium and boron or between strontium and titanium. In Figures 4.5 (d) and (f), the microstructures correspond to 0.5% B and 0.4% B levels, respectively; the figures clearly indicate that the Sr available for the modification of silicon particles decreases with an increase in boron addition. The silicon particles in these two microstructures clearly possess a flake-like acicular morphology, i.e. the eutectic silicon becomes *demodified* at boron-contents which are higher than 0.1%, while below that, or at around 0.1% B, the eutectic silicon retains its fibrous morphology to a greater extent. There is thus no interaction between Ti and Sr at Ti levels of up to 0.5%, even in the presence of boron-contents of less than 0.1 %, whereas the addition of boron in excess of 0.1% is apt to



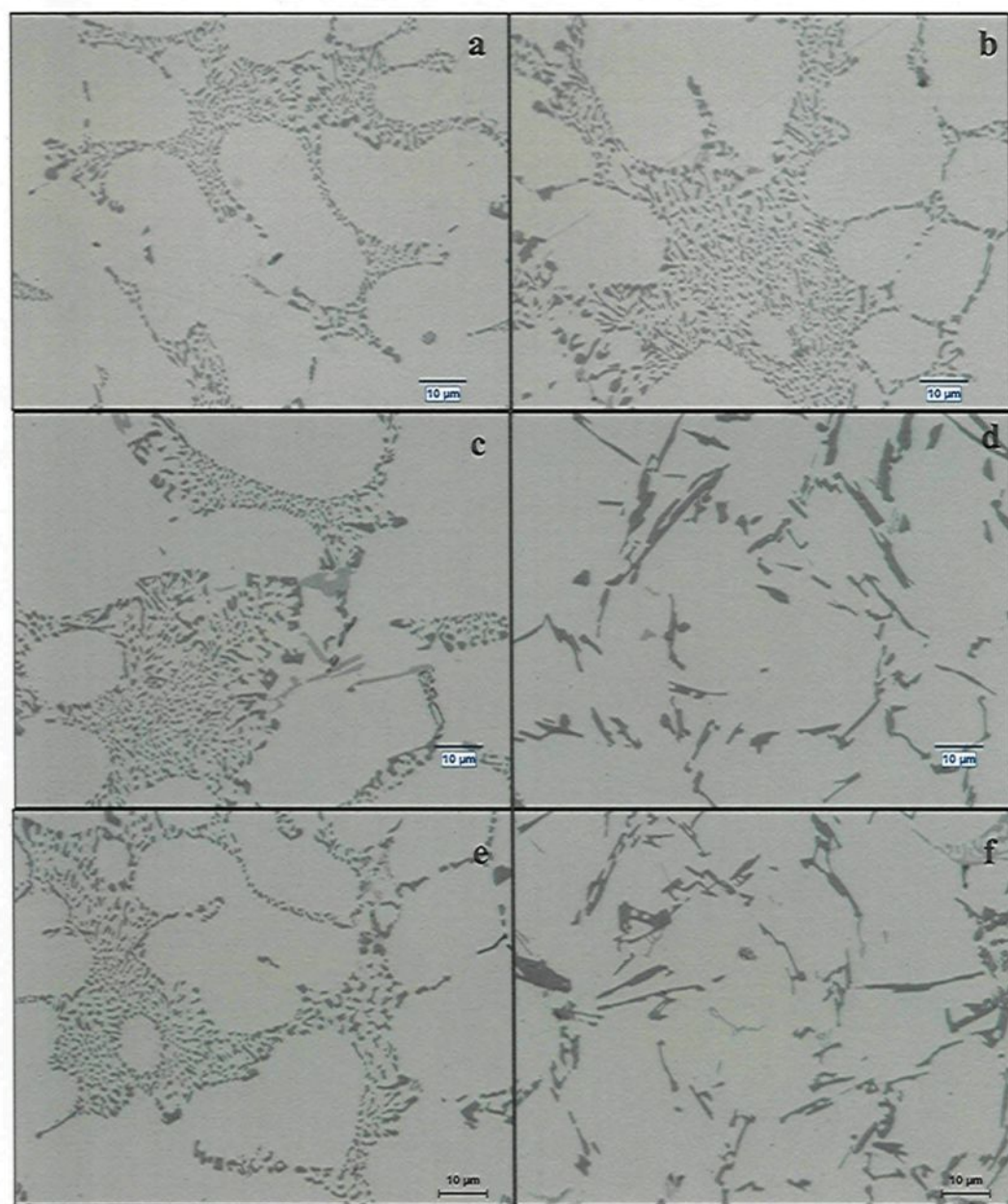


**Figure 4.5** Optical micrograph of microstructures of 200 ppm Sr-modified A356.2 as-cast alloy refined by addition of : (a,b) Al-5%Ti-1%B, (c,d) Al-2.5%Ti-2.5%B, and (e,f) Al-1.7%Ti-1.4%B master alloys; (a,c,e) 0.1% Ti addition; (b,d,f) 0.5% Ti addition.

reduce the level of modification considerably. Hence, the addition of boron may be deemed responsible for the changes in the morphology of eutectic Si particles. Table 4.1 summarizes the silicon particle characteristics for the as-cast 200 ppm Sr-modified samples of A356.2 alloy containing different types and addition levels of grain refiner.

In order to study the effects of the addition of different master alloys on the level of modification observed in the microstructures of the A356.2 alloy samples in each individual case, eutectic silicon particle length was chosen as the indicative parameter of the extent of modification of the Si particles. The results are shown in Figures 4.6 (a) and (b) for low and high levels of grain refiner additions, respectively. It is important to note that, in all the these figures, the X-axis label "Ti/B addition" refers to the additions of Ti in increments of 0.01% Ti or 0.1% Ti for the lower and higher addition level ranges, respectively, when these additions are carried out using Al-10%Ti or any of the Al-Ti-B master alloys. It should be noted that only in the case of the Al-4%B master alloy does the X-axis represent additions of boron in increments of 0.01%.

At lower additions of the master alloy, as shown in Figure 4.6 (a), the average length of the Si particles remains virtually unchanged, a fact which may be accounted for by the low B-content in each of the master alloy additions. Figure 4.6 (b) shows that, at higher master alloy additions, different observations may be noted depending on the master alloy under discussion. As in the case of Figure 4.6 (a), Figure 4.6 (b) also indicates that there is a lack of any significant change in the Si particle length for the Al-10%Ti master alloy, suggesting that there is no interaction between Ti and Sr over the range of Ti levels which were considered for this study.

**Table 4.1** Silicon particle characteristics of 200 ppm Sr-modified, grain refined as-cast A356.2 alloys

Grain Refiner type/level		Area ( $\mu\text{m}^2$ )		Length ( $\mu\text{m}$ )		Roundness Ratio		Aspect Ratio	
		Avg.	SD	Avg.	SD	Avg.	SD	Avg.	SD
No addition		1.18	2.66	1.66	1.70	0.48	0.19	1.95	0.90
Al-10%Ti	0.02% Ti	0.92	1.86	1.49	1.41	0.50	0.18	1.88	0.83
	0.08% Ti	1.03	2.28	1.64	1.67	0.47	0.19	2.0	0.89
	0.1% Ti	1.18	2.63	1.68	1.76	0.48	0.19	2.00	0.963
	0.5% Ti	1.44	3.07	1.87	1.91	0.48	0.19	1.99	0.952
Al-5%Ti-1%B	0.02% Ti	1.3	6.85	1.66	3.66	0.51	0.18	1.83	0.80
	0.08% Ti	1.05	2.7	1.62	1.78	0.48	0.19	1.95	0.86
	0.1% Ti	0.72	1.46	1.27	1.21	0.51	0.18	1.84	0.799
	0.5% Ti	2.13	4.81	2.31	2.55	0.46	0.20	2.07	1.10
Al-2.5%Ti-2.5%B	0.02% Ti	1.17	7.48	1.55	4.03	0.516	0.18	1.80	0.747
	0.08% Ti	0.81	2.72	1.35	1.34	0.52	0.18	1.83	0.76
	0.1% Ti	1.24	2.61	1.71	1.73	0.48	0.19	1.98	0.98
	0.5% Ti	6.75	12.8	4.96	5.97	0.39	0.26	2.85	2.10
Al-1.7%Ti-1.4%B	0.02% Ti	1.76	9.92	1.95	5.09	0.50	0.19	1.89	0.85
	0.08% Ti	1.06	4.55	1.59	1.74	0.49	0.19	1.95	0.90
	0.1% Ti	1.53	3.18	1.94	1.96	0.469	0.19	2.01	0.96
	0.5% Ti	6.08	11.8	4.33	5.22	0.41	0.25	2.57	1.97
Al-4%B	0.01% B	0.94	1.96	1.49	1.47	0.488	0.19	1.93	0.89
	0.05% B	0.915	2.06	1.43	1.42	0.5	0.19	1.89	0.85

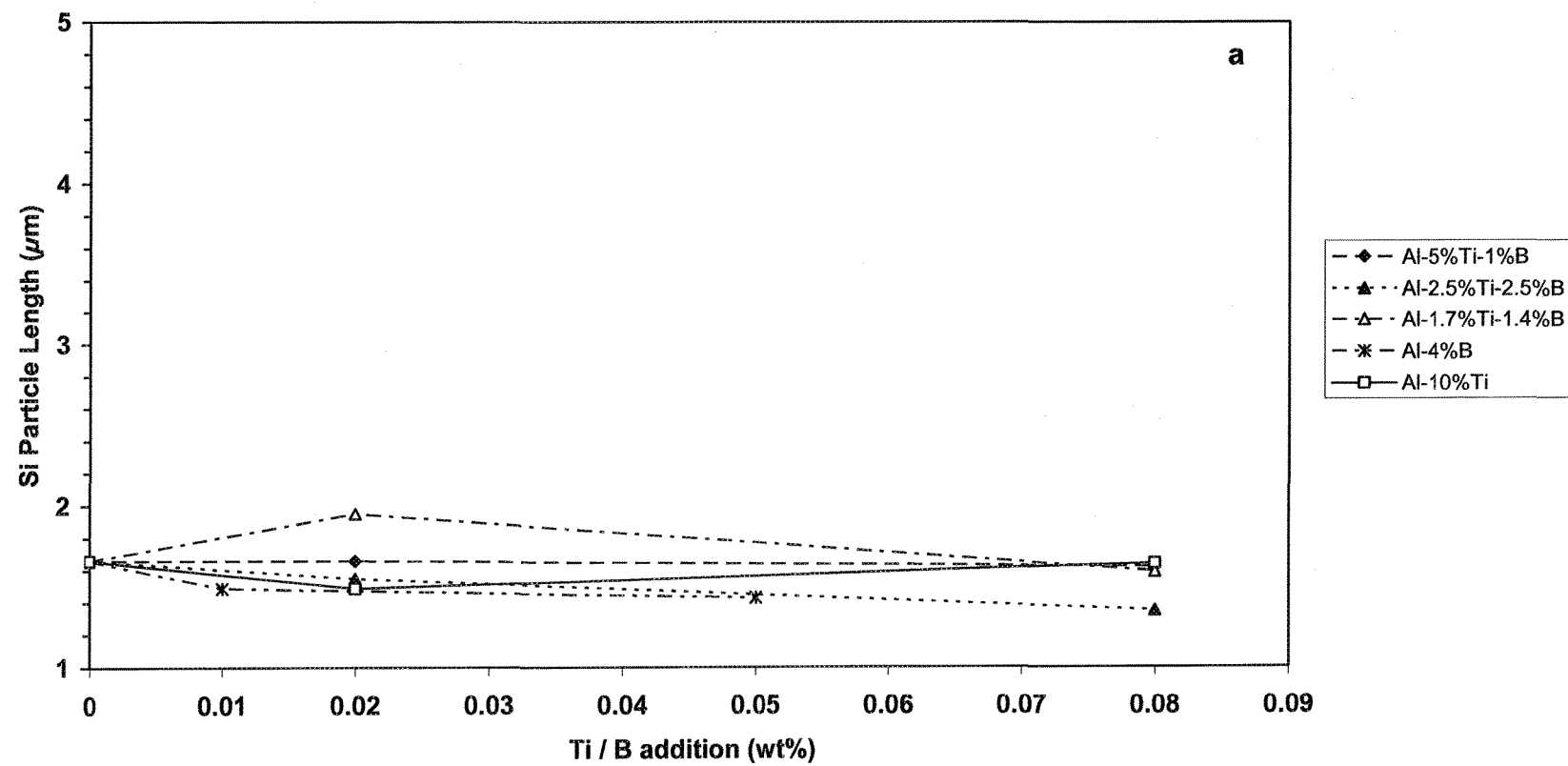
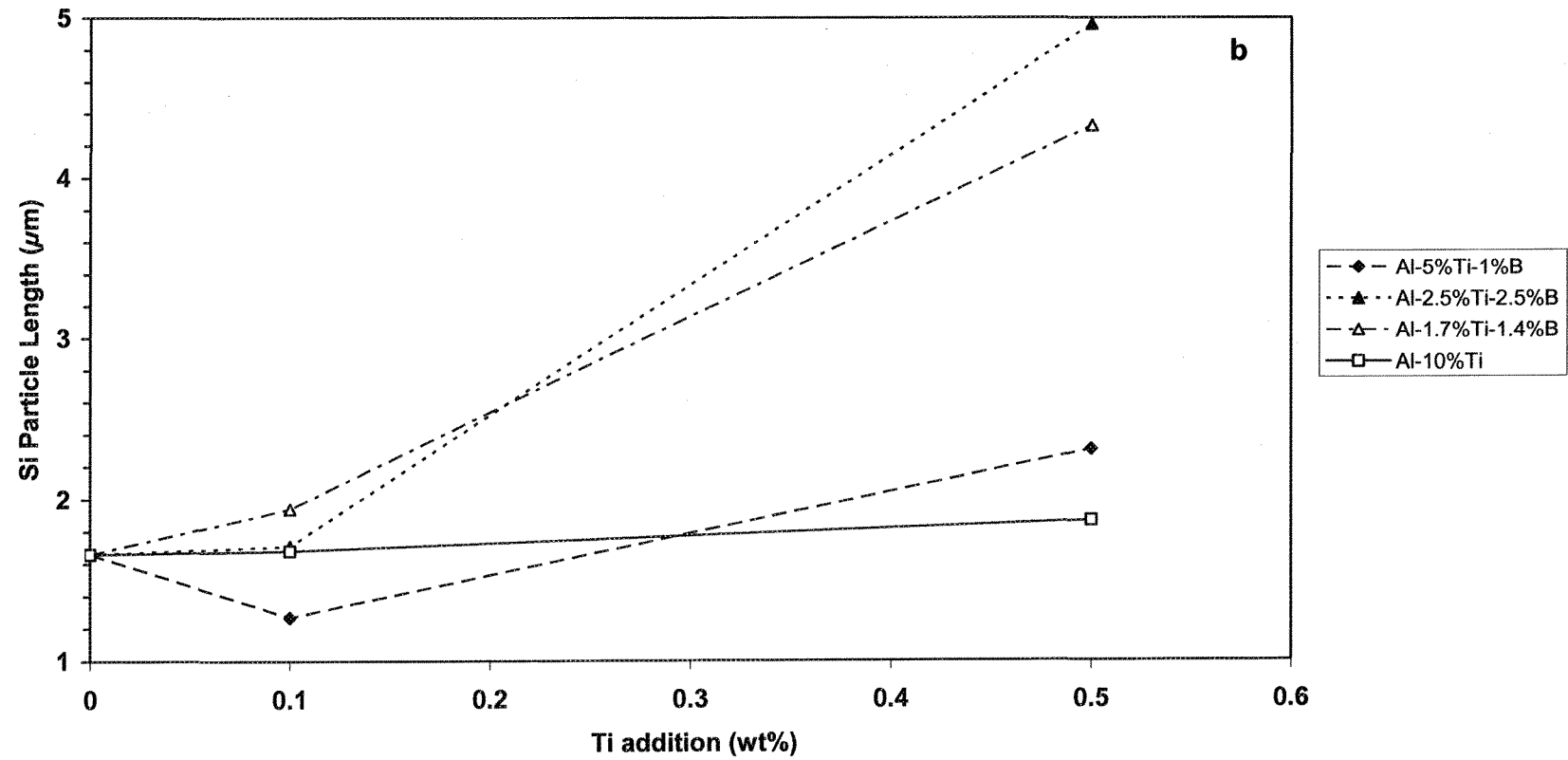


Figure 4.6 (a)



**Figure 4.6** Variation of eutectic Si particle length in 200 ppm Sr-modified as-cast A356.2 alloy grain refined with different types and amounts of master alloy: (a) lower addition levels, and (b) higher addition levels.

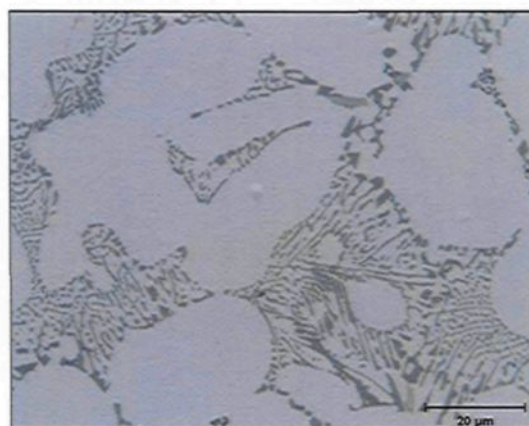
Similar observations were noted for the Al-4%B master alloy, leading to a similar conclusion regarding the Sr-B interaction for boron levels of up to 0.05%. The Al-5%Ti-1%B master alloy behaves in the same manner as Al-10 %Ti and Al-4%B, in that no interaction between Sr and B occurs up to 0.1% B-content. However, Al-2.5%Ti-2.5%B and Al-1.7%Ti-1.4%B appear to behave differently, a fact which may be related to the higher B-to-Ti ratios in these master alloys, *i.e.* the presence of higher B levels for the same Ti additions.

Figure 4.6 (b) shows that the average Si-particle length increases for additions beyond 0.1%Ti in the case of the master alloys Al-2.5%Ti-2.5%B and Al-1.7%Ti-1.4%B, implying that a certain boron level, over 0.1%, must be attained for the Sr-B interaction to take place and to affect the modification of the silicon particles adversely. Thus, with a boron-content in excess of 0.1%, the interaction of Sr and B results in a considerable decrease in the effective Sr and B levels in the melt; Figures 4.5 (d) and (f), and Figure 4.6 (b) show the corresponding consequences observed as the demodification of Si particles.

The adverse effect which occurs in the modification of the silicon particles was demonstrated by experimental observation of strontium boride with a 3:4 atomic ratio of Sr to B.<sup>23</sup> In this regard, other factors such as diffusion, solidification rate, the effect of other alloying elements, and local segregation effects may also be expected to influence the Sr-B interaction.

### 4.1.3 ADDITION OF 30 ppm STRONTIUM

The addition of Sr at levels as low as 30 ppm is insufficient for complete modification to be obtained. The undermodified structure comprises areas of fibrous and lamellar eutectic Si. Figure 4.7Error! Reference source not found. shows the as-cast microstructure of the 30 ppm Sr-modified sample, without the addition of any grain refiner. In comparison with the microstructure shown in Figure 4.1, the principal difference to be observed is the lamellar form of the eutectic silicon in certain areas, implying that the partial modification of eutectic silicon particles is due to an insufficient addition of strontium. This difference, however, is not clearly apparent as a result of the high cooling rate caused by casting in a metallic mold.



**Figure 4.7** Optical micrograph showing the microstructure of as-cast A356.2 alloy modified by addition of 30 ppm Sr.

Observation of the microstructures shown in Figure 4.8 (a) and (b) reveals that in the A356.2 alloy with low levels of Sr addition, the same conclusion may be drawn as in the case of high addition levels of this element; specifically, that titanium and strontium do



not interact with each other to weaken Si modification, instead, a certain amount of refining in Si particles may be observed and can be attributed to Ti. When comparing microstructures illustrating the addition of Al-4%B for low levels of Sr addition, as shown in Figures 4.8 (c) and (d), some coarsening in Si particles may be observed, causing the modification level to appear less than the one shown in Figure 4.7; as a result, the threshold of boron-content for demodification may occur earlier. A comparison of Figure 4.8 (c) and Figure 4.4 (c) provides a certain amount of evidence for this conclusion.

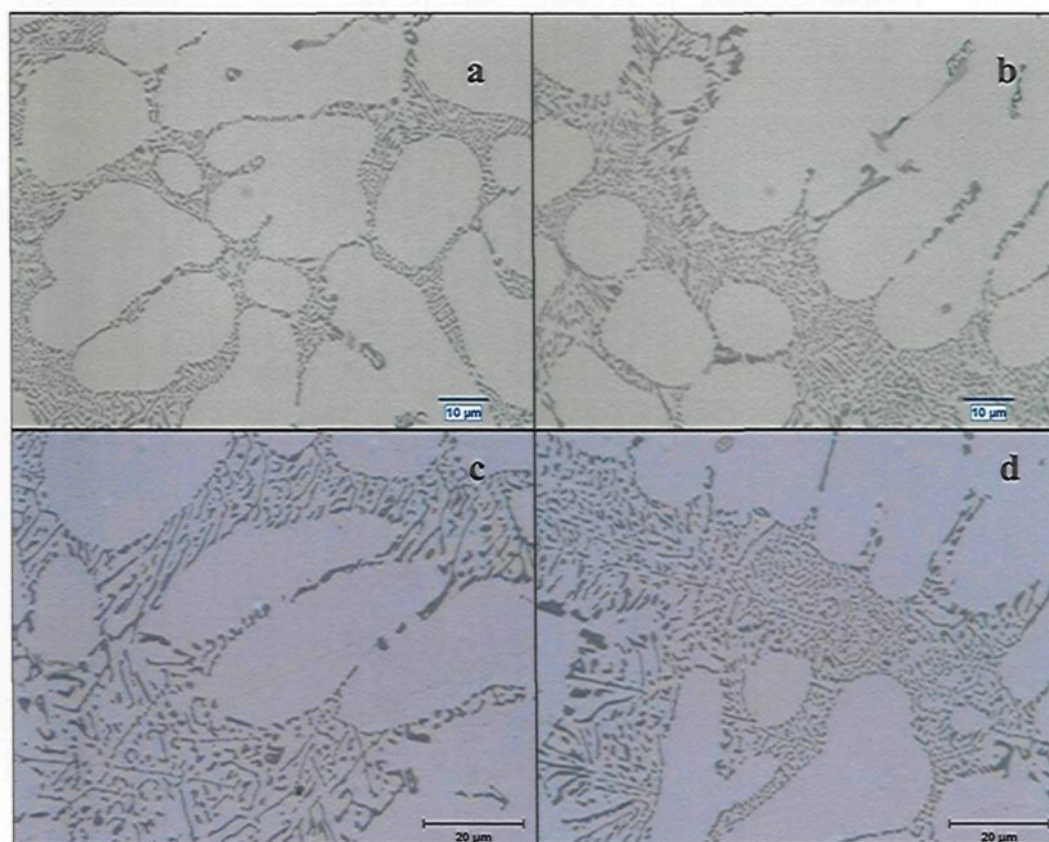


**Figure 4.8** Optical micrographs of the microstructures of 30 ppm Sr-modified as-cast A356.2 alloy refined using addition of Al-10%Ti and Al-4%B, (a) 0.1%Ti, (b) 0.5% Ti, (c) 0.01% B, and (d) 0.05% B.



Figures 4.9 (a) to (f) also illustrate the microstructures of the 30 ppm Sr-modified A356.2 alloy refined by three types of Al-Ti-B master alloys at two levels of Ti addition: 0.1% and 0.5% Ti. Only in Figures 4.9 (d) and (f) does the amount of boron addition exceed 0.1% B when using the master alloys Al-2.5%Ti-2.5%B and Al-1.7%Ti-1.4%B. It will be observed that the size of the silicon particles is somewhat coarser in the presence of a certain percentage of boron, *i.e.* over 0.1%. This fact is attributable to the interaction between boron and strontium, which appears to be one of the adverse effects to be observed in the length of silicon particles, regardless of the addition levels of strontium, as is shown by this study.

Table 4.2 shows the Si-particle characteristics for the 30 ppm Sr-modified samples of A356.2 alloy with different types and addition levels of grain refiner, in the as-cast condition. Figure 4.10 illustrates the variation in silicon-particle length as a function of the addition of boron in the form of four different master alloys, indicating that the potency of the Sr-B interaction causes demodification of silicon particles for any additions beyond 0.1% B. It is interesting to note that the average length of the silicon particles diminishes with boron additions of less than 0.1%, in other words, there is a possibility that boron might have a slightly modifying action on the silicon phase in the microstructure of the as-cast A356.2 alloy.

Particles classified as unmodified, as well as others which appear well-modified, may be observed in these undermodified microstructures, considering that there is a gradual change in morphology, from plate-like to fibrous, within the microstructure itself. In each one of these, it is possible to observe a number of isolated portions of partially or fully

modified silicon particles whose presence is attributable to a change in the local growth rate during the solidification process.

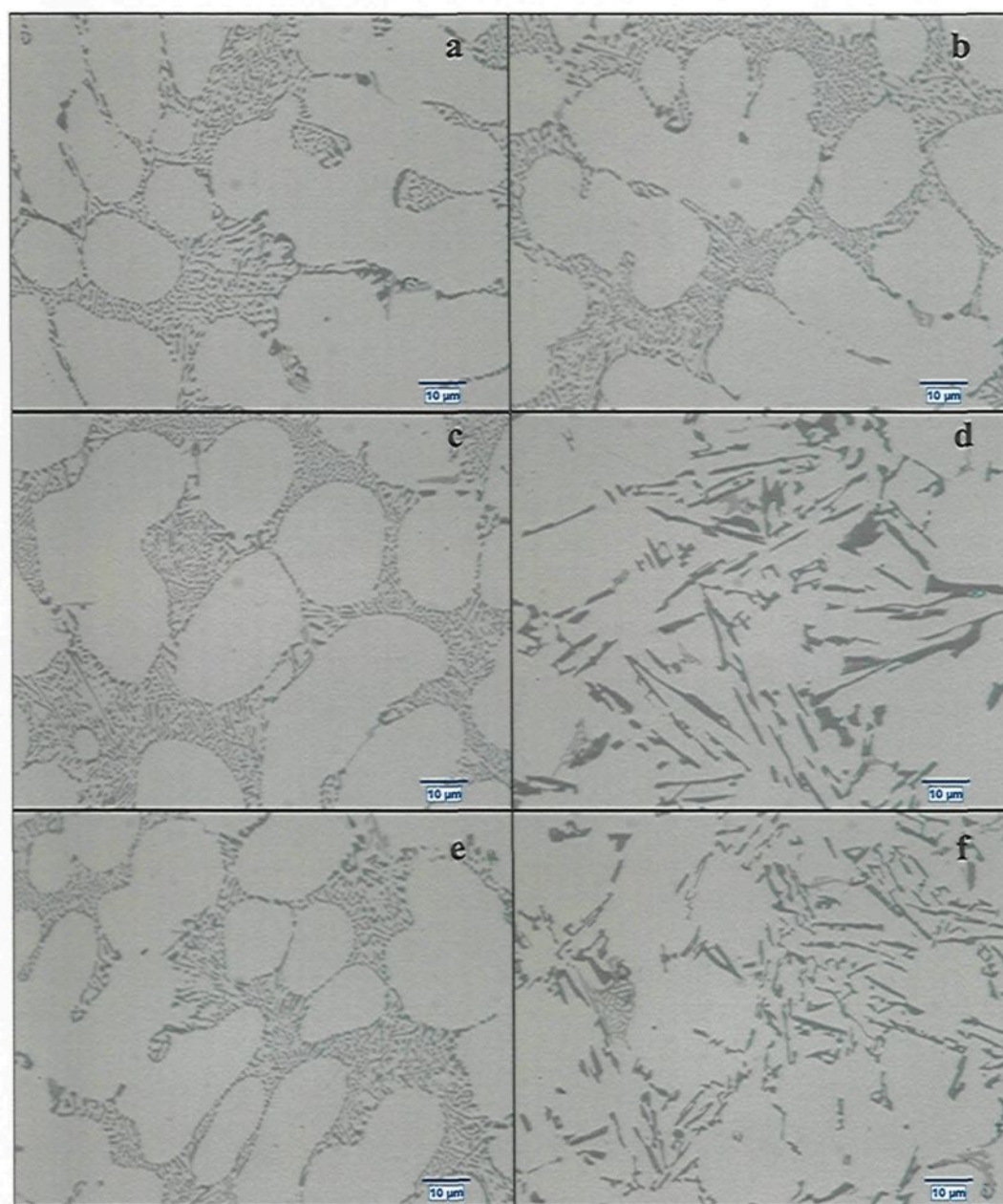


**Figure 4.9** Microstructures of the 30 ppm Sr-modified as-cast A356.2 alloy refined by addition of master alloys: (a,b) Al-5%Ti-1%B; (c,d) Al-2.5%Ti-2.5%B; (e,f) Al-1.7%Ti-1.4%B; (a,c,e) 0.1% Ti addition; (b,d,f) 0.5% Ti addition.

**Table 4.2** Particle characteristics of the 30 ppm Sr-modified as-cast A356.2 alloy.

Grain Refiner type/level		Area ( $\mu\text{m}^2$ )		Length ( $\mu\text{m}$ )		Roundness Ratio		Aspect Ratio	
		Avg.	SD	Avg.	SD	Avg.	SD	Avg.	SD
No addition		1.11	2.37	1.79	2.09	0.95	0.21	2.08	1.06
A†	0.1% Ti	0.79	1.66	1.41	1.53	0.49	0.20	1.94	0.93
	0.5% Ti	0.93	4.38	1.48	2.21	0.49	0.19	1.92	0.85
B†	0.1% Ti	1.44	4.29	2.12	2.76	0.44	0.21	2.18	1.20
	0.5% Ti	0.90	3.36	1.56	1.91	0.48	0.20	2.04	1.05
C†	0.1% Ti	0.81	3.03	1.45	1.80	0.48	0.20	1.99	0.97
	0.5% Ti	4.88	8.10	4.71	5.14	0.35	0.24	3.16	2.38
D†	0.1% Ti	0.86	2.98	1.52	2.04	0.48	0.20	2.01	1.02
	0.5% Ti	3.81	6.95	3.98	4.29	0.356	0.23	2.76	1.80
E†	0.01% B	1.00	2.15	1.65	1.83	0.48	0.20	2.03	1.06
	0.05% B	0.83	1.66	1.44	1.50	0.50	0.19	1.91	0.93

†A: Al-10%Ti, B: Al-5%Ti-1%B, C: Al-2.5%Ti-2.5%B, D: Al-1.7%Ti-1.4%B, E: Al-4%B

Thus, as shown in Table 4.2 and based on the data calculated from the 50 fields measured from the microstructures of the corresponding samples, the average parameter values may not be representative of a typical undermodified structure, principally because of the variations occurring from one field to another.

Based on the microstructural study presented here, it may be concluded that the growth mode of Si is sensitive to the amount of B available in the melt during solidification. Such a conclusion suggests that the plate-like form of silicon particles is apt to prevail when the concentration of boron exceeds 0.1 %.

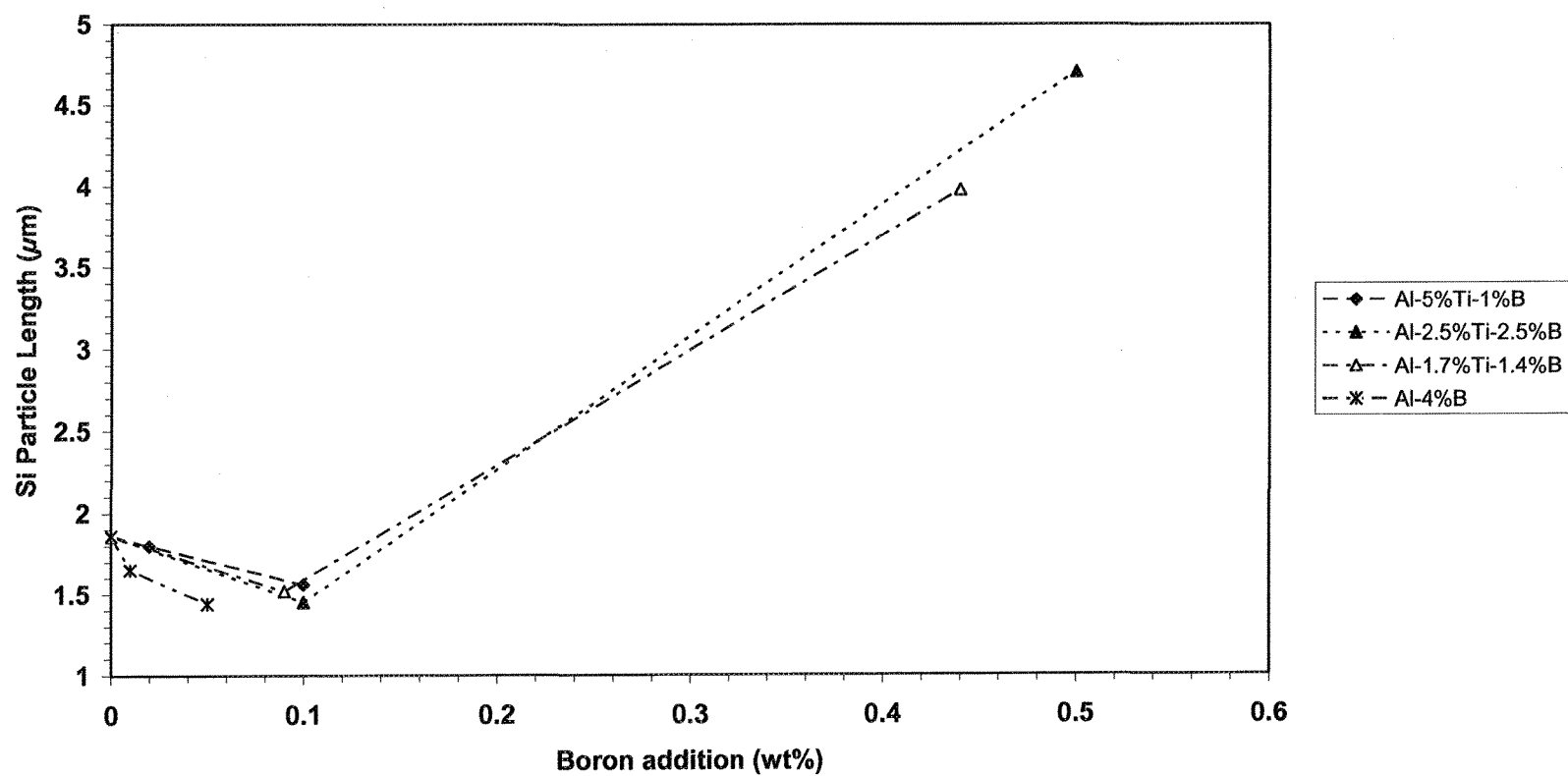


**Figure 4.10** Variation in the length of eutectic Si for the 30ppm Sr-modified as-cast A356.2 alloy samples, after grain refinement using various types and amounts of master alloys.

## 4.2 ELECTRON PROBE MICROANALYSIS

### 4.2.1 INTRODUCTION

This section will discuss the results obtained from EPMA and energy dispersive spectroscopy (EDS) analyses of the various A356.2 alloy samples discussed in the previous section. These two techniques were applied with a view to identifying the phases formed in these samples, in particular, the precipitation of Ti, Sr, B, and Mg-containing intermetallic compounds, under different conditions of grain refining and Sr additions.

### 4.2.2 UNREACTED PARTICLES

Figures 4.11 (a) and (b) show backscattered images of the 200 ppm Sr-modified A356.2 alloy, which had previously been refined using two levels of Al-10%Ti addition. When the Al-10%Ti master alloy is added to the A356.2 alloy melt, which itself contains 0.11% Ti, all the Ti atoms will react with the Al atoms in the melt to form  $\text{Al}_3\text{Ti}$  particles. The reaction may be expressed by the following equation:



The amount of master alloy added may result in raising the amount of Ti-based intermetallic compounds, particularly  $\text{Al}_3\text{Ti}$ . The situation is complicated, however, by the fact that aluminides often cluster into irregular islands. Figure 4.11(b) show a group of rodlike aluminide particles. It may clearly be seen from the images that the size of the  $\text{Al}_3\text{Ti}$  particles in these samples lies within the range of 15-50  $\mu\text{m}$ .

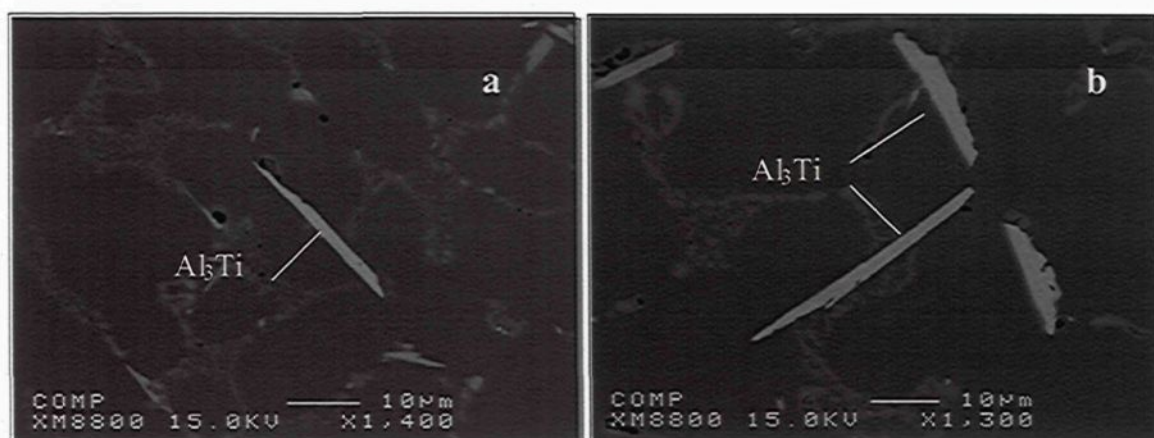


**Figure 4.11** Backscattered images of titanium aluminide particles observed in 200 ppm Sr-modified A356.2 alloy at two addition levels of Al-10%Ti: (a) 0.1% Ti, and (b) 0.5% Ti.

Figures 4.12(a) and (b) display the backscattered images obtained from an as-cast sample solidified from the A356.2 alloy melt after treatment with a combination of 200 ppm Sr and high addition levels of the Al-5%Ti-1%B master alloy (0.1% and 0.5% Ti); the clusters of extremely fine particles visible in the image are believed to be  $\text{TiB}_2$  particles. From these observations, it may be expected that agglomerates of  $\text{TiB}_2$  and other small particles cause the quality problems which arise in certain applications, for example,  $\text{TiB}_2$  particles are much harder than aluminum, and are also prone to nucleate porosity.<sup>11</sup>

### 4.2.3 INTERACTION OF GRAIN REFINER AND MODIFIER

Figure 4.133 shows a backscattered image of an as-cast A356.2 alloy sample containing 0.5% Ti and 200 ppm Sr, and the corresponding EDS analysis of the particles observed in the image. The sample contains a number of tiny bright particles, approximately 1  $\mu\text{m}$  or less in diameter which were originally believed to constitute a Sr-Ti compound, but this deduction has since been proven inaccurate.



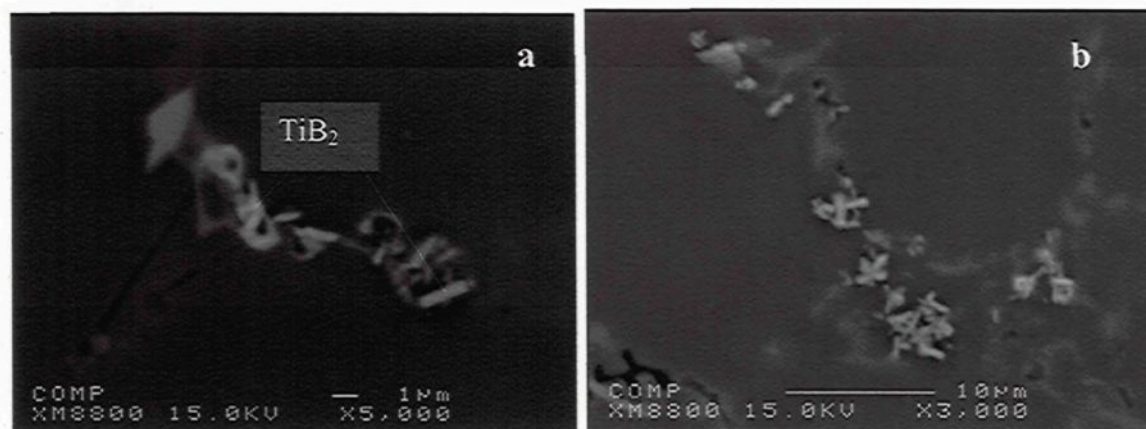


Figure 4.12 Backscattered images of  $\text{TiB}_2$  particles observed at two Al-5%Ti-1%B addition levels in A356.2 alloy: (a) 0.1% Ti, and (b) 0.5% Ti.

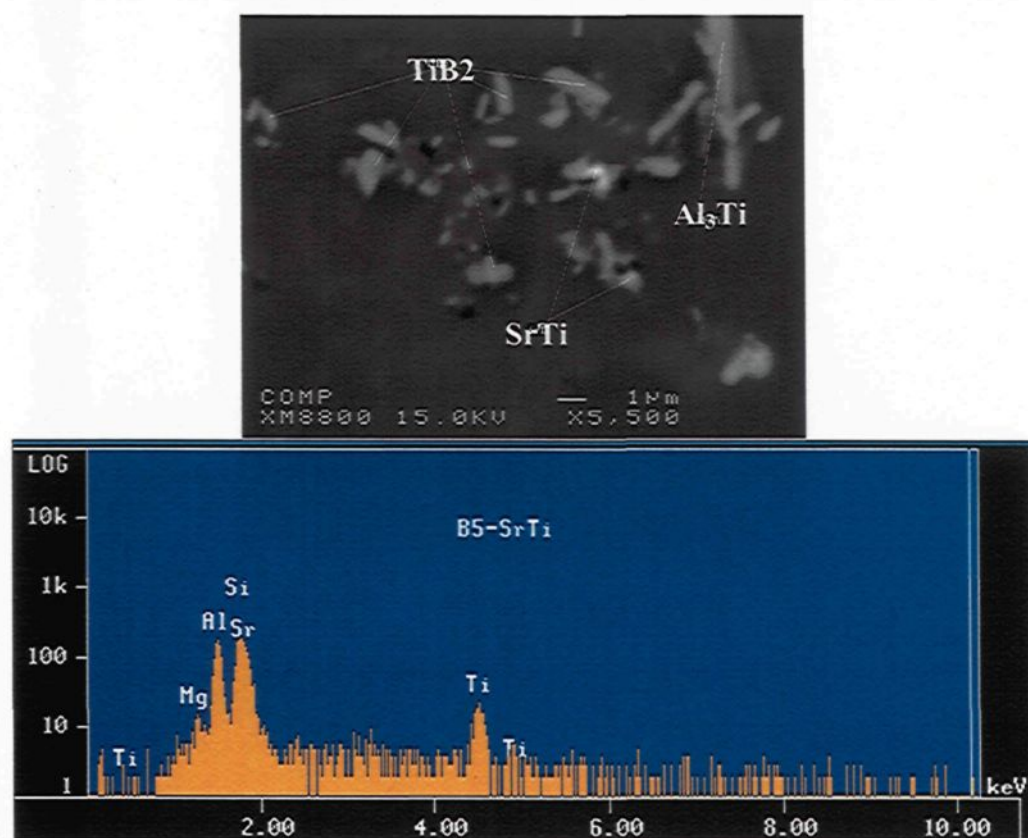
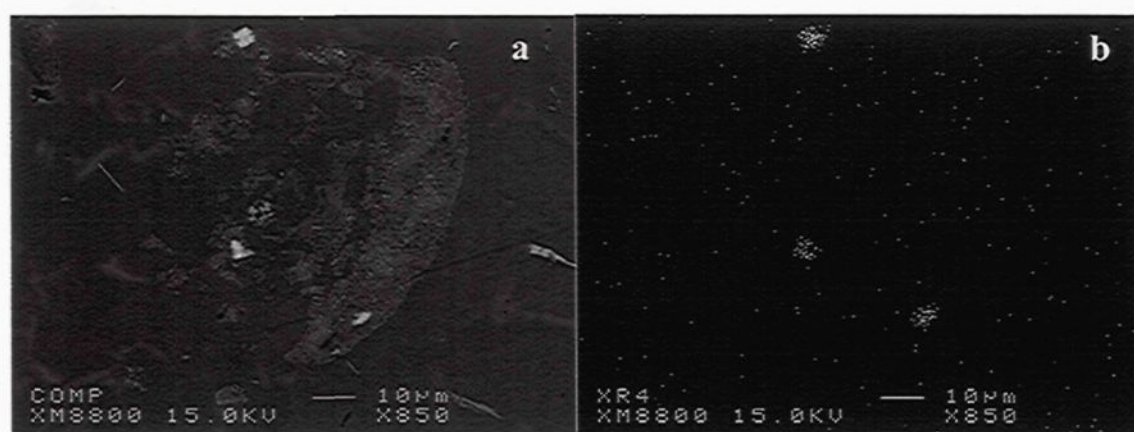


Figure 4.13 Backscattered image of different particle types observed in the sample refined with Al-5%Ti-1%B master alloy (0.5% Ti), and corresponding EDS spectrum.

In order to determine the chemical composition of these particles, an EDS analysis was conducted at 15 kV, but since the  $K\alpha$  line for silicon is very close to the  $L\alpha$  line for strontium, no conclusions may be drawn with any certainty regarding the interaction between Ti and Sr. Such particles also appear in the corresponding images of the samples which have been refined with Al-2.5%Ti-2.5%B, as shown in Figure 4.14.

Figures 4.15 (a), (b), and (c) show the backscattered image and corresponding distribution of Sr and Ti in the as-cast 200 ppm Sr-modified A356.2 alloy sample containing 0.5%Ti added in the form of Al-10%Ti master alloy. In this figure, the backscattered image (a) and the X-ray image of Ti (b) show that the tiny bright particles do not contain Ti, *i.e.* the presence of these particles is not necessarily to be interpreted as evidence for a Ti-Sr interaction. The gap in the Sr element distribution map, as shown in Figure 4.15 (c), clearly reveals that there is no diffusion between Ti and Sr atoms, or any tendency towards interaction between them.



**Figure 4.14** (a) Backscattered image of tiny, bright particles in the sample refined with Al-2.5%Ti-2.5%B master alloy (0.5% Ti), and (b) X-ray image of Sr.



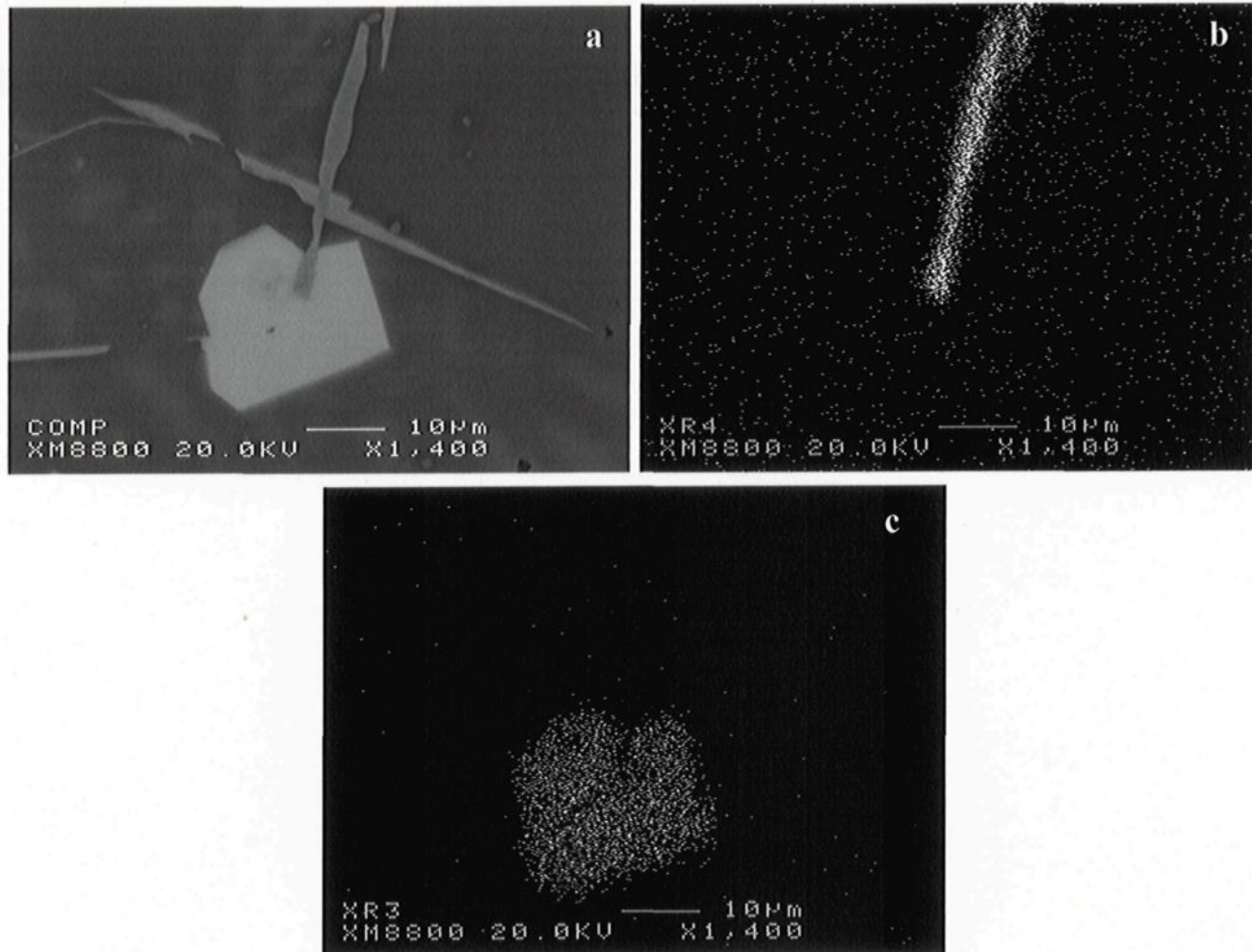
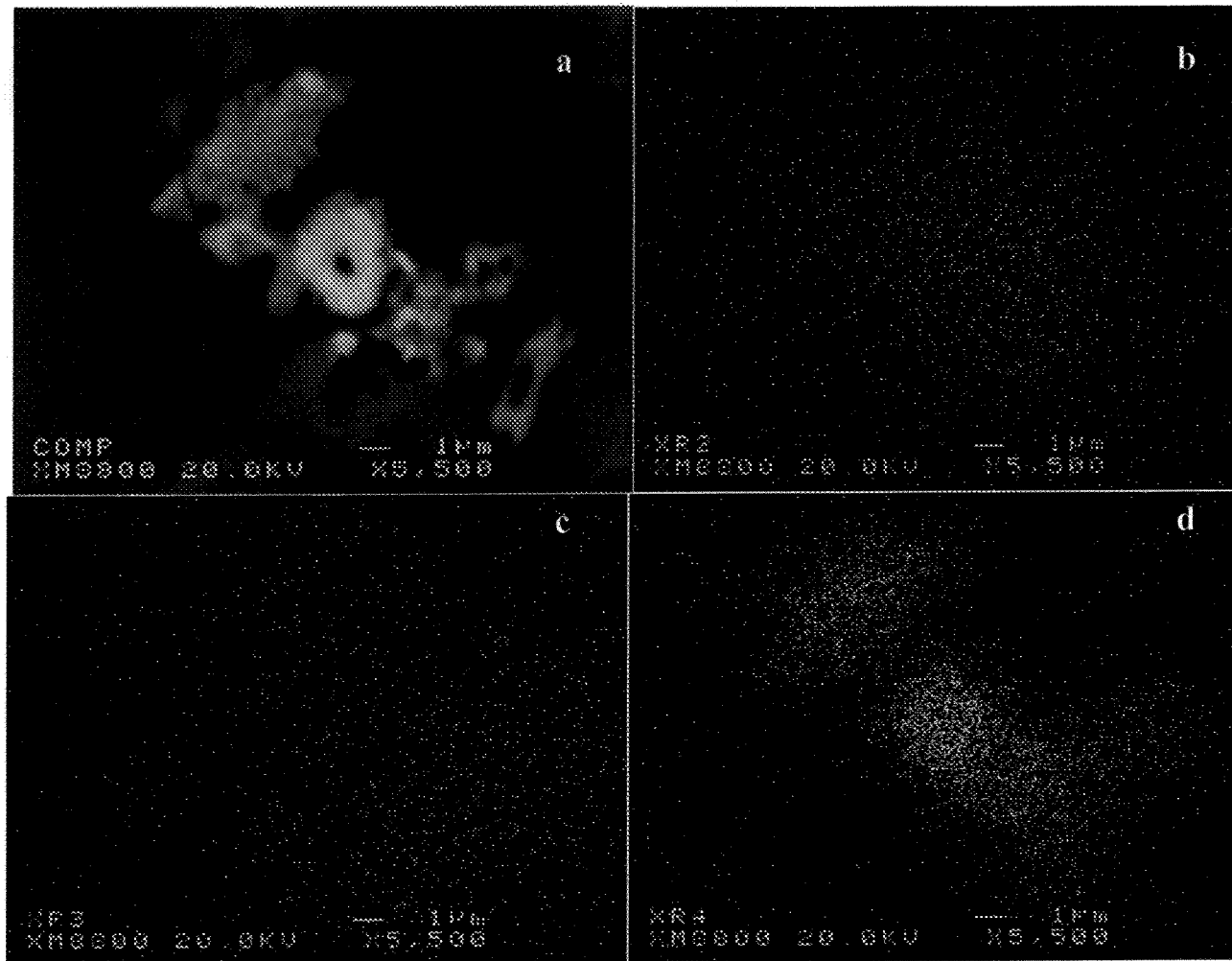


**Figure 4.15** Proximity of Al<sub>3</sub>Ti particle with Sr-rich particle in 200 ppm Sr-modified alloy refined with addition of 0.5%Ti in the form of Al-10%Ti: (a) back scattered image; (b) X-ray image of Ti distribution; and (c) X-ray image of Sr distribution.

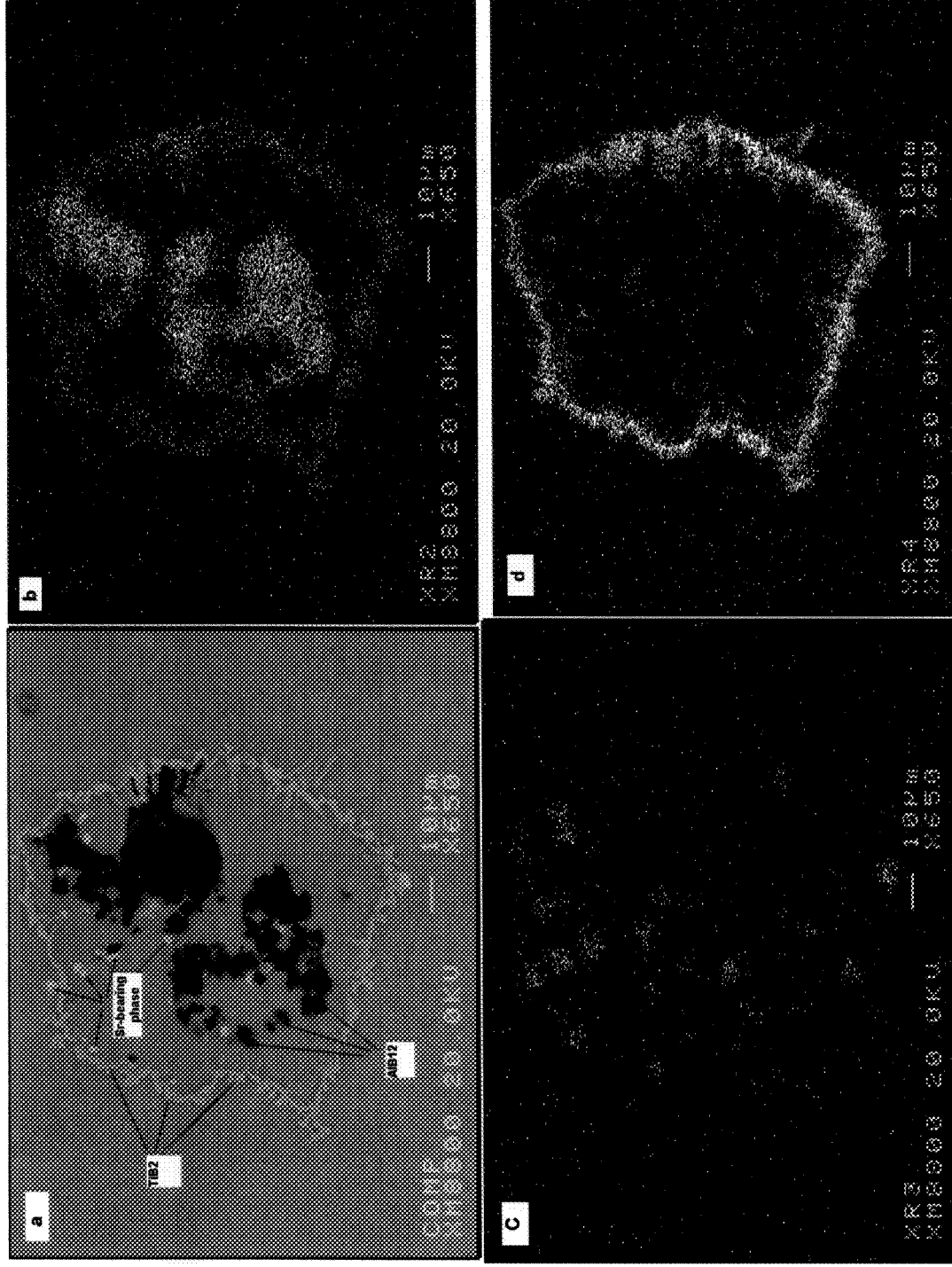
Figures 4.16 (a) to (d) illustrate the elemental distribution in the particles found in the as-cast sample of the 200 ppm Sr-modified A 356.2 alloy, grain refined with 0.01 % B added in the form of Al-4% B master alloy. A comparison of the X-ray images of Ti, B, and Sr suggests that, at low addition levels of B, there appears to be no given Sr potency which takes precedence over another for a reaction to take place with either Ti or B atoms.

Figure 4.17 (a) shows a backscattered electron image of a cluster of  $\text{AlB}_{12}$  particles surrounded by a ring of  $\text{TiB}_2$  particles; this configuration was observed with the addition of 0.05%B to the A356.2 alloy using the Al-4%B master alloy. The corresponding X-ray images for B, Sr, and Ti are provided in Figures 4.17 (b), (c), and (d), respectively. These images are presented as evidence for the greater tendency of B to react with Sr to form a Sr-B compound, as opposed to Ti.

The fact that an  $\text{AlB}_{12}$  phase may be observed is, in all likelihood, the result of the excessive amount of Al-4%B master alloy (0.05% B) present in the melt, which would tend to explain why part of this phase remains unreacted. The composition of the intermetallic compounds shown in Figure 4.17 (a) and Figure 4.18 were analyzed using wavelength dispersive spectroscopy (WDS) and the average compositions are listed in Table 4.3. An increase in the Sr-content of the alloy would thus eventually lead to the formation of the non-heat-treatable intermetallic compound  $\text{Al}_4\text{SrSi}_2$  which causes alloy embrittlement.<sup>34</sup> Electron probe microanalysis of the particles observed showed that the composition of several of them is close to  $\text{Al}_4\text{SrSi}_2$ .



**Figure 4.16** (a) Backscattered electron image showing intermetallic particles found in 200 ppm Sr-modified as-cast A356.2 alloy refined by addition of 0.01 %B using Al-4%B, and corresponding X-ray images of (b) B, (c) Sr, and (d) Ti.



**Figure 4.17** (a) Backscattered electron image showing intermetallic particles found in 200 ppm Sr-modified as-cast A356.2 alloy refined by addition of 0.05% B using Al-4%B, and corresponding X-ray images of (b) B, (c) Sr, and (d) Ti.

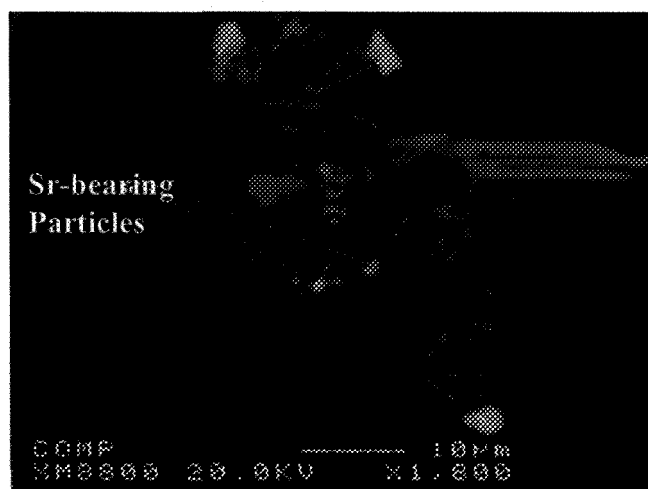


**Figure 4.18** Backscattered electron image of intermetallic particles found in the same sample as the one shown in Figure 4.17.

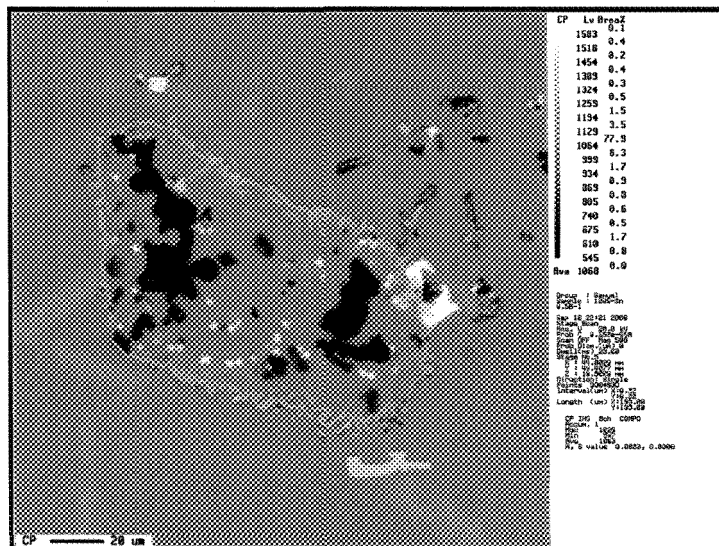
**Table 4.3** Average chemical composition of particles observed in as-cast A356.2 alloy (200 ppm Sr-modified, refined with 0.05% B using Al-4%B).

Figure Reference	Elements Present	Average (wt %)	Average (at. %)	Calculated Formula	Suggested Formula
Figure 4.18	Si	23.73	25.34	$\text{Al}_{4.5}\text{SrSi}_{2.4}$ + B	$\text{Al}_4\text{SrSi}_2$ + B
	B	4.24	12.42		
	Ti	0.68	0.40		
	Al	40.74	46.92		
	Sr	27.73	10.38		
	Mg	0.90	1.08		
	Total	98.02	96.54		
Figure 4.17	B	81.06	92.19	$\text{AlB}_{11..85}$	$\text{AlB}_{12}$
	Al	17.06	7.78		
	Total	98.16	99.97		

Figures 4.19 and 4.20 display the backscattered images with their corresponding WDS analysis of a 200 ppm as-cast Sr-modified alloy refined with the addition of 0.5% B using Al-4%B. Figure 4.19 includes some bright particles with a broad size-range, where the corresponding WDS image, shown in Figure 4.20 (c), confirms that these are Sr-rich particles. The proximity of the B-rich zones to the Sr-rich zones, and the fact that these elements co-exist in bright-particle locations, suggest that the particles contain, predominantly, B and Sr.

The WDS analysis results shown in Table 4.4 suggest further that the composition of these particles is very close to the stoichiometric value of  $\text{SrB}_6$ . This observation indicates that certain portions of the boron tend to combine with Sr, instead of with Ti. The formation of this compound consumes a large amount of Sr and B in the melts simultaneously, resulting in the reduction of freely available Sr and B for modification or refinement, respectively.

These  $\text{SrB}_6$  particles are relatively high in density,<sup>23</sup> with a theoretical density of  $3.422 \text{ g/cm}^3$ , and they are therefore expected to precipitate gradually in the melt. As a result, a Sr and B rich intermetallic compound is expected to accumulate in the bottom layer of the melt, while the concentration of solute Sr in the melt decreases to a significant extent.



**Figure 4.19** Backscattered image of a region which includes Sr-rich particles in as-cast 200 ppm Sr-modified A356.2 alloy refined with 0.5% B using Al-4%B.

**Table 4.4** Chemical composition of particles observed in Figure 4.19 as obtained from WDS analysis.

Figure Reference	Elements Present	Average (wt%)	Average (at.%)	Calculated Formula	Suggested Formula
Figure 4.19	B	48.32	87.35	SrB <sub>7</sub>	SrB <sub>6</sub>
	Al	0.12	0.09		
	Sr	55.82	12.46		
	Total	103.26	99.90		



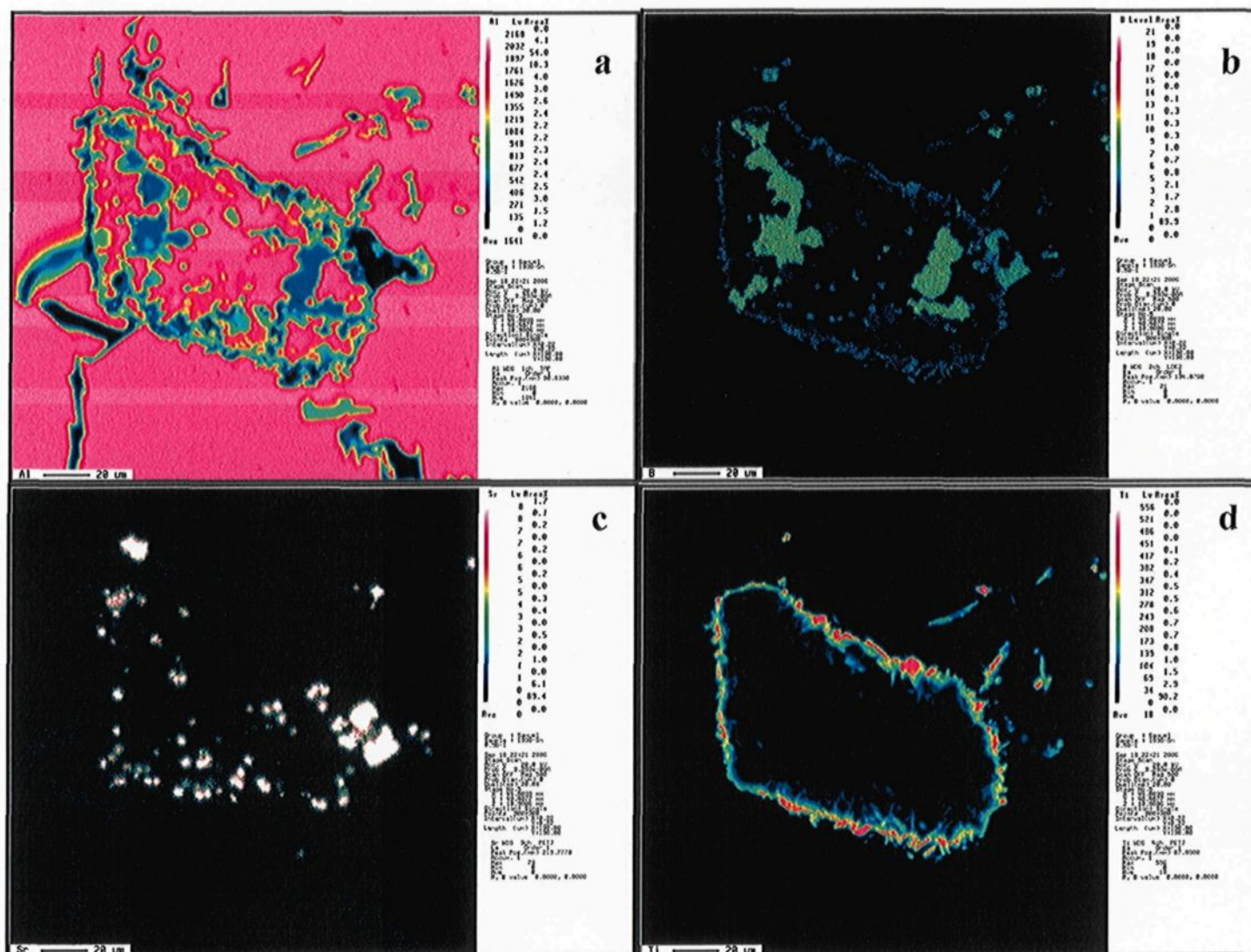


Figure 4.20 X-ray images corresponding to the backscattered image of Figure 4.19 (a) Al; (b) B; (c) Sr; and (d) Ti.



#### 4.2.4 THERMAL ANALYSIS

The general trend is that with decreasing Al-Si eutectic temperatures, the extent of Si modification increases. The principle method for determining Si-particle modification is to measure the suppression of the growth temperature of the Al-Si eutectic in the modified alloy and compare it to the same parameter in the unmodified alloy; this process is carried out by means of thermal analysis.

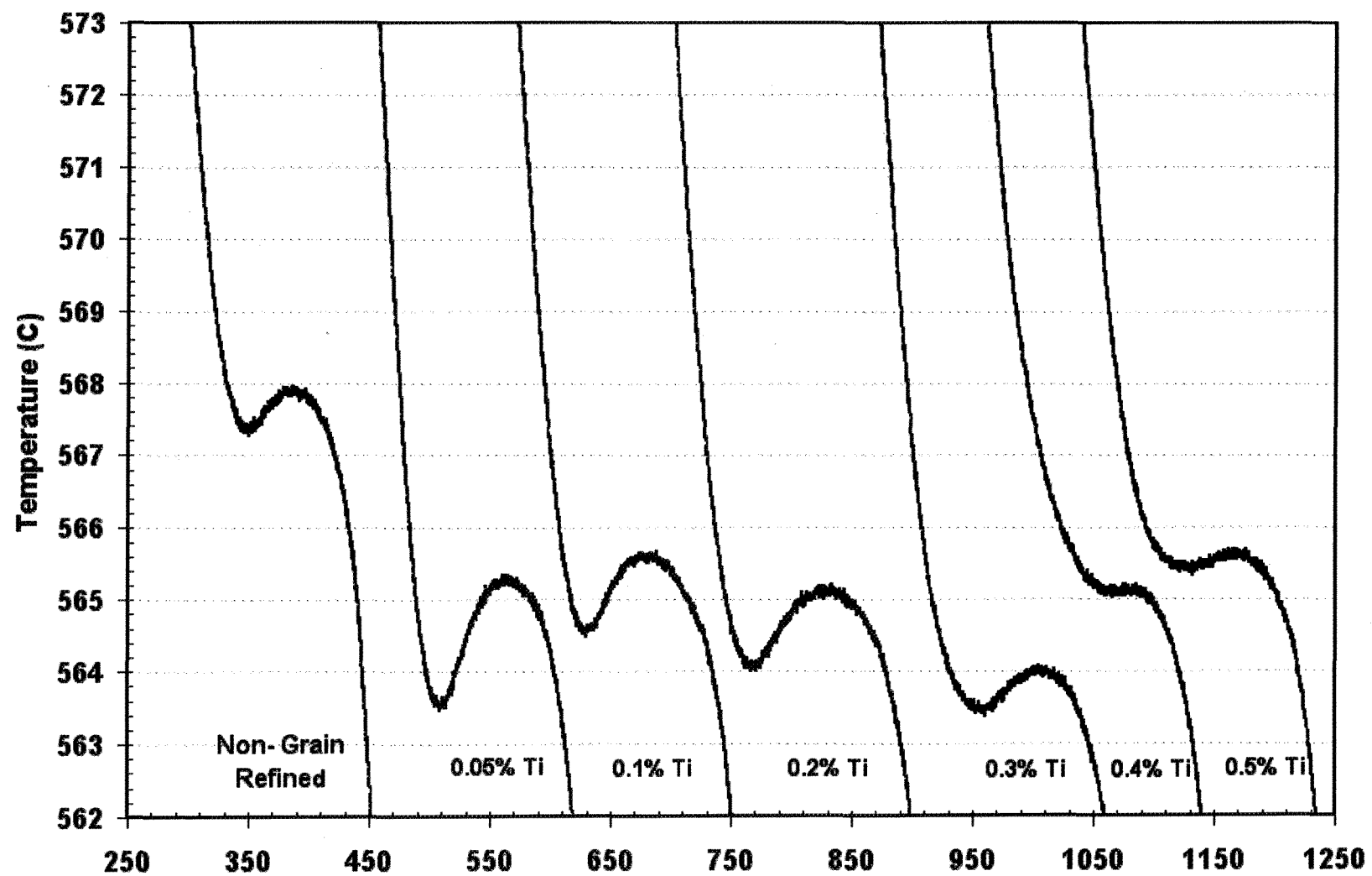
In order to evaluate interactions between Sr and B, as well as between Sr and Ti, a number of thermal analysis experiments were conducted for this study. Both the influence of boron on strontium fading and the effect of the Sr-B interaction on the eutectic silicon in the Sr-modified A356.2 alloy were investigated using the master alloy Al-4%B; whereas Al-10% Ti was used to examine Ti for the same purpose. The results are summarized in Figures 4.21 and 4.22.

Figure 4.21 illustrates that, within the range of 0.05% – 0.5% Ti used in this study, the eutectic temperature drops as Ti increases in comparison with the non-grain-refined 200 ppm Sr modified alloy, with a minimum at 0.3%Ti. The eutectic temperature thus shows signs of being affected by this range of Ti addition, implying that the presence of Ti in the melt promotes the modification of Si in this alloy.

Figure 4.22 shows a corresponding set of cooling curves for additions of boron ranging from 0.05% to 0.5%. This figure illustrates two distinct regions: one in which the eutectic temperature decreases when the boron addition is less than approximately 0.20%B; and the other in which the eutectic temperature increases rapidly, rising even beyond the

original temperature when B addition increases from approximately 0.20 to 0.50%B. It will be observed, therefore, that when the B increases, the eutectic growth temperature drops initially by almost 2°C until a 0.1%B level is attained, but when the boron is increased to higher levels, the eutectic growth temperature also increases. This behavior indicates that the interaction of Sr with B affects the modification of Si in A356.2 alloys, on condition that the amount of boron is raised by more than 0.1%.

A comparison between addition levels of B and Si modification shows that, in general, as the boron is increased to 0.1%, the degree of Si modification also increases. It is clear that the boron-content should not exceed 0.1% for Sr to modify the morphology of eutectic Si in the presence of a grain refiner. Also to be observed is the fact that the addition of boron has a slightly modifying effect on A356.2 alloys at low levels of addition. This information is consistent with the length measurements of silicon particles for low levels of Sr addition, as shown in Figure 4.10. It is important to mention that such a conclusion may only be drawn with any certainty after further experiments are carried out in greater detail while applying more highly refined measurements than were required for the purposes of this thesis.



**Figure 4.21** Cooling curves for thermal analysis of 200 ppm Sr-modified A356.2 alloy with different Ti additions using Al-10%Ti.

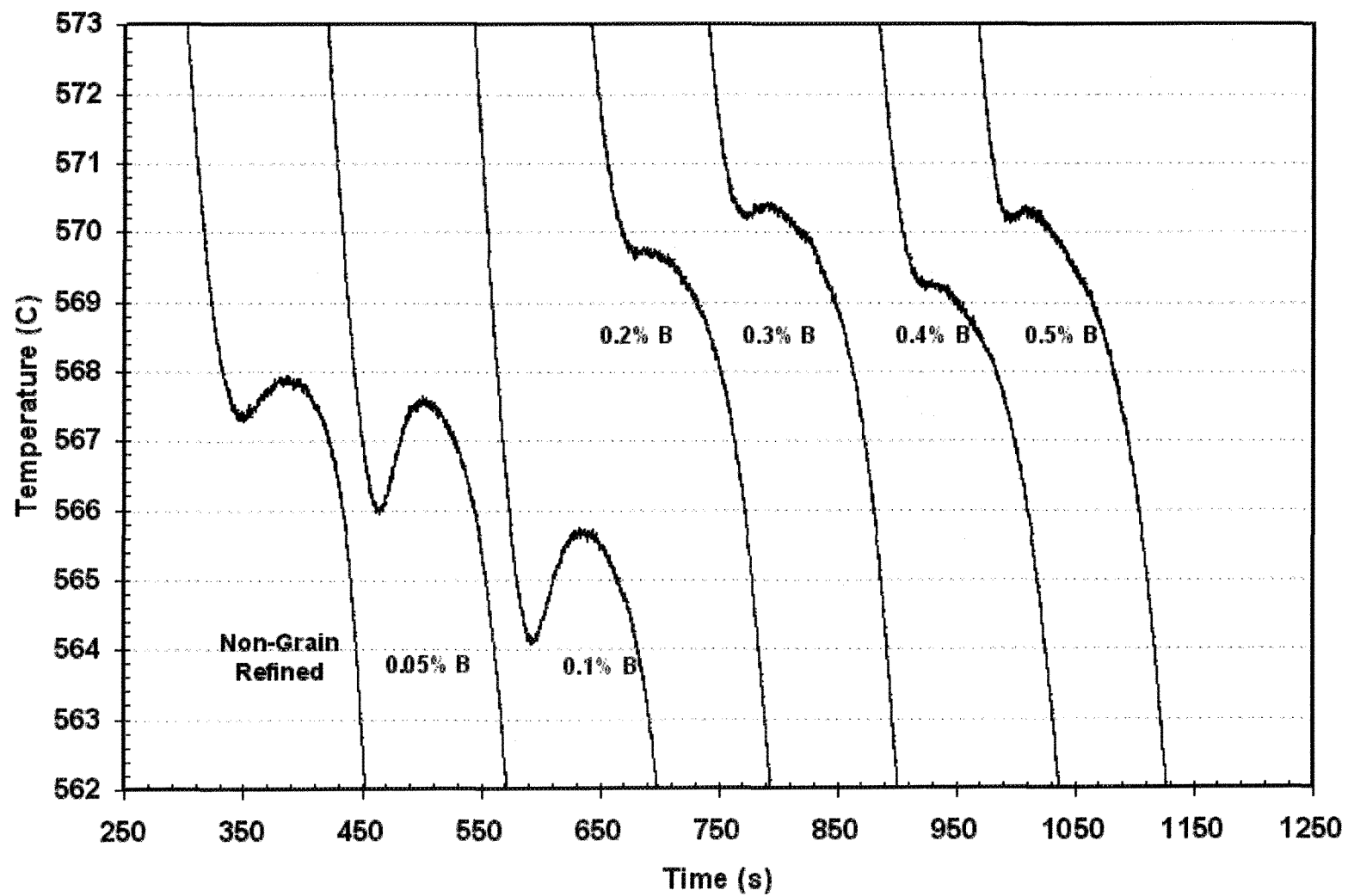


**Figure 4.22** Cooling curves for thermal analysis of 200 ppm Sr-modified A356.2 alloy with different B additions using Al-4%B.

### **4.3 CHARACTERIZATION OF MACROSTRUCTURE**

#### **4.3.1 INTRODUCTION**

The main aim of this section is to examine the influence of the potential interactions between refiners and modifiers in connection with the efficiency of the grain refining process. The following subsections will undertake to investigate the pertinent aspects of such potential interactions. For this purpose, a detailed examination was carried out with regard to the macrostructure of a number of specimens of the A356.2 alloy after they had undergone modification with strontium, and after they had been grain refined by means of different types of Al-Ti-B master alloys at various addition levels.

#### **4.3.2 EFFECTS OF ADDITION LEVEL OF GRAIN REFINERS**

In Figure 4.23, the 200 ppm Sr-modified A356.2 alloy sample without any grain refiner addition is shown in (e). The samples shown in (a) and (b) were refined using 0.1 and 0.5% Ti, respectively, added in the form of Al-10%Ti, while those shown in (c) and (d) were refined using 0.01% and 0.05% B, respectively, added in the form of Al-4%B. As will be observed from the figures, with an increase in the addition level of grain refiner, the grain structure of the A356.2 alloy becomes finer for each subsequent addition level. Satisfactory grain refinement i.e. a fine equiaxed grain structure was obtained in this alloy by the addition of 0.05% B using Al-4%B; this is supported by the fact that numerous fine  $\text{TiB}_2$  particles were formed, as is proved by the following reaction:



The influence of three different Al-Ti-B master alloys on 200 ppm Sr-modified A356.2 alloy is illustrated in Figure 4.24 (a) through (f). A large number of the fine  $\text{TiB}_2$  particles will ultimately be transformed into heterogeneous nucleation sites for liquid aluminum, as will the excess titanium atoms occurring in the form of  $\text{Al}_3\text{Ti}$ . Grain size is sufficiently fine at the high addition rates for all boron-bearing master alloys as is made abundantly clear in Figure 4.24. A critical conclusion to be drawn at this juncture is that the Al-Ti-B and Al-4%B types of master alloy have a greater influence on the grain refining of the A356.2 alloy than does Al-10%Ti, as may be observed from Figure 4.25. It is evident that the grain size of the A356.2 alloy decreases rapidly with an increase in boron-content for the lower levels of boron addition.

Lower additions of master alloy (corresponding to 0.02-0.08% Ti additions) were also made to the Sr-modified A356.2 alloy using different Al-Ti-B master alloys so as to investigate the poisoning effect of Sr on the grain refining effect of B. Figure 4.26 (a) and (b) display the macrostructures of the 200 ppm Sr-modified alloy, refined with 0.02 and 0.08% Ti, respectively, using Al-10%Ti. There appears to be no significant difference between the corresponding grain sizes for 0.02 and 0.08% Ti additions. In both cases, heterogeneity of grain size may be observed, while for higher addition levels, grain sizes show increased homogeneity. Nevertheless, the finest grain size obtained by this grain refiner is coarser, after the addition of 0.5% Ti, than any obtained using other master alloys at the same level of addition.

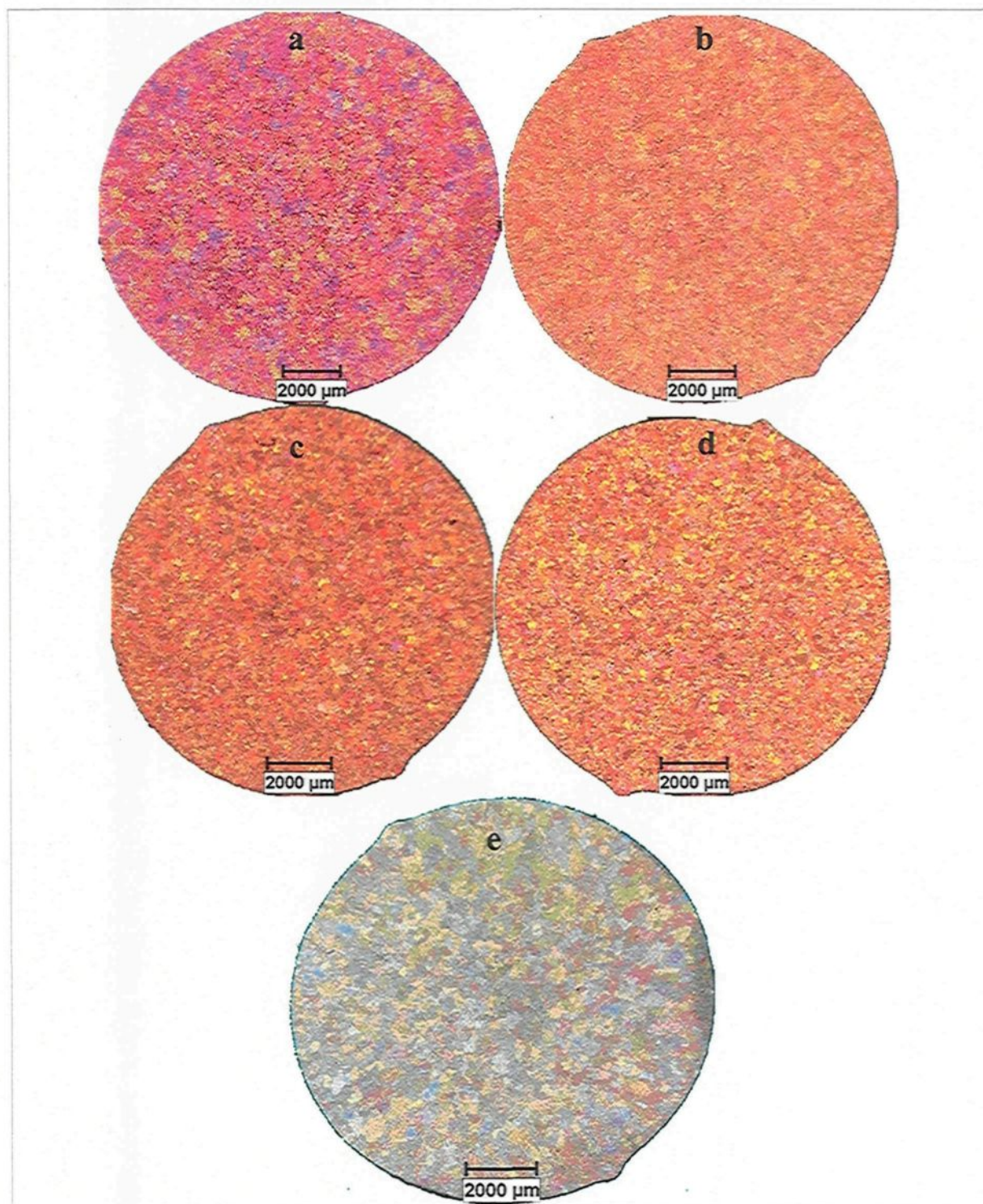


**Figure 4.23** Macrostructures of 200 ppm Sr-modified A356.2 alloy refined with: (a, b) 0.1% Ti and 0.5% Ti, using Al-10%Ti; (c, d) 0.01% B and 0.05% B, using Al-4%B; and (e) without any grain refiner addition.



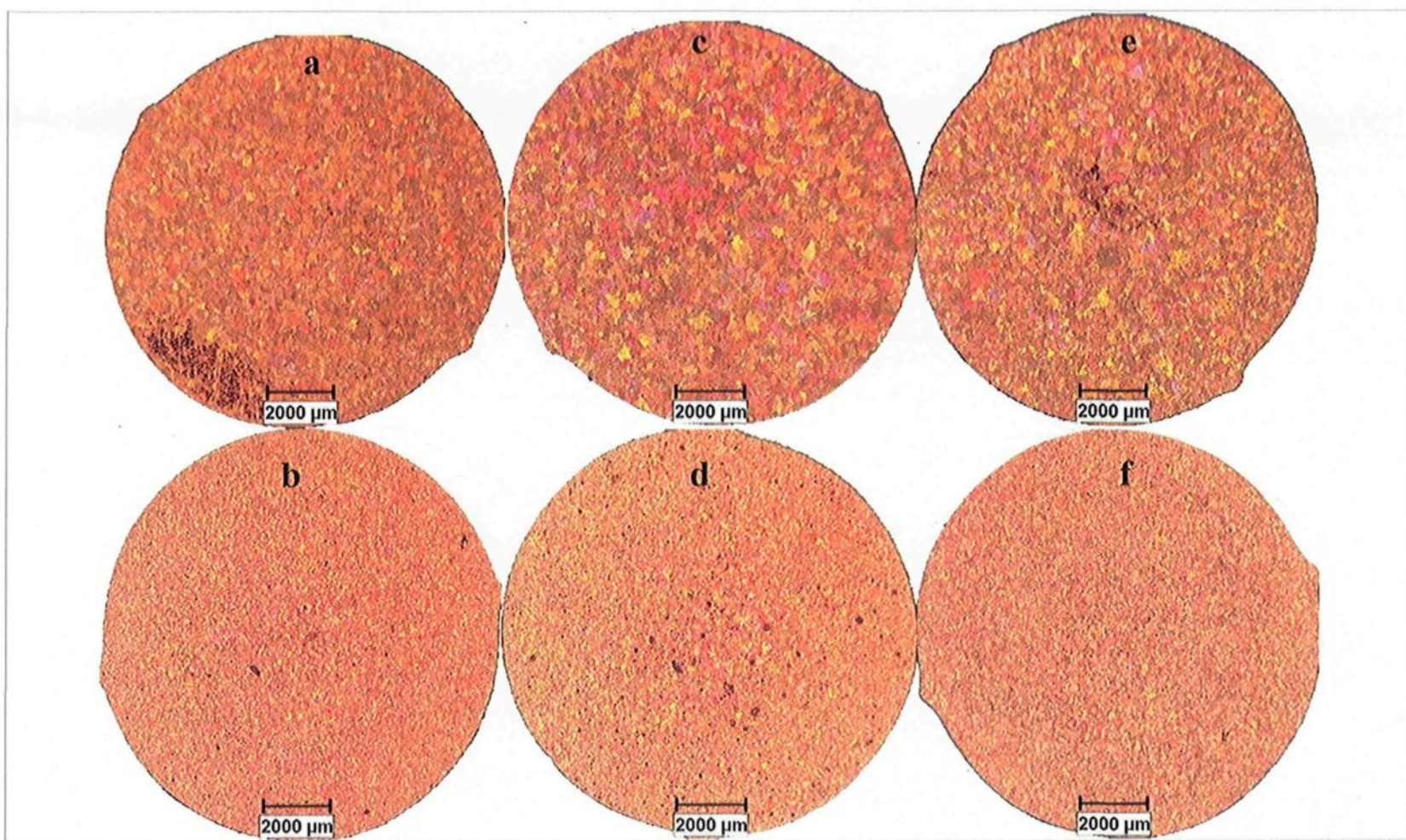


**Figure 4.24** Macrostructures of 200 ppm Sr-modified A356.2 alloy refined with: (a, b) 0.1% and 0.5% Ti, using A1-5%Ti-1%B; (c, d) 0.1% and 0.5% Ti, using A1-2.5%Ti-2.5%B; and (e, f) 0.1% and 0.5% Ti, using A1-1.7%Ti-1.4%B master alloys, respectively.



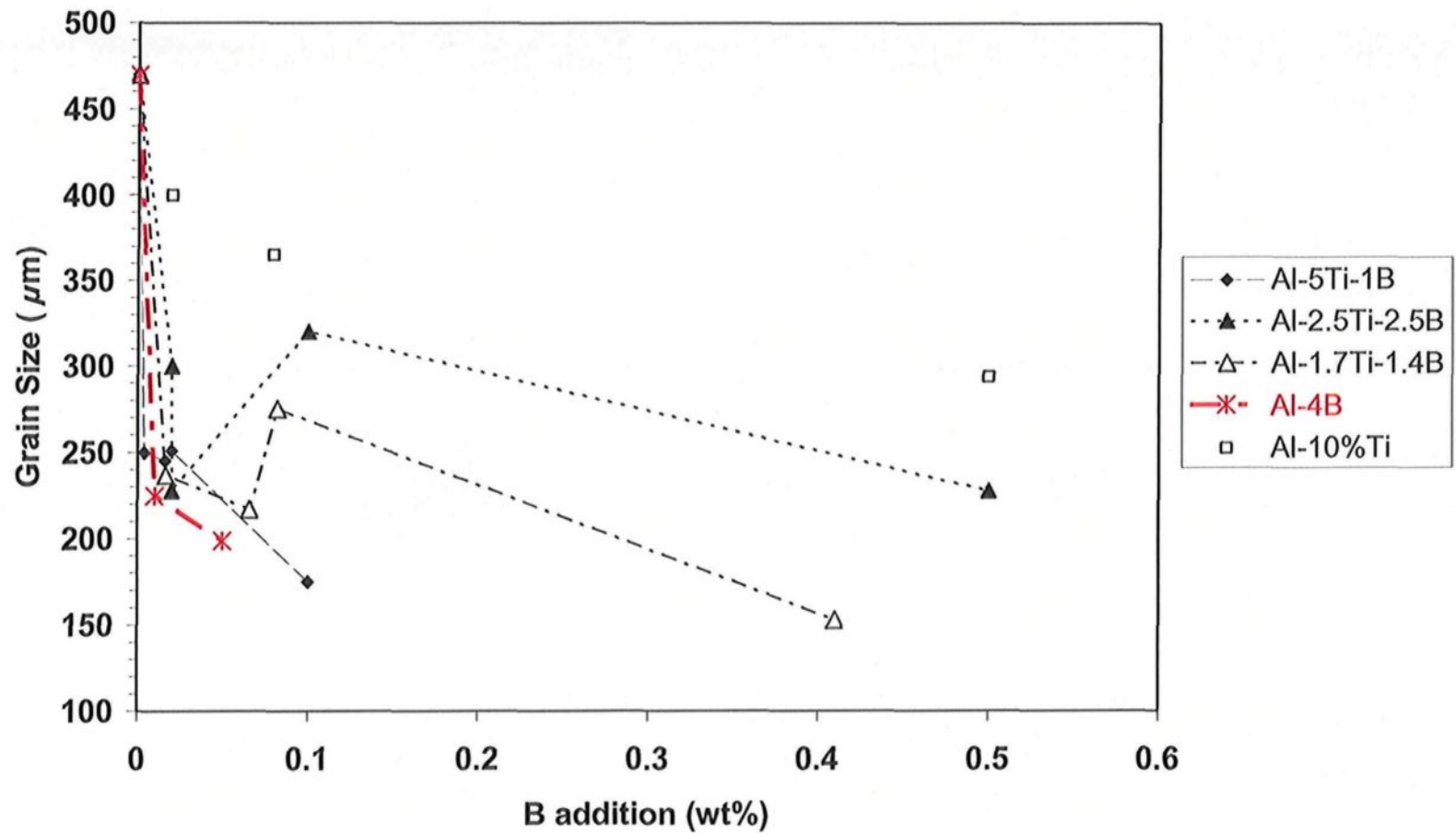


**Figure 4.25** Graph showing average measured grain sizes in 200 ppm Sr-modified A356.2 alloy as a function of boron addition levels using different grain refiners. Corresponding data for Ti additions using Al-10%Ti are also shown (see individual squares).

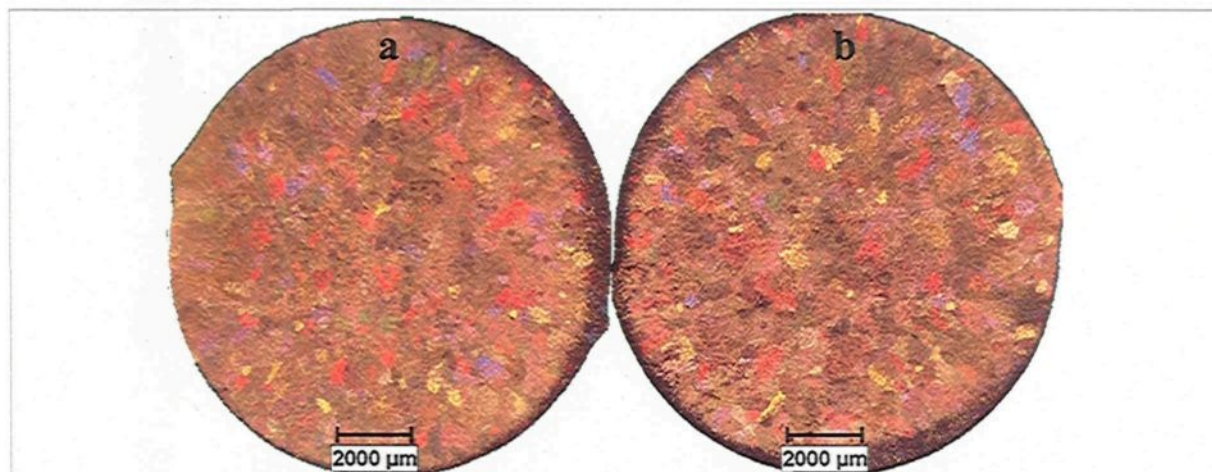


**Figure 4.26** Macrostructures of 200 ppm Sr-modified A356.2 refined with: (a) 0.02% Ti, and (b) 0.08% Ti, using Al-10%Ti master alloy.

As regards the Al-5%Ti-1%B master alloy, significant refining is achieved with the sole addition of 0.02% Ti (or 0.004% B), yet no further refining occurs with increasing additions of up to 0.1% Ti (or 0.02% B), and with an addition of 0.5% Ti (or 0.1% B) a further drop in grain size may be observed. An interesting point emerges in connection with the master alloys Al-2.5%Ti-2.5%B and Al-1.7%Ti-1.4%B when the addition level shifts from 0.08% to 0.1% B. Measurements indicate a certain amount of coarsening, or deterioration in the grain-refining effect, when the abovementioned range of boron additions is made to the 200 ppm Sr-modified 356.2 alloy using these two master alloys. The adverse effect of the Sr-B interaction may be considered for justifying this coarsening. It is interesting to note that this coarsening is not evident in the case of Al-5%Ti-1%B compared to the other Al-Ti-B master alloys, as shown in Figure 4.25. This figure also shows that when the boron content is further increased to over 0.1%B, the refining recommences, which may be attributed to the increased number of  $\text{TiB}_2$  and  $\text{Al}_3\text{Ti}$  particles made available due to the higher addition, thereby restoring the grain-refining effect.

As Figure 4.27 shows, the samples which have received a 0.02% Ti addition in the form of Al-Ti-B master alloys display a high degree of grain refinement, although it is preferable to add at least 0.1% Ti in order to obtain improved homogeneity of grain size. The improved grain refining response of the A356.2 alloy at a higher addition level of grain refiner would, in all likelihood, be a result of the availability of a number of aluminide and boride particles which retain their potency for heterogeneous nucleation. Also, an interaction between Sr and B might be responsible for the coarsening effect because of a decrease in the amount of boron available, thereby leading to a drop in  $\text{TiB}_2$  formation. Such a situation would result in the creation of fewer potent nucleating sites causing a tendency towards unsatisfactory grain refining. The evidence presented here confirms the importance of the addition of 0.1% B as the initiating point for this type of interaction when using the master alloys Al-2.5%Ti-2.5%B and Al-1.7%Ti-1.4%B.



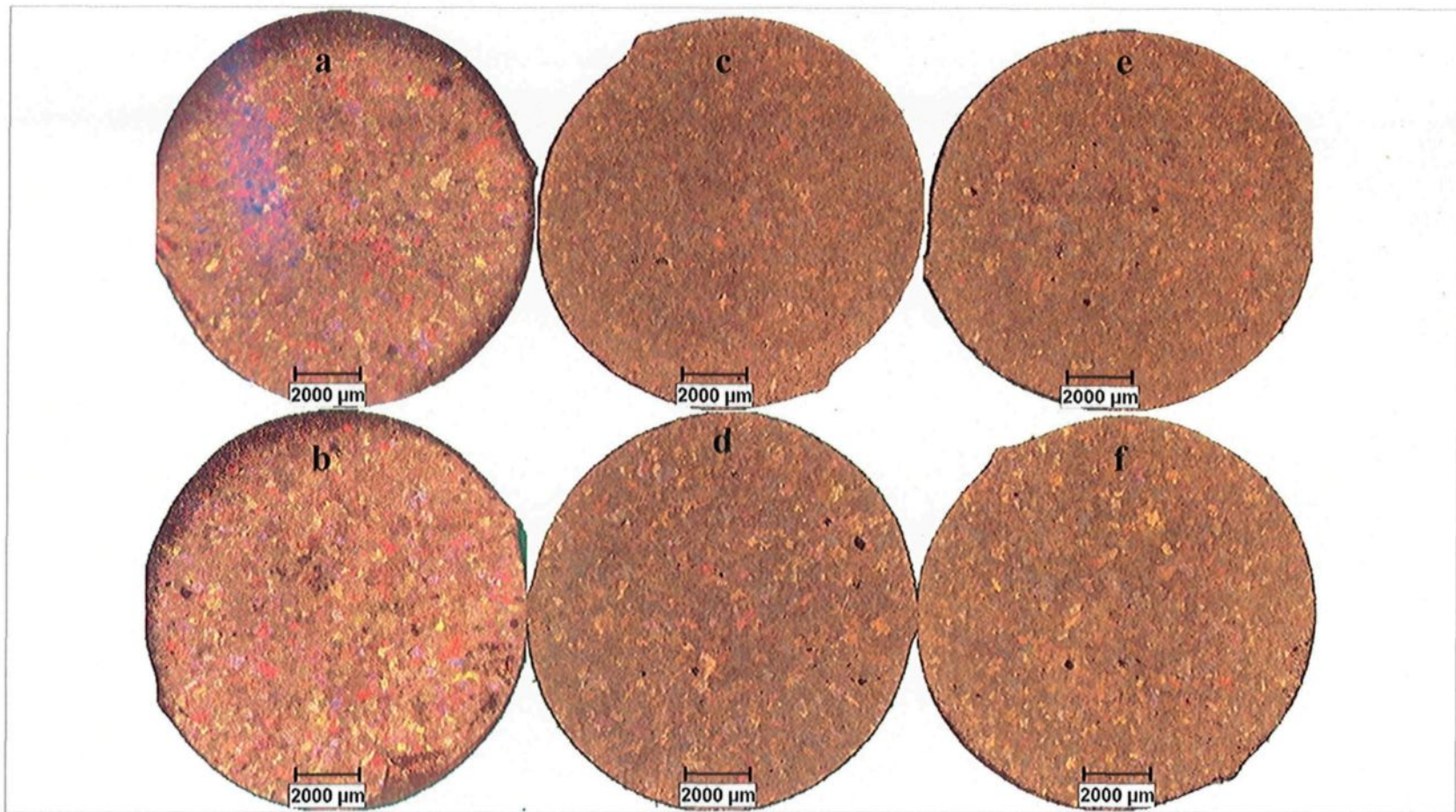


**Figure 4.27** Macrostructures of 200 ppm Sr-modified A356.2 refined with: (a, b) 0.02% and 0.08% Ti, using A1-5%Ti-1%B; (c, d) 0.02% and 0.08% Ti, using A1-2.5%Ti-2.5%B; and (e, f) 0.02% and 0.08% Ti, using A1-1.7%Ti-1.4%B master alloys, respectively.

### 4.3.3 EFFECTS OF ADDING LOWER LEVELS OF MODIFIER

The undermodified structure of the A356.2 alloy was examined at this stage, after the addition of 30 ppm Sr, in order to investigate its effect on the grain-refining efficiency of different master alloys. In Figure 4.28, the macrostructure of the 30 ppm Sr-modified A356.2 alloy sample without any grain refiner addition is shown in (e). Upon comparison with Figure 4.23 (e), the 200 ppm Sr-modified alloy seems to display the same grain size.

Figure 4.28 (a) and (b) show the macrostructures of the 30 ppm Sr-modified alloy samples refined with 0.1% and 0.5% Ti using Al-10%Ti master alloy, while those shown in (c) and (d) were refined with 0.01% and 0.05% B, respectively, using Al-4%B. A comparison of the macrostructures indicates that, in the case of the 30 ppm Sr-modified alloy, grain sizes at both Ti levels of 0.1 and 0.5% are finer than those in the corresponding samples obtained from the 200 ppm Sr-modified alloy, Figure 4.23 (a) and (b), although the average measurements for grain sizes indicate no significant difference. This outcome may be attributed to greater heterogeneity in grain size observed at the 200 ppm Sr-modified samples.

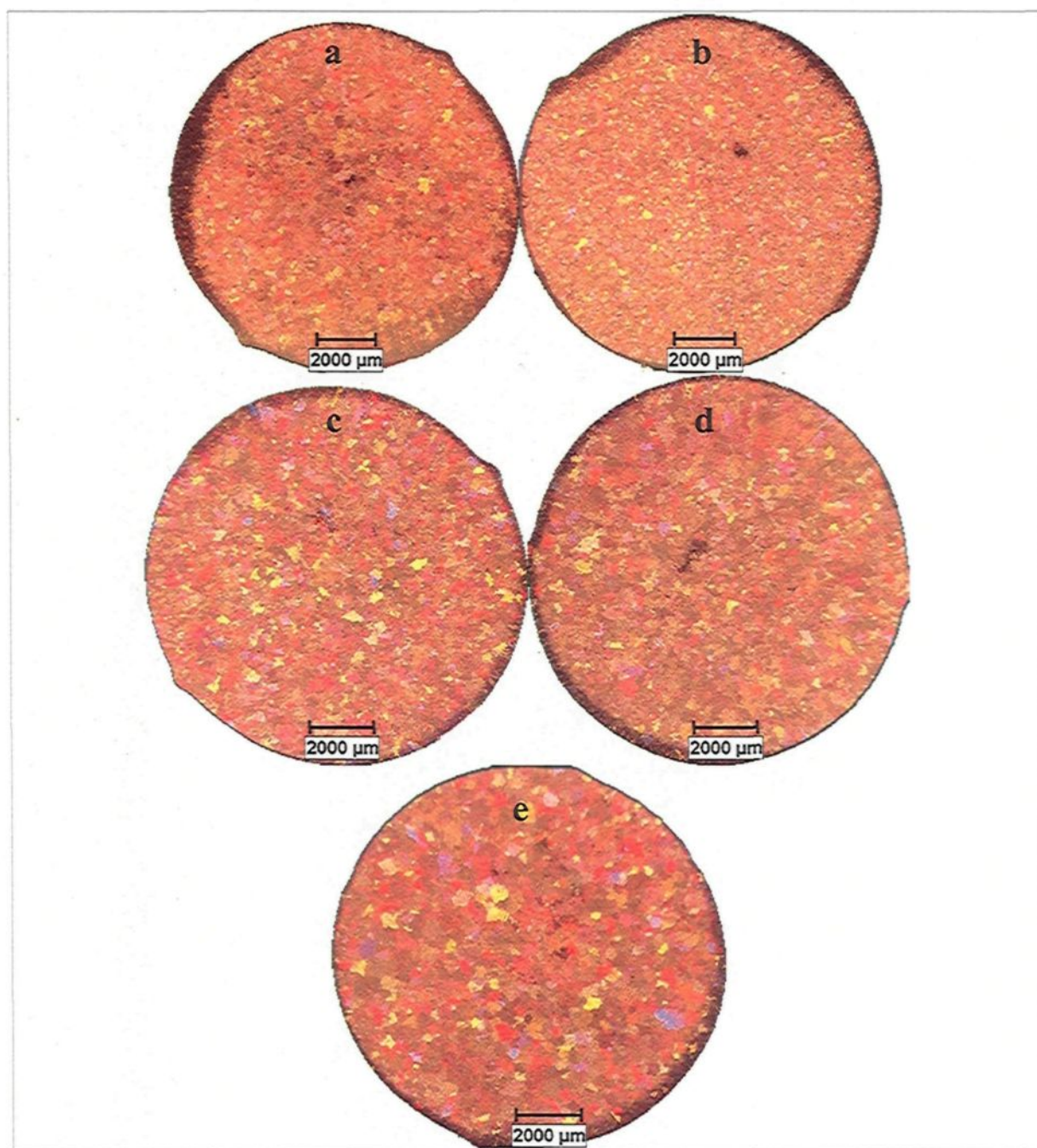
In contrast to the above, grain size appears to be coarser in the Al-4%B refined samples of the 30 ppm Sr-modified A356.2 alloy, as shown in Figure 4.28 (c) and (d), as opposed to those observed for the similarly refined samples of the 200 ppm Sr-modified alloy, Figure 4.23 (c) and (d). It would be possible to conclude that if the Sr-B interaction were known to be responsible for this coarseness, then the addition of less Sr would lead to a drop in the threshold level of boron-content required to activate the Sr-B interaction. Such

a conclusion will, indeed, be confirmed by drawing a comparison between the coarser grained 30 ppm Sr-modified 356.2 alloy samples refined with Al-5%Ti-1%B, and the corresponding 200 ppm Sr-modified counterparts, as shown in Figure 4.24 (a) and (b) and Figure 4.29 (a) and (b), respectively, where Figure 4.29 compares the influence of Al-Ti-B grain refiners on the macrostructures of the 30 ppm Sr-modified A356.2 alloy. Moreover, where the master alloys Al-2.5%Ti-2.5%B and Al-1.7%Ti-1.4%B are concerned, the same type of grain coarseness also occurs, and thus corroborates the above conclusion.

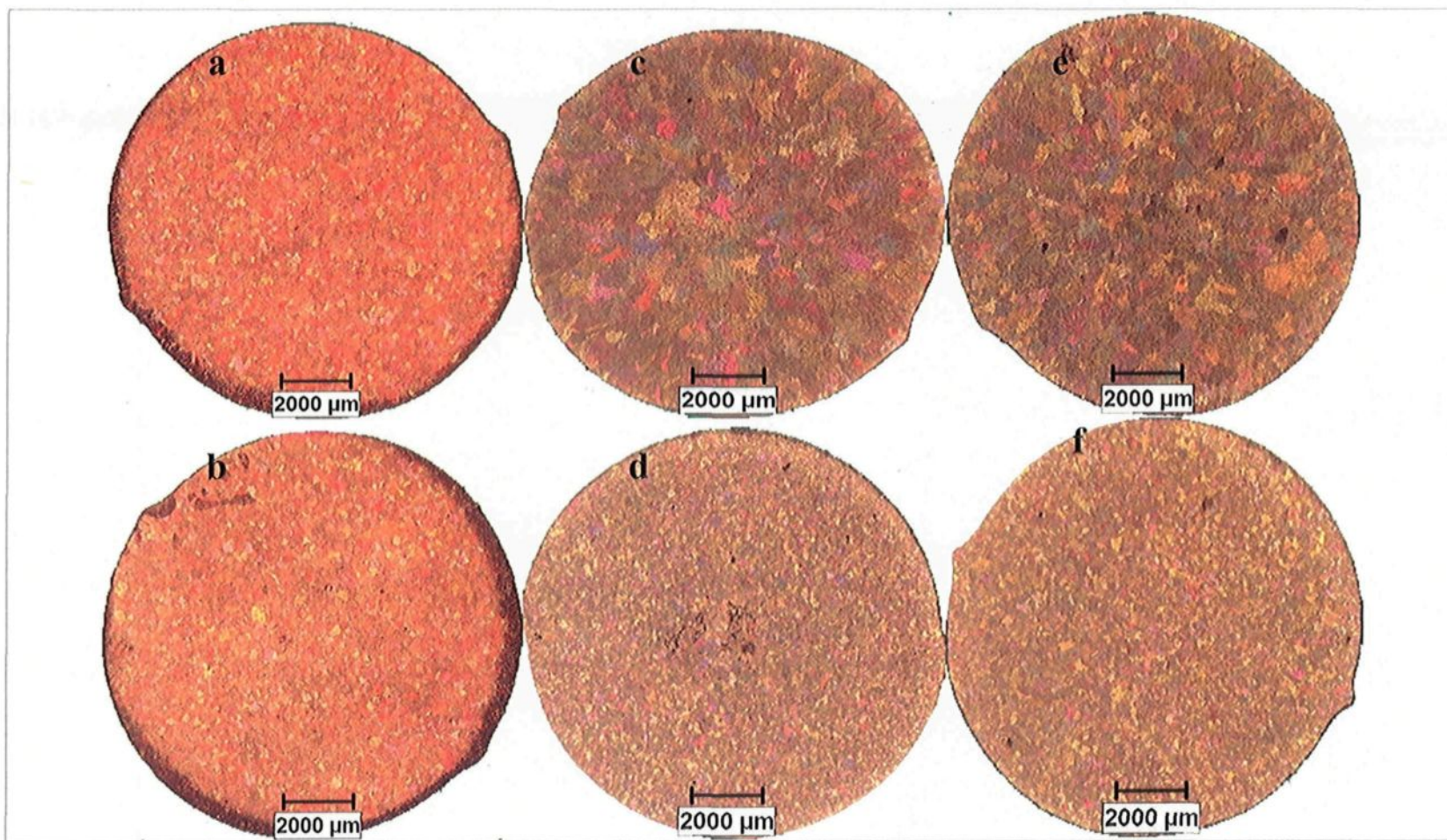
As stated in subsection 4.2, boron in the form of additions to the A356.2 alloy by means of a master alloy may result in the removal of strontium atoms from the bulk of the melt through the formation of such relevant boride particles as  $\text{SrB}_6$  as a result of the interaction of B and Sr.<sup>67</sup> The atomic ratio of the Sr and B indicates that the reaction between them will result in the exhaustion of the boron atoms necessary for grain refinement. The occurrence of this interaction represents a noticeable change in the effectiveness of added grain refiners, hence a higher level of grain refiner would be required to obtain a given grain size. The results indicate that the mean grain size of the samples should not be interpreted as adequate evidence for the fading of grain refiners due to the interaction of Sr and B; particularly if such a deduction is based on the pronounced heterogeneity of the grain size in the sample.

Figure 4.30 summarizes these results in graphic form for the 30 ppm Sr-modified A356.2 alloy samples refined using the different grain refiner types. Data for the Al-10%Ti master alloy additions are also given.





**Figure 4.28** Macrostructures of 30 ppm Sr-modified A356.2 alloy refined with: (a, b) 0.1% and 0.5% Ti, using Al-10%Ti; (c, d) 0.01% and 0.05% B, using Al-4%B; and (e) without any grain refiner addition.



**Figure 4.29** Macrostructures of 30 ppm Sr-modified A356.2 alloy refined with: (a, b) 0.1% and 0.5% Ti, using Al-5%Ti-1%B; (c, d) 0.1% and 0.5% Ti, using Al-2.5%Ti-2.5%B; and (e, f) 0.1% and 0.5% Ti, using Al-1.7%Ti-1.4%B master alloys, respectively.



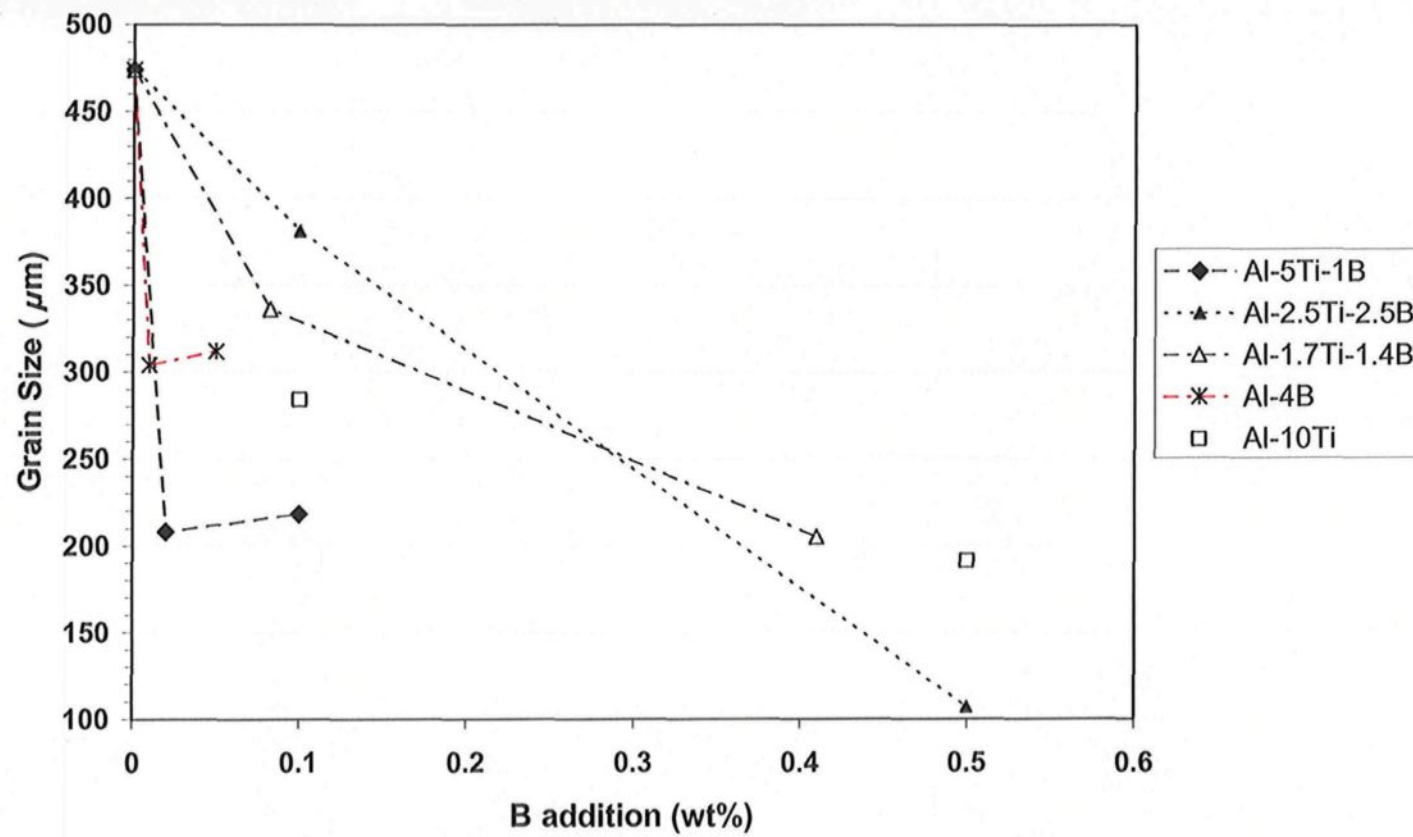


**Figure 4.30** Graph showing average grain sizes measured in 30 ppm Sr-modified A356.2 alloys as a function of boron addition level using different grain refiners. Corresponding data for Ti additions using Al-10%Ti are also shown (see individual squares).

**CHAPTER 5**

**MECHANICAL PROPERTIES**

## **CHAPTER 5**

### **MECHANICAL PROPERTIES**

#### **5.1 INTRODUCTION**

This chapter will discuss and analyze variations and interactions pertaining to the tensile properties and impact toughness values of the A356.2 casting alloy insofar as these relate to addition levels and type of master alloy used. The chapter will thus attempt to shed light on the combined effects of adding silicon modifiers and grain refiners to this alloy. Also discussed will be an approach to tempering the characteristics of eutectic silicon particles in the alloy in order to regulate its mechanical properties by means of chemical modification and T6 heat treatment after the said alloy has undergone modification.

#### **5.2 TENSILE PROPERTIES**

##### **5.2.1 AS-CAST CONDITION**

The most important parameters affecting the mechanical properties of alloy A356.2 in the as-cast condition are silicon particle morphology, intermetallics, inclusions, and porosity. Large, acicular silicon particles will tend to crack at an earlier stage of the testing, while the high cooling rate in permanent molds may lead to improved tensile properties.

Different results were obtained when the Sr-modified A356.2 alloy was refined using the various grain refiners as shown in Figure 5.1. Figure 5.1 (a) illustrates the percent elongation values for the 30 ppm Sr-modified as-cast A356.2 alloy. For all grain refiners used at this addition level of Sr, the first addition level causes an increase in elongation, whereas different consequences are brought about by further successive additions. Elongation values remain stable between Ti additions of 0.1 and 0.5% for the master alloys Al-10%Ti, Al-5%Ti-1%B, and Al-1.7%Ti-1.4%B. In the case of Al-2.5%Ti-2.5%B, the increase in elongation with the addition of 0.1%Ti, is lowered to a value below than exhibited by the non-refined sample when the grain refiner addition is increased to 0.5% Ti. In the case of Al-4%B, however, both addition levels of 0.01 and 0.05% B result in increased elongation values. Upon comparison, it is interesting to note that those samples which have been refined with Al-10%Ti and Al-5%Ti-1%B show greater ductility than those refined using the master alloys Al-1.7%Ti-1.4%B and Al-2.5%Ti-2.5%B.

In general, silicon particles in the form of coarse acicular needles act as crack initiators when there is an insufficiency of Sr in the A356.2 alloy, thereby diminishing mechanical properties, including ductility. It may be concluded from Figure 5.1 (a) that elongation increases with additions of boron to the master alloy if 0.1% is not exceeded. A decrease in the amount of Sr available for modification resulting from the interaction between strontium and boron can have an impact on the ductility of the alloy. Furthermore, supplementary additions of Ti and B may lead to the formation of a large amount of intermetallics, some of which are significant in size from the outset, or are otherwise capable of agglomerating into larger quantities. Hence, elongation of the A356.2 alloy

samples refined with Al-1.7%Ti-1.4%B and Al-2.5%Ti-2.5%B master alloys would show a certain degree of deterioration. This fact is perfectly consistent with the microstructures and X-ray images presented in Chapter 4.

Figure 5.1 (b) shows the changes in percentage elongation of the as-cast A356.2 alloy samples modified with modification with 200 ppm Sr and refined using low Ti and B additions. Except for Al-4%B, all other grain refiners show an arc-shaped variation with the Ti level for this range of additions. The best elongation at this low addition range of grain refiner is obtained for a addition level of 0.02% Ti using Al-5%Ti-1 %B, thereby confirming the importance of the boron content in achieving optimum ductility at low addition levels.

When the alloy contains a sufficient amount of Sr as modifier, the refining action associated with modification *i.e.* the change in the morphology of eutectic silicon from acicular to fibrous improves the mechanical properties, in particular, the ductility. A comparison of the elongation values of the alloy observed in Figures 5.1 (a) and (b) illustrates this fact. The elongation values in the 200 ppm Sr-modified A356.2 alloy samples are significantly higher than the corresponding values of the 30 ppm Sr-modified samples. It should be noted that no sign of the adverse effects of the interaction between Sr and B may be observed in terms of a decline in elongation due to additions of boron. In fact, at such low addition levels of grain refiner, the critical boron content of 0.1 % is not exceeded.

Figure 5.1 (c) shows the results for the 200 ppm Sr-modified A356.2 alloy for higher levels of Ti addition. With regard to the Al-5%Ti-1%B and Al-10%Ti master alloys,

the trend of the data points is almost horizontal, whereas a downward tendency is observed in the case of the Al-1.7%Ti-1.4%B and Al-2.5%Ti-2.5%B master alloys; in other words, the elongation values decrease as the Ti and B content increase. This downward trend is observed to be somewhat steeper for additions made using the Al-2.5%Ti-2.5%B master alloy than it is for those made using Al-1.7%Ti-1.4%B. The best ductility value at this high addition range of grain refiner is observed at 0.2% Ti addition using the Al-5%Ti-1%B master alloy.

In Figure 5.1 (c) some signs of interaction between Sr and B are evident for both Al-1.7%Ti-1.4%B and Al-2.5%Ti-2.5%B, particularly for the latter. In the case of both these grain refiners, the amount of boron addition exceeds 0.1%, a figure which is recognized as the threshold percentage for the abovementioned interaction. This percentage of B-content is in agreement with the corresponding microstructures containing coarse acicular eutectic silicon particles, as discussed in Chapter 4. This type of Si-particle morphology may act as a crack initiator in the A356.2 alloy and thus influence the elongation adversely. The downward trend in elongation values for these two grain refiners is attributed to the reduction in Sr resulting from the interaction between strontium and boron. A further significant parameter which plays a role with respect to the addition levels of grain refiners is the existence of large quantities of intermetallic compounds capable of agglomerating into larger quantities and affecting the ductility of the alloy.

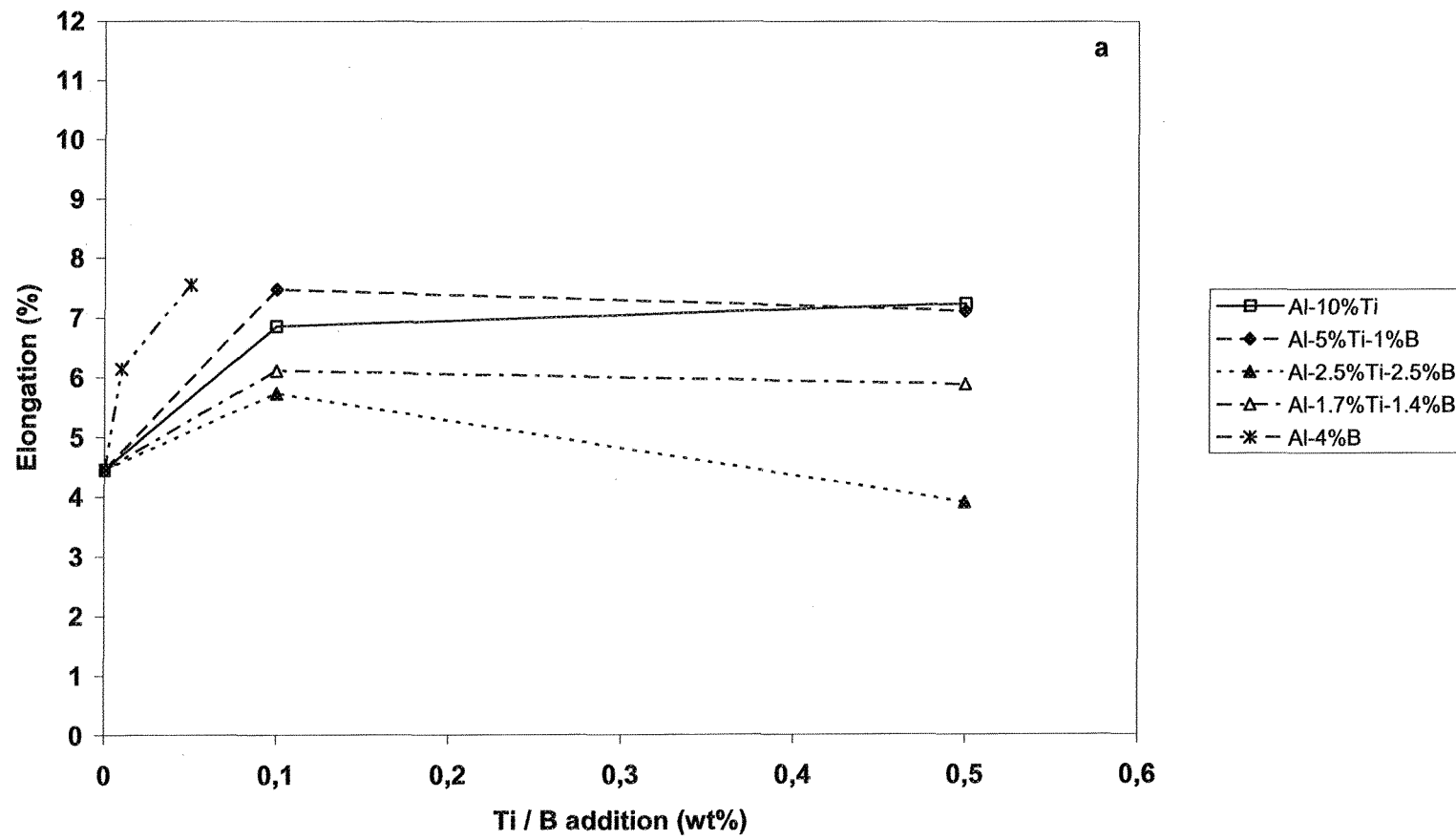


Figure 5.1 (a)

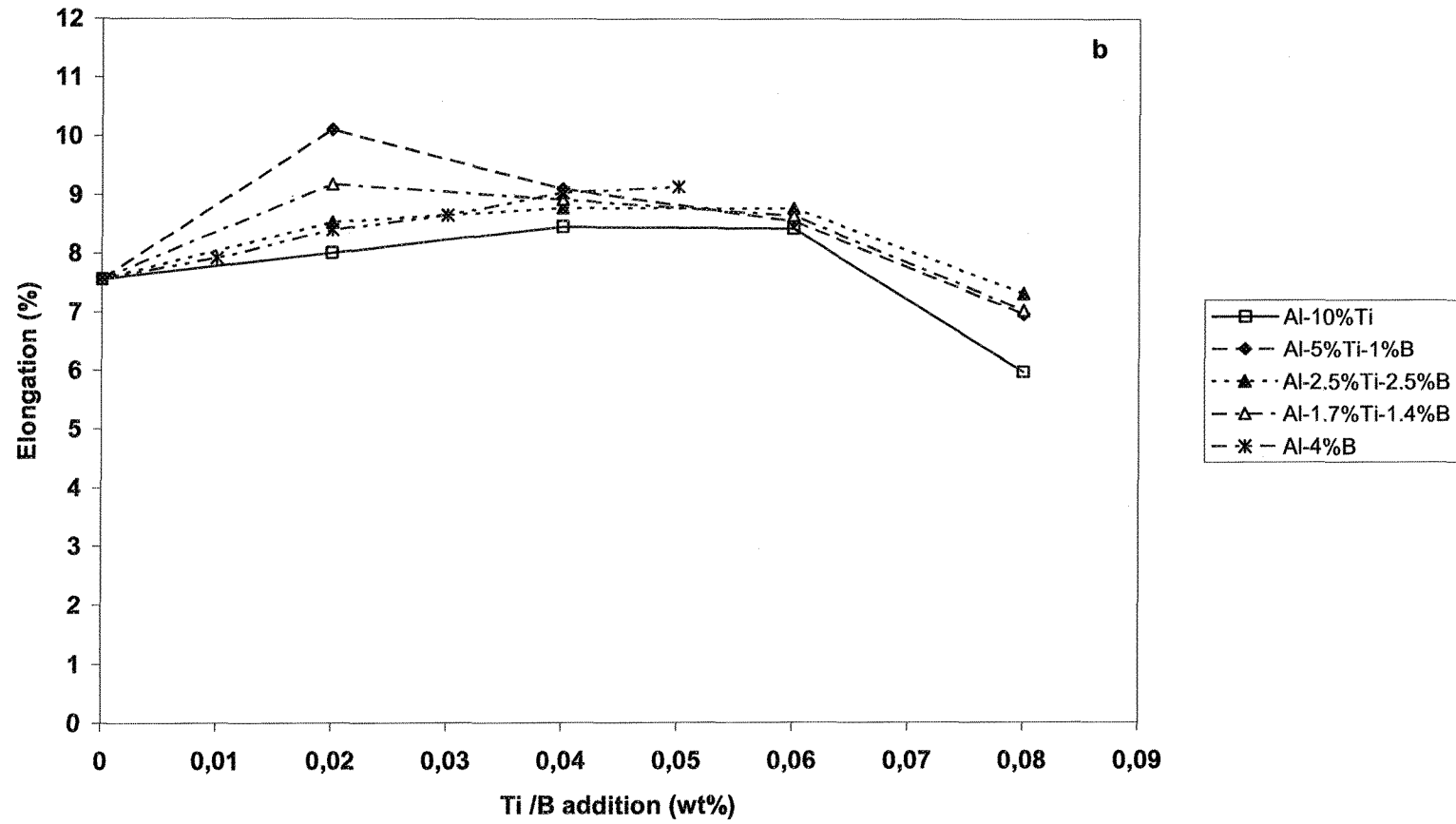
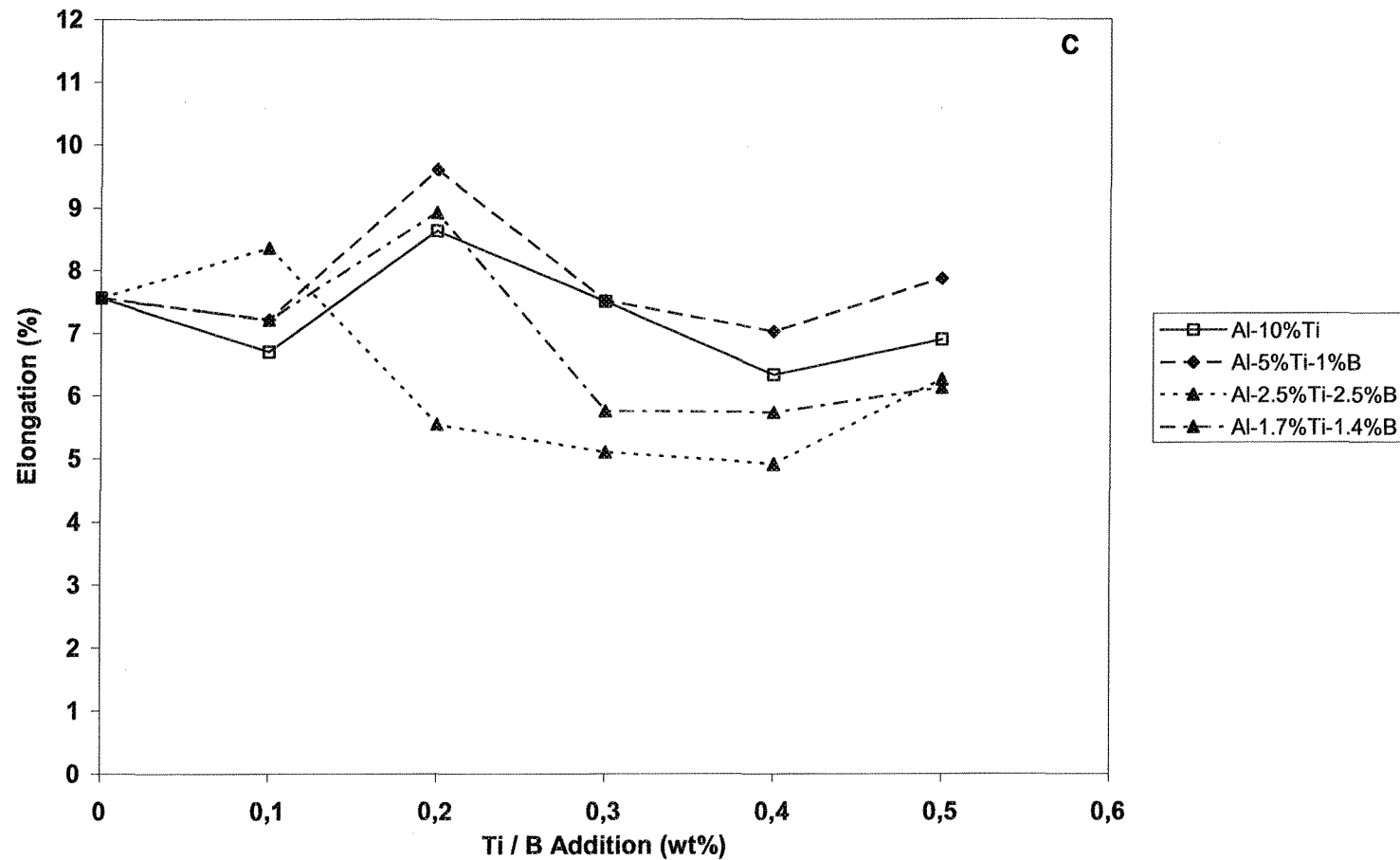


Figure 5.1 (b)





**Figure 5.1** Percentage elongation as a function of Ti or B content in Sr-modified grain-refined as-cast A356.2 alloy: (a) modified with addition of 30 ppm Sr; (b, c) modified with addition of 200 ppm Sr. Note the low and high Ti/B addition ranges in (b) and (c).

Figures 5.2 (a) to (c) show the variations in ultimate tensile strength (UTS) of the Sr-modified A356.2 alloy as a function of the addition of Ti and B, at both levels of Sr addition of 30 ppm and 200 ppm each. Figure 5.2 (a), which shows the 30 ppm Sr-modified samples, reveals two types of consequences caused by adding different master alloys. The Al-5%Ti-1%B, Al-10%Ti, and Al-4%B master alloys improve the tensile strength, whereas Al-2.5%Ti-2.5%B and Al-1.7%Ti-1.4%B master alloys behave in a contrary manner, *i.e.* they reduce the tensile strength of the alloy. From the figure, a growing trend in tensile strength values is evident for Al-10%Ti, while a certain amount of stability between corresponding levels of additions is also to be observed for Al-5%Ti-1%B and Al-4%B.

With reference to Figure 4.30, grain size in the corresponding alloys is observed to have diminished after the addition of various master alloys. Despite the theoretical inverse correlation between tensile strength and grain size, a comparison of Figure 4.30 and 5.2 (a) suggests that a number of alternative influencing factors should be taken into account to explain some of the data obtained regarding tensile strength. A decline in the tensile strength values of the samples refined using Al-2.5%Ti-2.5%B and Al-1.7%Ti-1.4%B master alloys may be attributed to the influence of a 0.1 %B addition as a threshold amount for the effects of the Sr-B interaction to become apparent, as is clear from Figure 5.2 (a).

Figure 5.2 (b), which relates to low levels of Ti and B addition to the 200 ppm Sr-modified A356.2 alloy, is almost the inverse of Figure 5.2 (a), leading to the assumption that Al-2.5%Ti-2.5%B and Al-1.7%Ti-1.4%B master alloys cause a certain amount of improvement in tensile strength, while other master alloys are responsible for reducing the strength. Furthermore, as shown in Figure 5.2 (b), the stability which is to be observed in

tensile strength may also be pinpointed as characteristic of low levels of grain refiner additions.

It is worthy of note that the tensile strength value recorded for the non-refined 30 ppm Sr-modified alloy, as shown in Figure 5.2 (a), is about 10 MPa lower than it is for the alloy which was modified using 200 ppm Sr, as shown in Figure 5.2 (b). This difference, however, is not relevant in view of the fact that a metallic mold is used thereby inducing a high cooling rate in the castings, which in turn promotes refining of the eutectic silicon particles.

Figure 5.2 (c) shows the UTS values for the 200 ppm Sr-modified A356.2 alloy, but for higher levels of Ti addition. A stable situation prevails for the samples refined with Al-5%Ti-1%B and Al-10%Ti master alloys, although tensile strength decreases when both Al-1.7%Ti-1.4%B and Al-2.5%Ti-2.5%B master alloys are used, more noticeably with regard to the latter. Contrary to case of low levels of Ti addition, Figure 5.2 (b), alloy refined with Al-5%Ti-1%B and Al-10%Ti master alloys show higher tensile strength than do does refined with other master alloys.

The following summary may be drawn up based on a comparison of Figures 5.1 and 5.2. For lower levels of Ti addition, refining the Sr-modified A356.2 alloy with Al-1.7%Ti-1.4%B and Al-2.5%Ti-2.5%B master alloys produces higher ductility and tensile strength values, whereas at higher levels of Ti addition, these advantages are lost to some extent. Such an impairment of the properties may be attributed to the interaction of strontium with boron, and is consistent with the microstructural analysis and quantitative Si-particle measurements reported in the previous chapter. Moreover, at high levels of Ti and B

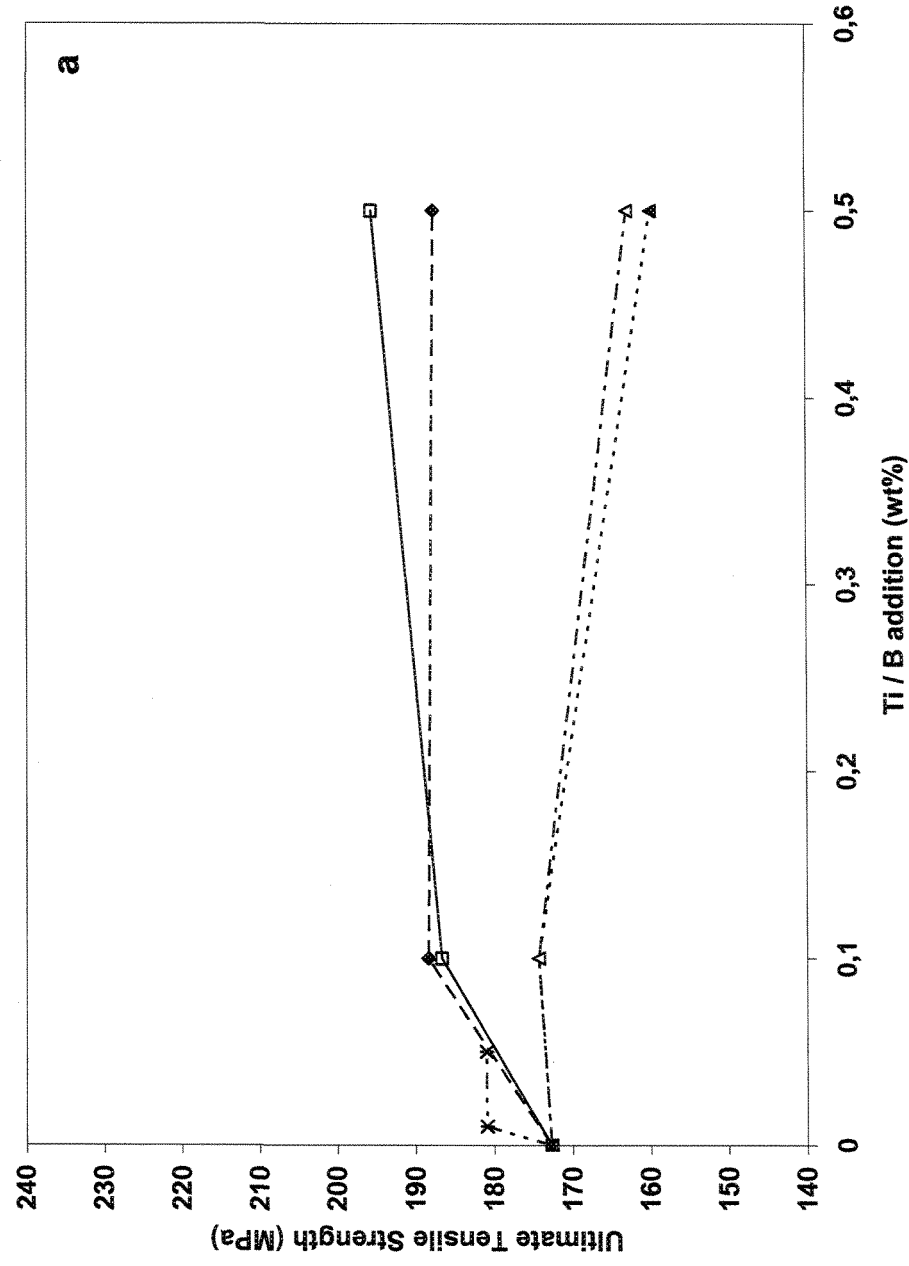


Figure 5.2 (a)

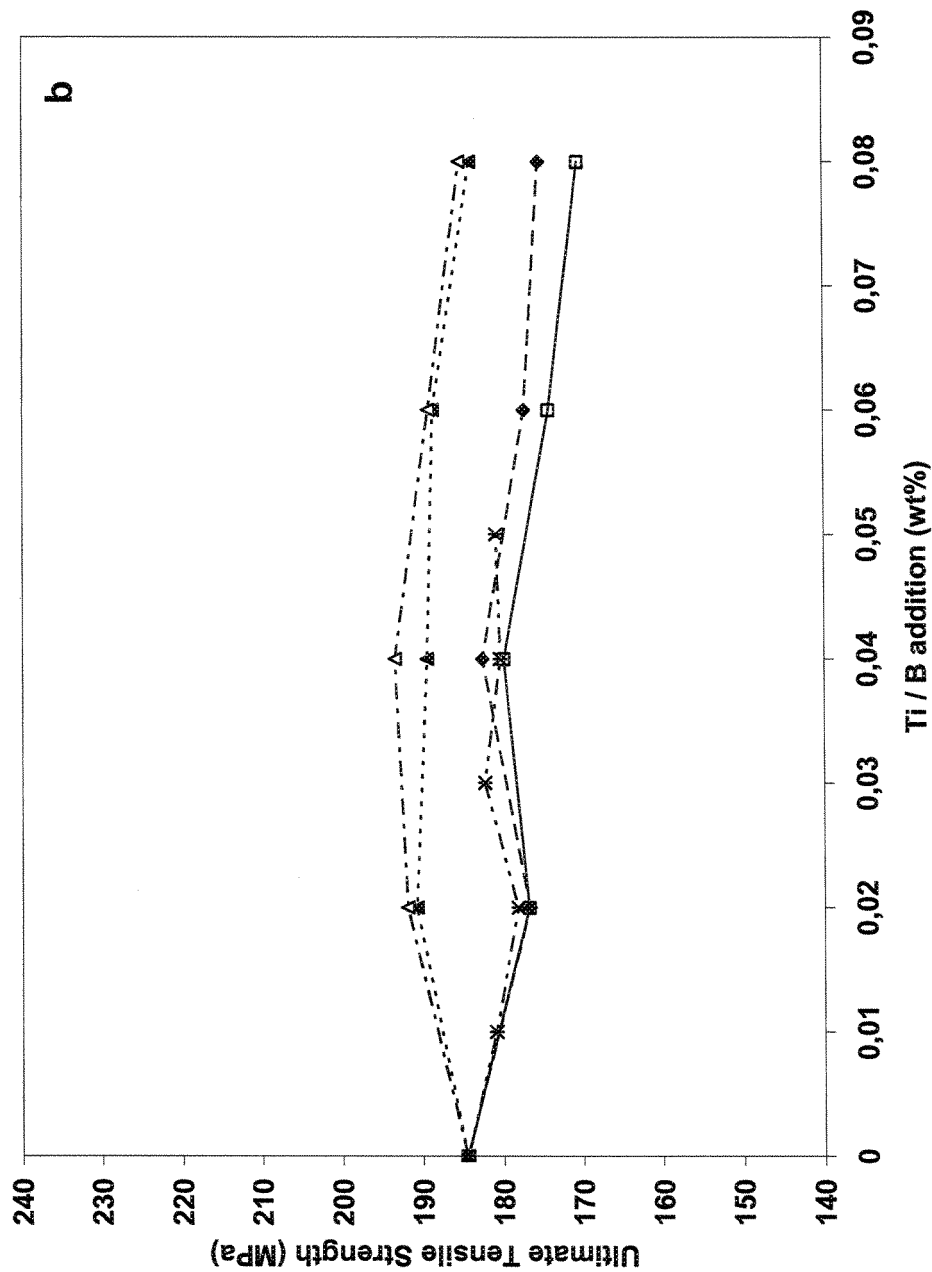
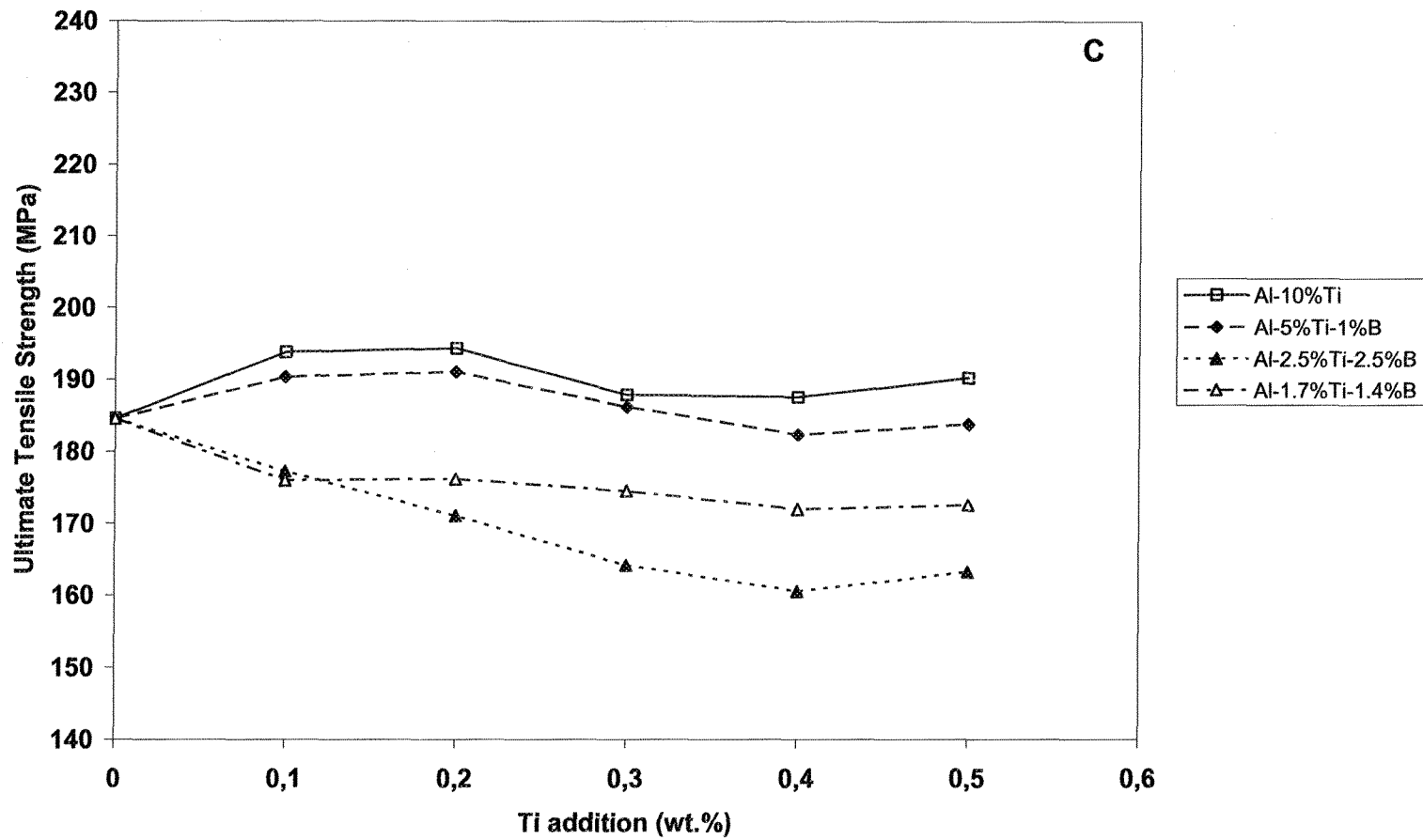


Figure 5.2 (b)



**Figure 5.2** Variation of tensile strength as a function of Ti or B content in the Sr-modified grain-refined as-cast A356.2 alloy:(a) modified with addition of 30 ppm Sr; (b, c) modified with addition of 200 ppm Sr.

addition, namely, 0.1–0.5 %, there is a possibility that the  $\text{Al}_3\text{Ti}$ ,  $\text{TiB}_2$  and other Ti-based intermetallic compounds might agglomerate in the form of short fine needles adversely affecting the mechanical properties of the alloy. It should be noted that the possibility of the formation of these agglomerates is expected to be higher as the addition of grain refiners increases.

Figures 5.3 (a) to (c) show the variations in yield strength (YS) , defined as 0.2% proof stress, of the Sr-modified as-cast A356.2 alloy as a function of Ti and B additions for the two levels of Sr addition. Figure 5.3 (a) shows the variation in YS values of the as-cast A356.2 alloy after modification with 30 ppm Sr and grain refining with various master alloys. A linear increase in YS values may be observed for the case of Al-10%Ti. Although some improvement in YS values is evident for Al-5%Ti-1%B and Al-4%B, no further increase is to be observed with supplementary additions of these master alloys. The addition of Al-1.7%Ti-1.4%B and Al-2.5%Ti-2.5%B leads to different outcomes, including a decrease in YS.

In general, YS depends on the type and size of grain, as well as on the size and distribution of precipitates, and to some extent on the presence of such structural discontinuities as porosity. With reference to Figure 4.30, the grain size of the 30 ppm Sr-modified alloys will be seen to have undergone reduction after the addition of various master alloys. The variation observed in the YS values of the alloy for the grain refiners Al-5%Ti-1%B, Al-10%Ti and Al-4%B are all in agreement with results of measurements obtained for grain size. However, with regard to the remaining master alloys, Al-1.7%Ti-

1.4%B and Al-2.5%Ti-2.5%B, both YS and grain size may be observed to have diminished.

As a result of cooling in a metallic mold, the alloys have the potential for more uniform microstructures with more closely distributed and finer particles in the form of eutectic silicon and intermetallic compounds. The addition of 30 ppm Sr, however, does not provide the capacity for leading to complete modification of the eutectic silicon particles; also, some demodification may be caused by the addition of Al-1.7%Ti-1.4%B and Al-2.5%Ti-2.5%B master alloys.

Increases in YS values for additions using Al-4%B, Al-10%Ti, and Al-5%Ti-1%B are consistent with a reduction in grain size as a result of the action of the grain refiner. In the case of Al-1.7%Ti-1.4%B and Al-2.5%Ti-2.5%B, YS values were expected to increase as a result of the decrease in grain size as shown in Figure 4.30, however, the stability observed in YS values of these master alloys may be related to the presence of demodified eutectic silicon in the as-cast microstructures and a decrease in the corresponding elongations.

Figure 5.3 (b) illustrates the variation in yield strength (YS) as a function of Ti addition in the as-cast A356.2 alloy after modification with 200 ppm Sr and grain refining with various master alloys. Further addition of modifiers, for alloys free of grain refiner, does not appear to have any marked influence on the yield strength. This observation is in agreement with Campbell's findings which state that, in the as-cast condition, microstructural features such as Si shape, size, and distribution, as well as dendrite arm spacing have essentially no effect on YS.<sup>68</sup> Although grain size diminishes after grain



refining, as shown in Figure 4.25, further additions reveal that the process has only a minimal effect on improving YS. Overall, for low addition levels of grain refiner, no significant variations in YS values are to be observed.

According to Figure 4.25, it may also be concluded that the interaction of Sr and B has a fading effect on grain refiners. The adverse effects of this interaction, however, will appear when boron additions are made in the range of 0.02% to 0.1%. It may be concluded, therefore, that the fading effect of the Sr-B interaction causes the stability of YS values at this low addition range of grain refiner. As shown in the same figure, the addition of the boron-free grain refiner, Al-10%Ti, is not sufficiently satisfactory in terms of grain size. This observation confirms that the stability of YS values may also be explained by the weak performance of the grain refiner.

Figure 5.3(c) illustrates the YS values for the 200 ppm Sr-modified A356.2 alloy, for high addition levels of grain refiner. As in the case of low levels of addition, no substantial changes are to be observed on condition that a few minimal fluctuations are disregarded. The slight increases in YS which may be observed with the addition of Al-5%Ti-1%B and Al-10%Ti master alloys are attributable to the refining performance of these grain refiners, as shown in Figure 4.25. Negligible decreases in the YS values of alloys samples refined with Al-2.5%Ti-2.5%B and Al-1.7%Ti-1.4%B master alloys are not sufficiently meaningful to be attributed to the amount of the intermetallic compounds which enter the melt through master alloys.

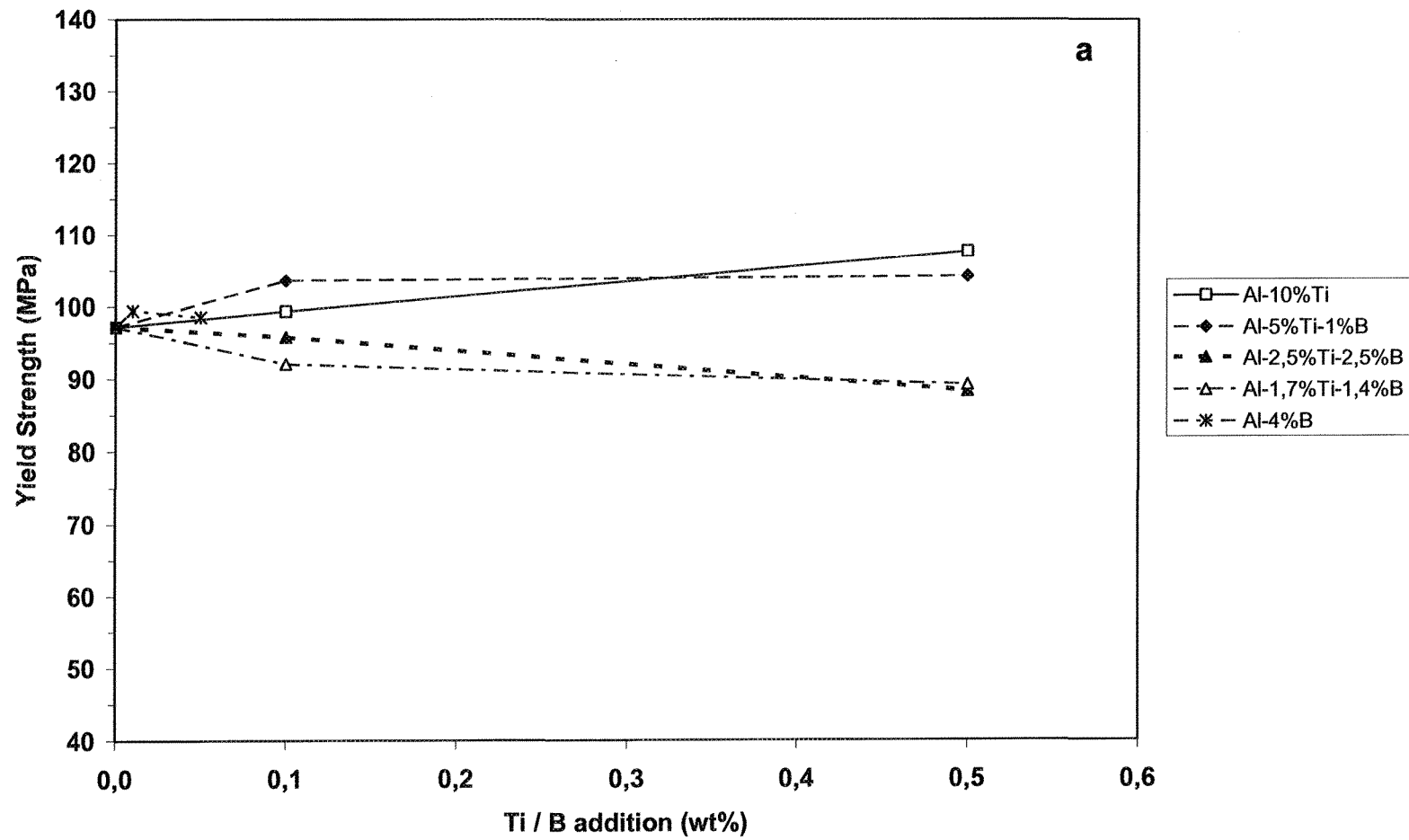


Figure 5.3 (a)

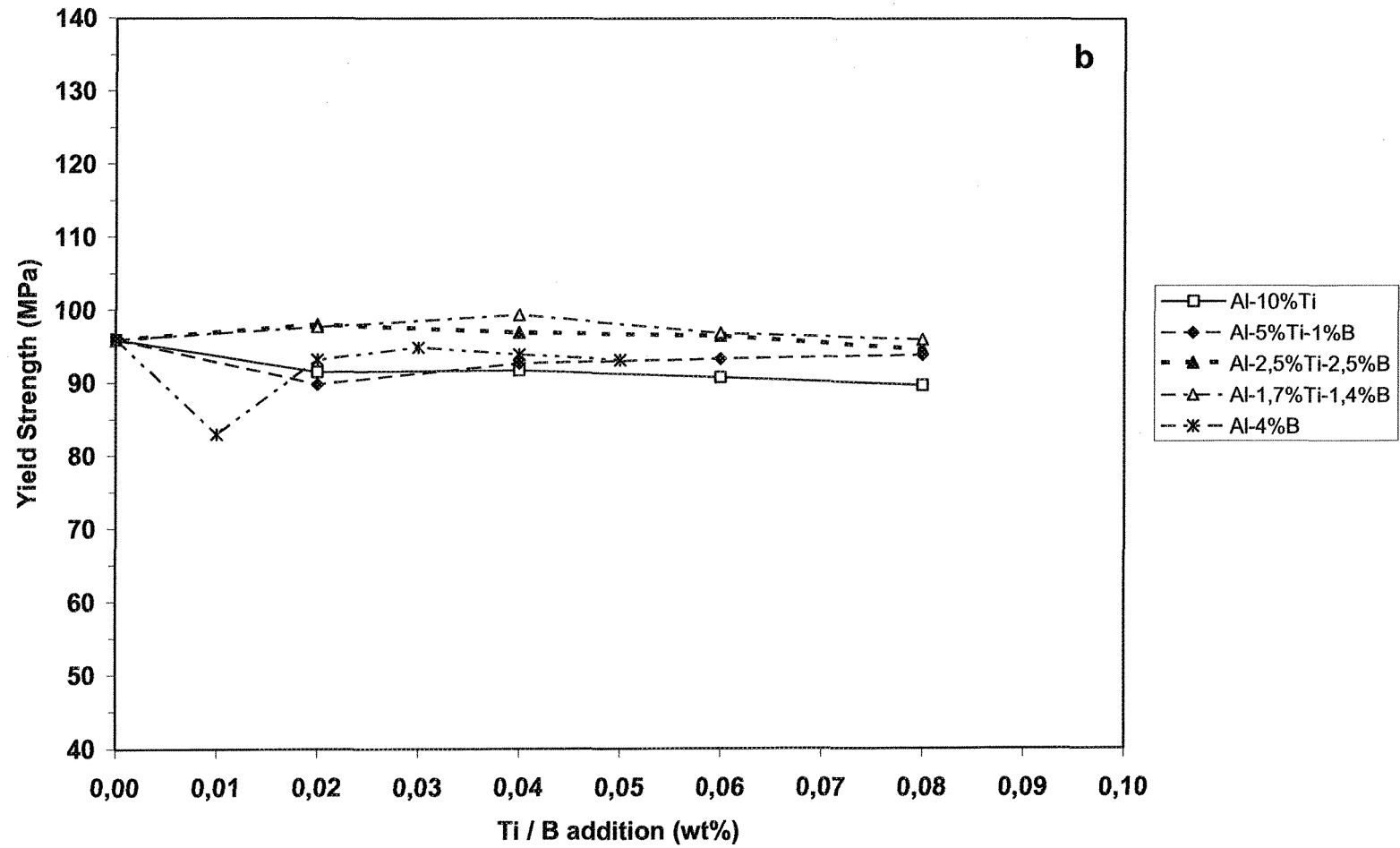
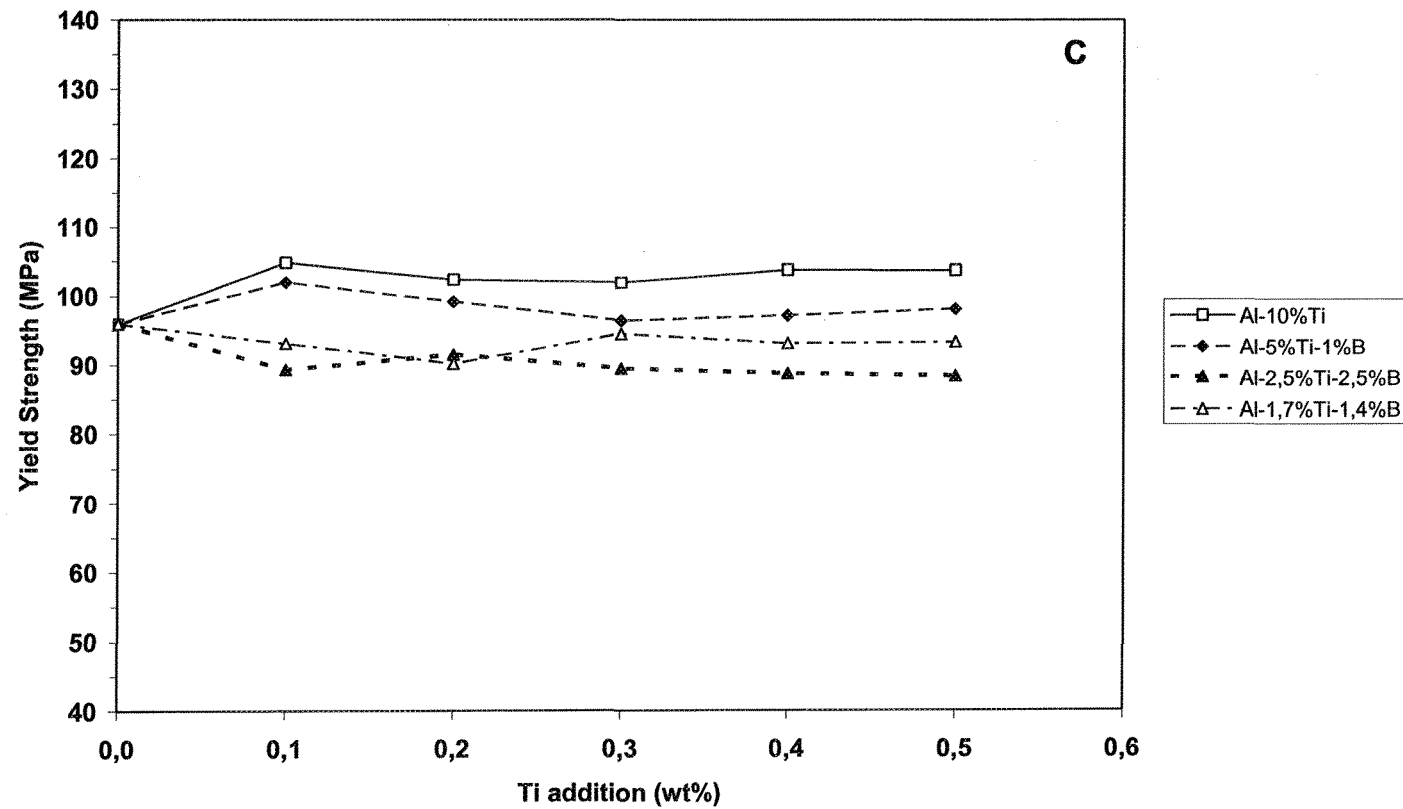


Figure 5.3 (b)



**Figure 5.3** Variation of yield strength as a function of Ti or B content in the Sr-modified grain-refined as-cast A356.2 alloy: (a) modified with addition of 30 ppm Sr; (b, c) modified with addition of 200 ppm Sr.

### 5.2.2 T6-TEMPERED CONDITION

Applying an appropriate heat treatment technique is one of the decisive factors affecting the improvement of the mechanical properties of heat-treatable Al-Si alloys.<sup>69, 70</sup> The coring phenomenon, or the chemical composition gradient, particularly for Mg and Si, has an observable influence on the mechanical properties of the as-cast A356.2 alloy. The T6 temper, comprising of a solution heat treatment, followed by quenching and aging, is the heat treatment normally applied to A356.2 type Al-Si-Mg casting alloys. The solution treatment stage of the T6 temper homogenizes the cast structure and minimizes the segregation of alloying elements in the casting. This stage of the T6 temper will also tend to convert eutectic silicon particles to a finer and rounder morphology than that to be observed in the as-cast condition. As a result of the T6 temper, coarse particles, which form when a casting solidifies, are also dissolved.

This subsection will therefore investigate the effects of T6 temper on the tensile properties of the Sr-modified A356.2 alloys refined using the various types and amounts of master alloy additions investigated in this study.

Figure 5.4 (a) shows the variation in percentage elongation of the T6-tempered 30 ppm Sr-modified A356.2 alloy grain refined using various master alloys. The significant improvement observed in the alloy sample which is free of grain refiners is caused by the T6 temper and can be attributed to homogenization of the casting, as well as to changes occurring in the morphology of eutectic silicon through fragmentation, spheroidization and coarsening. Only a narrow variation may be observed with Ti additions using Al-10%Ti,

Al-5%Ti-1%B and Al-1.7%-1.4%B master alloys; hence, T6 temper does not result in any noticeable beneficial consequences in terms of the elongations obtained with the use of these master alloys in comparison with the as-cast condition. The other master alloys, Al-4%B and Al-2.5%Ti-2.5%B, tend to display a rising trend in the same manner as the as-cast alloys, and a reducing trend with regard to all amounts added, respectively. The best results are obtained after using the Al-4%B master alloy following upon the addition of 0.05% B, while the least advantageous results are revealed after the addition of 0.5% Ti in the form of Al-2.5%Ti-2.5%B master alloys.

A comparison of Figures 5.1 (a) and 5.4 (a) shows that the T6 temper has a beneficial effect on the elongation values of the 30 ppm Sr-modified A356.2 alloy which has been refined using Al-4 %B. In the case of Al-2.5%Ti-2.5%B, however, the T6 temper does not lead to any improvement with regard to the coarse eutectic Si particles which are present in the corresponding as-cast microstructures, as shown in Figure 4.9 (d), and which would therefore require a longer fragmentation time. The behavior of the alloys which have been grain refined with Al-2.5%Ti-2.5%B may suggest that the duration of the solutionizing time of the T6 temper should be considered insufficient. Thus, one of the consequences of the demodification of Si particles as a result of the interaction between Sr and B is a prolongation of the heat treatment times.

The elongation values of the alloy samples refined with Al-1.7%Ti-1.4%B remain higher than those refined with Al-2.5%Ti-2.5%B, in the same manner as the alloys in the as-cast condition, in spite of the fact that the boron content is in excess of 0.1%.

Figure 5.4 (b) shows the variation in elongation for the 200 ppm Sr-modified A356.2 alloy for low addition levels of Ti and B in the T6-treated condition. There is a 20% increase in ductility to be observed for the alloy which is grain-refiner free, as compared to the same alloy in the as-cast condition. A sharp drop in elongation may be observed with an increase in the addition of boron using the Al-4%B master alloy. Refining the A356.2 alloy using Al-1.7%Ti-1.4%B leads to a gradual and moderate decrease; whereas the dispersed elongation values for Al-10%Ti and Al-5%Ti-1%B do not show any evident trend. A comparison of the elongation values of T6-tempered alloys with those of as-cast alloys shows that this form of tempering produces a beneficial effect on the elongation values of the grain-refined alloys, except for the case of the addition of Al-4%B. In this regard, the T6 temper has a most deleterious effect on the ductility of the alloy, and reduces the elongation to a value less than half of that observed for the grain-refiner free sample in the as-cast condition.

The effects of T6 temper on the percentage elongation of the 200 ppm Sr-modified A356.2 alloy samples for higher additions level of Ti may be observed in Figure 5.4(c). Once the above figure is compared against the data provided for the as-cast alloy in Figure 5.1(c), a sharper decline will be observed in the elongation, particularly for the cases when Al-2.5%Ti-2.5%B and Al-1.7%Ti-1.4%B grain refiners are used. As was mentioned in the case of the 30 ppm Sr-modified alloys, the reduction in elongation occurring in these alloys is related to the interaction between Sr and B. Moreover, in the case of the Al-10%Ti, and to some extent the Al-5%Ti-1%B refined alloys, elongation values decrease as Ti or B additions increase. This observation may be explained by the tendency of existing

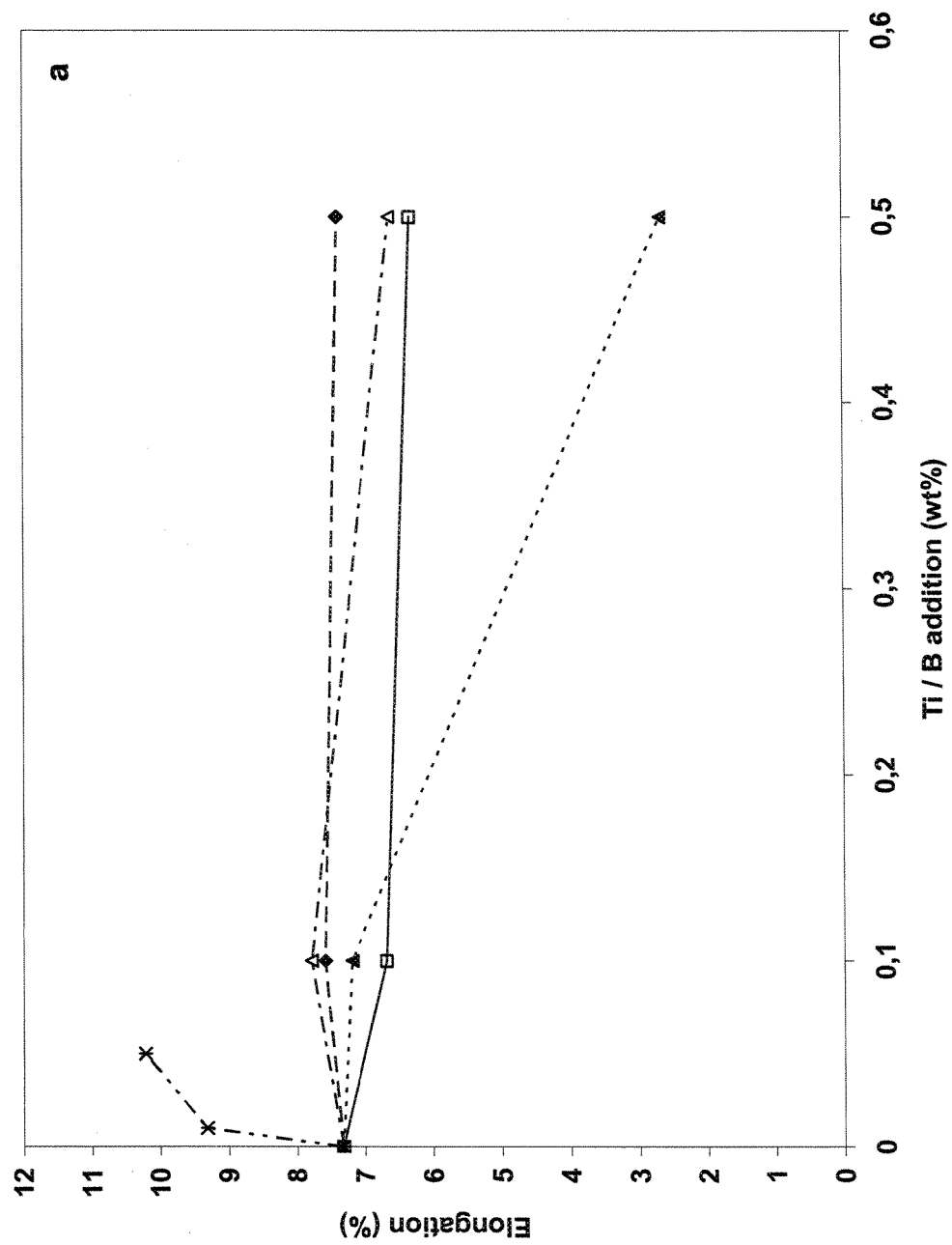


Figure 5.4 (a)



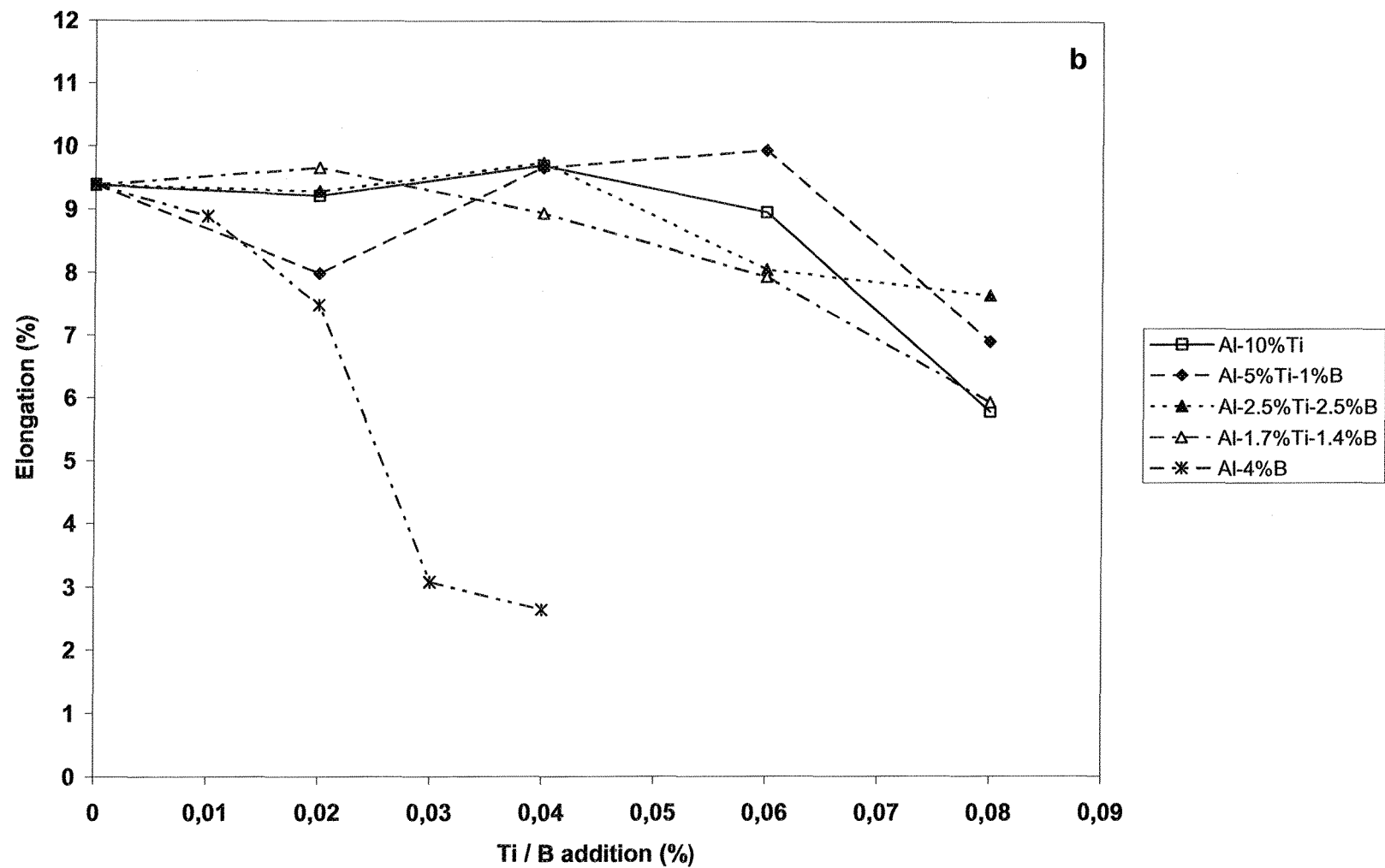
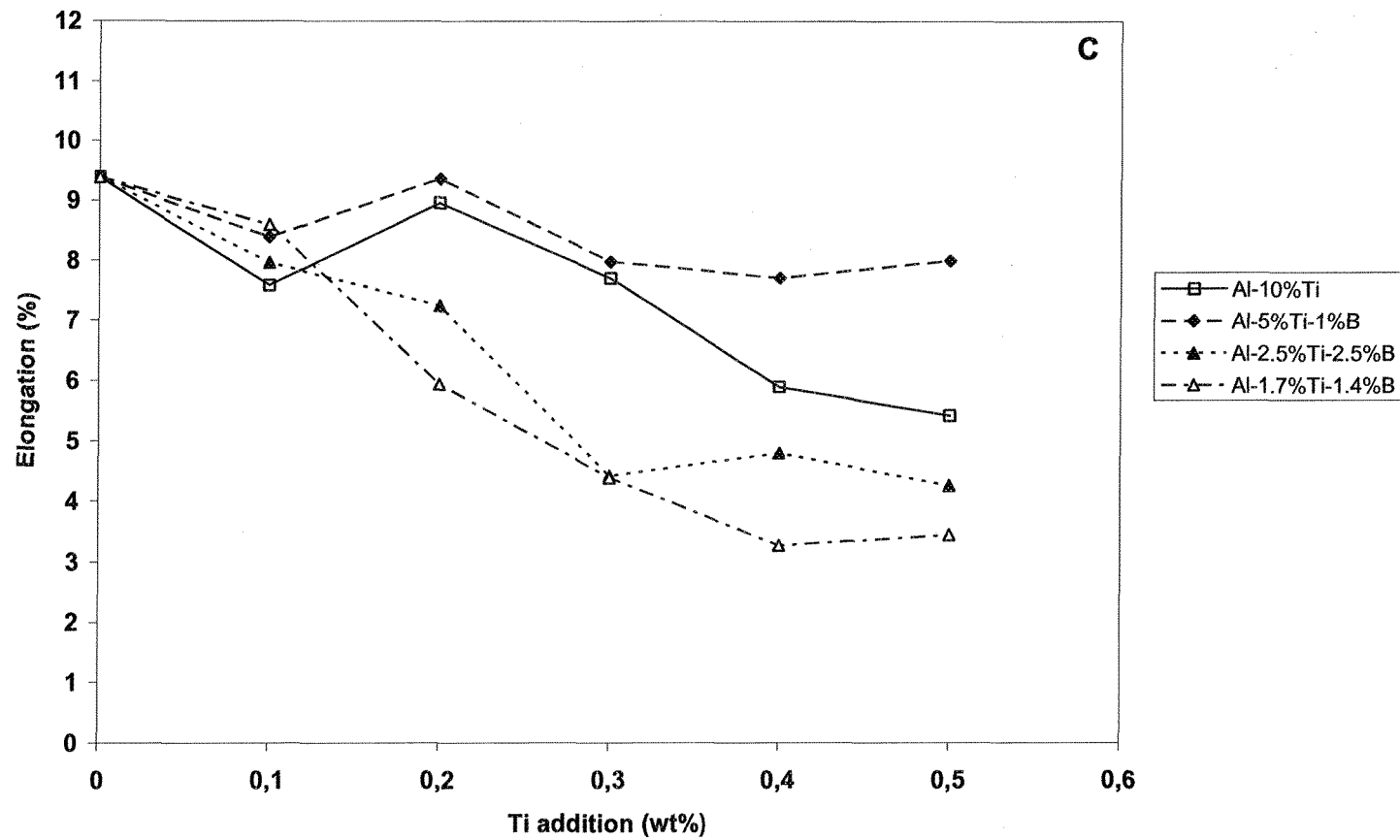


Figure 5.4 (b)



**Figure 5.4** Variation of percentage elongation as a function of Ti or B content in T6-tempered Sr-modified grain-refined A356.2 alloy: (a) modified with 30 ppm Sr addition; (b, c) modified with 200 ppm Sr addition.

intermetallic particles to agglomerate under the improved thermal conditions, promoting diffusion, and thereby forming large particles which have the potential for adversely affecting the mechanical properties of the alloy. Overall, as no serious improvement in elongation may be observed after application of the standard T6 temper, the solutionizing and aging periods should be determined with respect to the type and amount of grain-refining additions.

Figure 5.5 (a) to (c) show the variations in ultimate tensile strength (UTS) of the Sr-modified A356.2 alloy samples in the T6-treated condition as a function of Ti and B addition levels, at the two levels of Sr addition. As the regards 30 ppm Sr-modified samples, Figure 5.5 (a) shows that the tensile strength of the alloy samples refined with Al-5%Ti-1%B and Al-1.7%Ti-1.4%B remain almost unchanged, as the addition of Ti is increased from 0.1% to 0.5%Ti. Although the tensile strength of the alloy improves after an addition of 0.1%Ti using Al-10%Ti, no further change is observable at 0.5% Ti addition, whereas for Al-2.5%Ti-2.5%B, the addition of 0.5% Ti results in a considerable drop in tensile strength from the slight improvement observed at the 0.1% Ti level.

High tensile strength and high elongation are most desirable properties in structural design. The case for this may be made by comparing Figure 5.5(a) with Figure 5.4(a) which would show that the T6 temper improves both ductility and tensile strength after the addition of Al-4%B; whereas for Al-2.5%Ti-2.5%B, the T6 temper results in a decrease in both elongation and ductility when boron addition exceeds 0.1 %. Such results may suggest that the T6 temper, involving insufficient solutionizing time, does not entirely change the

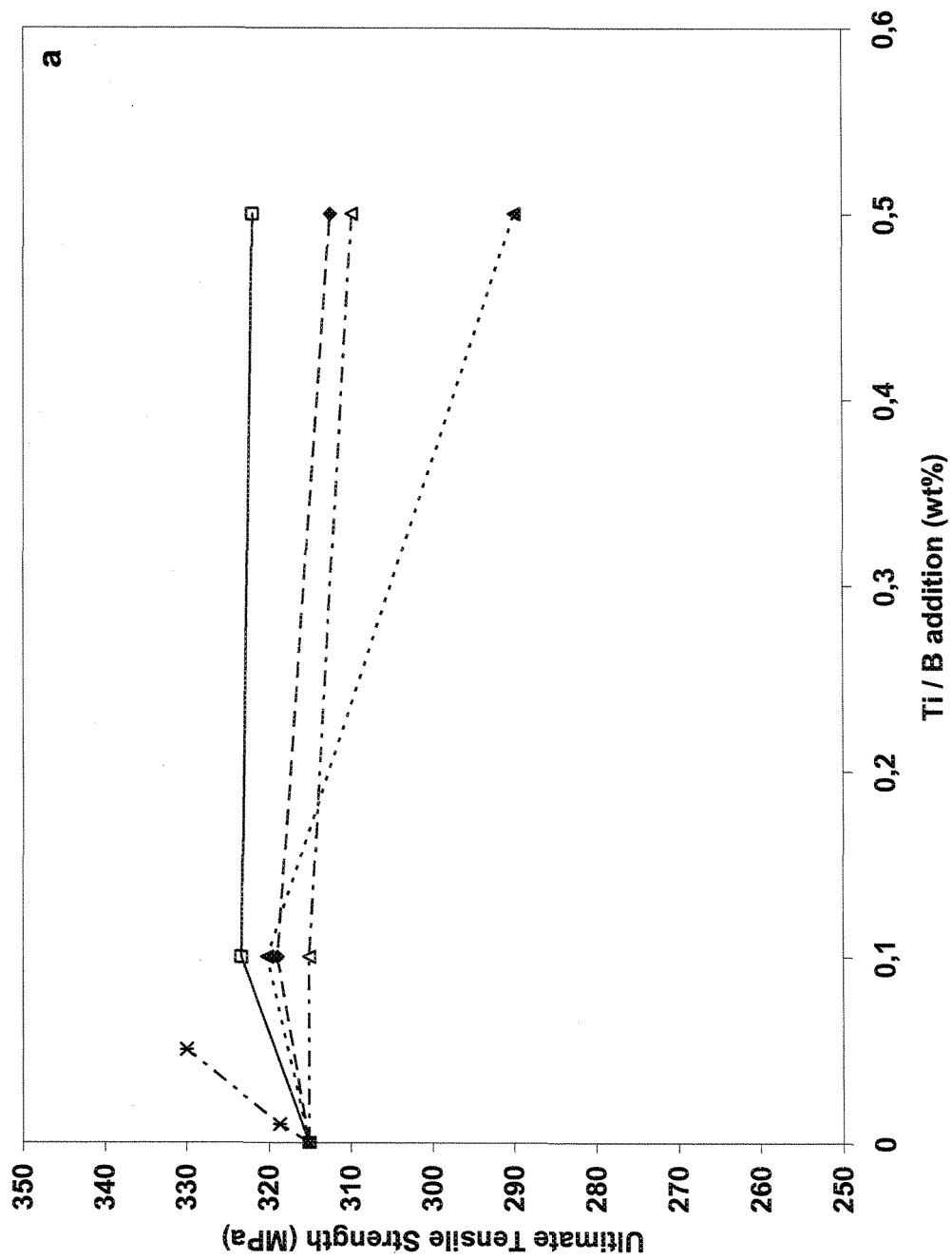


Figure 5.5 (a)

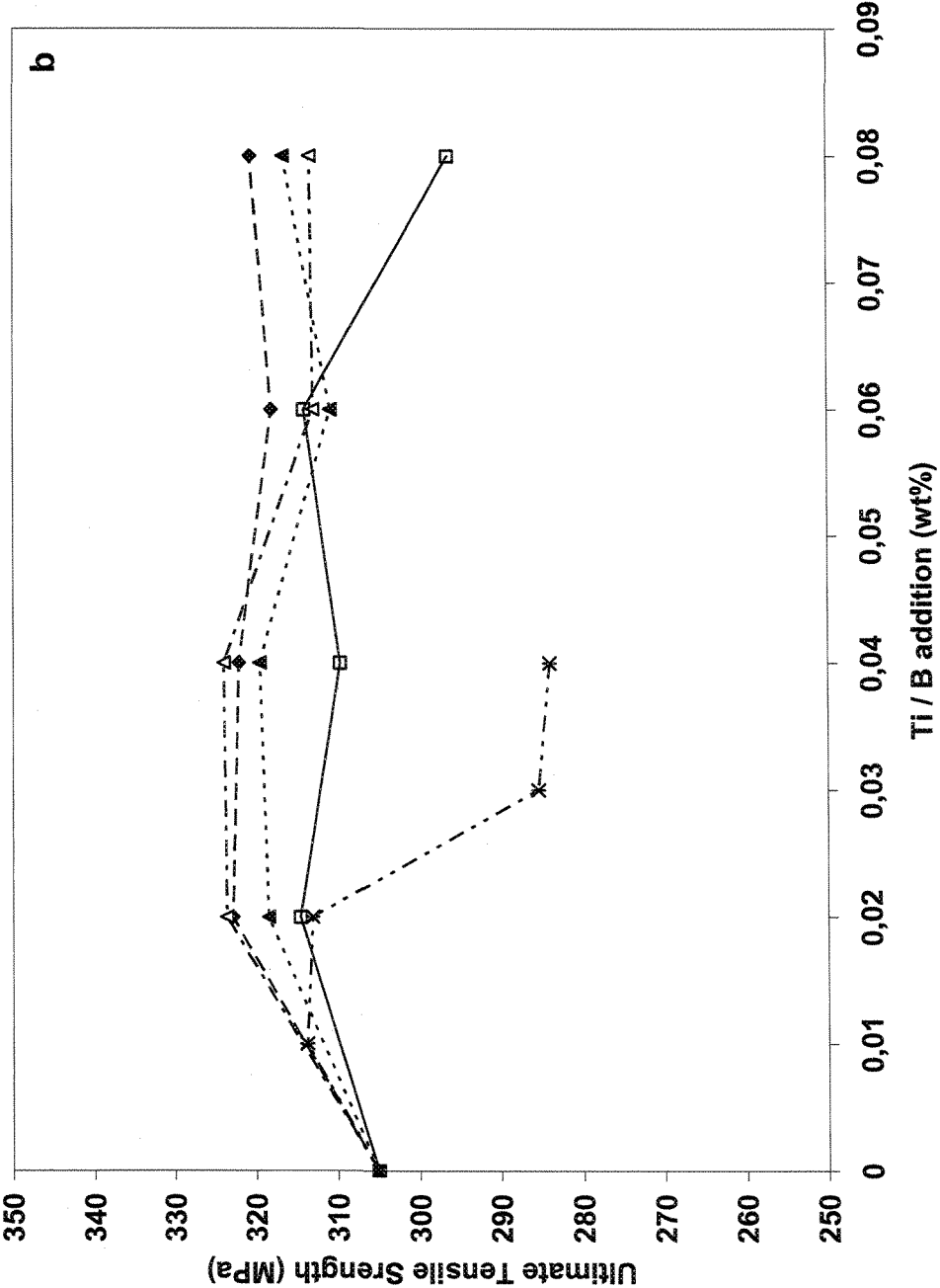
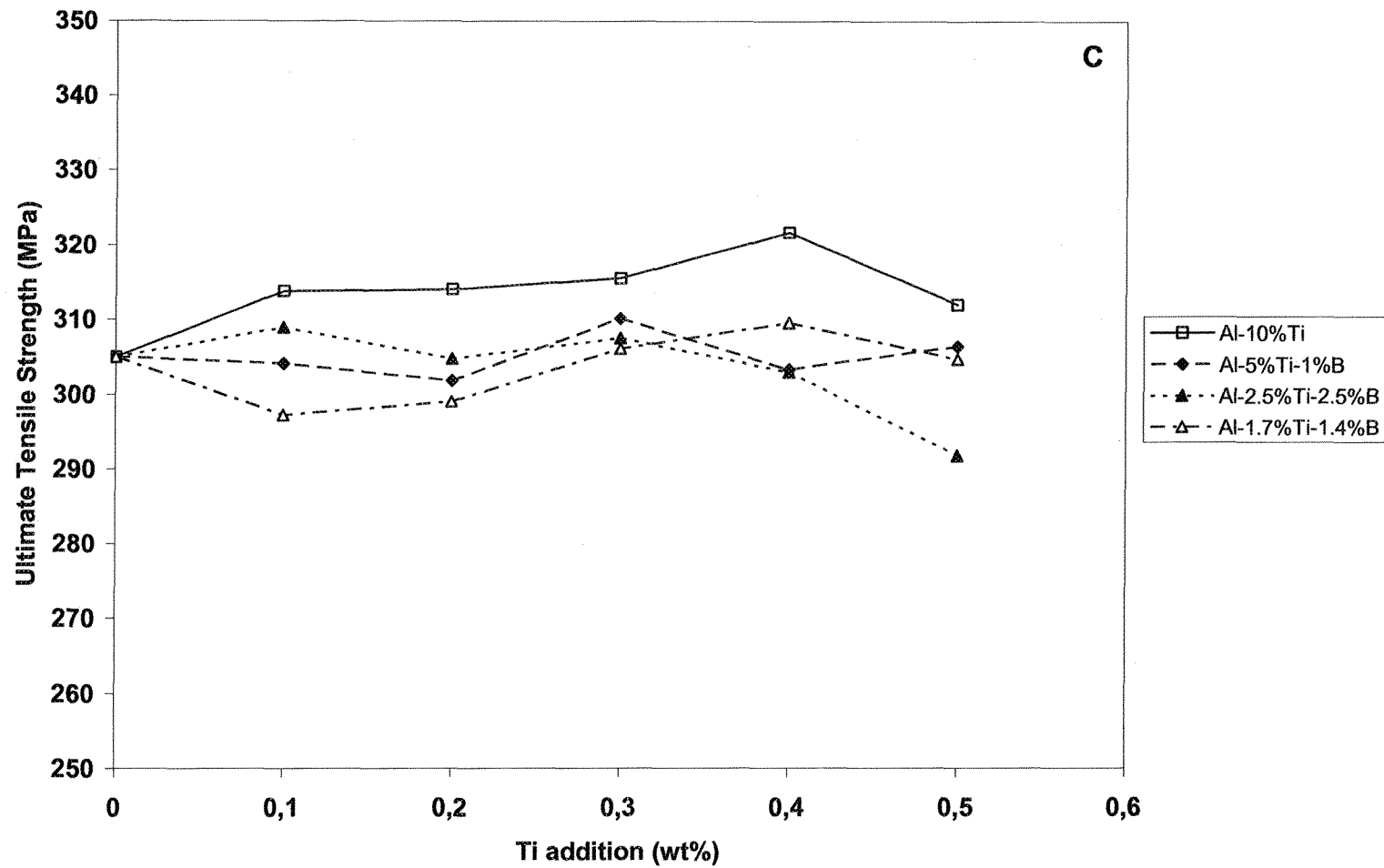


Figure 5.5 (b)



**Figure 5.5** Variation of tensile strength as a function of Ti or B content in T6-tempered Sr- modified grain-refined A356.2 alloy: (a) modified with 30 ppm Sr addition; (b, c) modified with 200 ppm Sr addition.

morphology of eutectic silicon which is present in the form of acicular particles in the corresponding as-cast microstructure. Since the Al-1.7%Ti-1.4%B master alloy also meets the requirement of exceeding 0.1 % B, the T6 temper results in improvement in UTS in the as-cast condition, while the elongation value decreases for an addition level of 0.5% Ti. The effect of a T6 temper, however, increases the strength in this alloy to almost twice that of the as-cast value.

It may be suggested that, for an addition of 0.1% Ti, the T6 temper results in improvements in both elongation and UTS due to changes in the initial morphology of coarse eutectic silicon, it also results in the dissolution of the existing  $Mg_2Si$  particles. For an addition of 0.5% Ti, however, the T6 temper is not as effective as it is for an addition of 0.1% Ti, since the solutionizing time may not have been long enough to dissolve the  $Mg_2Si$  particles, nor long enough to complete the fragmentation and spheroidization of coarse eutectic silicon particles. For Al-10%Ti and Al-5%Ti-1%B as well, improvements in UTS of the A356.2 alloy samples refined using these master alloys may be explained in terms of the same mechanisms as those associated with the T6 temper.

In the case of the 200 ppm Sr-modified A356.2 alloy, for low addition levels of Ti, some improvement in tensile strength is obvious for all the master alloys, excluding Al-4%B, as shown in Figure 5.5(b); this may be explained by the effects of the T6 temper, which include the dissolution of  $Mg_2Si$  particles and further fragmentation and spheroidization of Si particles. The as-cast microstructures of the 200 ppm Sr-modified alloys contain fine fibrous silicon particles and finer grain sizes after refining with low addition levels of master alloy. This feature would tend to indicate that such T6 temper

parameters as time and temperature were applied appropriately. Results for samples refined with Al-4%B display a drop in tensile strength when the boron content exceeds 0.02%, in other words, both tensile strength and ductility diminish under T6 temper condition, since the amount of boron addition exceeds 0.02 %. With regard to the corresponding as-cast microstructures shown in Figures 4.4 (c) and (d), there is no explanation available to account for this behavior, indicating the necessity for elucidation by means of further trials.

Figure 5.5 (c) illustrates the influence of high levels of added Ti and B on the tensile strength of the 200 ppm Sr-modified alloy. It will be observed that the tensile strength values for Al-10%Ti are the best of all those produced by the range of master alloys applied, whereas other master alloys resulted in a decrease in tensile strength values, compared to the values observed for lower addition levels, as shown in Figure 5.5 (b).

A comparison of Figures 5.5 (b) and (c) indicates that, under T6-temper, higher tensile strength values may be obtained through the addition of lower amounts of the master alloys, particularly in the range of 0.02% to 0.04% Ti. Based on this observation, it is important to choose the right grain refining agents in conjunction with appropriate amounts of additives. On the other hand, a comparison of Figures 5.4 (c) and 5.5 (c) with Figures 5.1 (c) and 5.2 (c) indicates that T6 temper results in greater improvement in UTS than in elongation for both Al-1.7%Ti-1.4%B and Al-2.5%Ti-2.5%B-refined samples. This difference in outcome of the application of the T6 temper may be explained by the adverse effects produced by the Sr-B interaction, as well as by the presence of demodified eutectic silicon particles. Solutionizing time may thus need to be prolonged in order to obtain improved ductility in these samples.



Figures 5.6 (a) to (c) show the variation in YS values of the T6-tempered Sr-modified A356.2 alloy samples as a function of Ti and B addition levels, at the two levels of Sr addition. The data provided for the YS values for additions of 30 ppm Sr, Figures 5.6 (a), and 200 ppm Sr, Figures 5.6 (b) and (c), show that the T6 tempered alloys result in much higher YS values compared to the as-cast alloys (Figure 5.3). Increase in the YS value after application of the T6 temper is more considerable with regard to the addition of 30 ppm Sr, compared to 200 ppm Sr for the alloy free of grain refiner.

Figure 5.6 (a) illustrates the influence that the addition of Ti may have on the YS of 30 ppm Sr-modified A356.2 alloy, through the addition of various grain refiners, after application of the T6 temper. No important difference among YS values is observed when the alloy is grain-refined using Al-10%Ti, Al-5%Ti-1%B and Al-4%B master alloys. The decreases in the YS values which are to be observed with the use of Al-2.5%Ti-2.5%B and Al-1.7%Ti-1.4%B master alloys may be attributed to the size and volume fraction of intermetallic particles remaining in the alloy microstructures after the T6 treatment.

Figure 5.6 (b) shows the variation in YS of the 200 ppm Sr-modified A356.2 alloy samples for low addition levels of grain refiners, following T6 treatment. Despite a certain amount of scatter in values observed in the figure, overall, the increase in YS values is discernible in comparison to the YS values of the as-cast samples, Figure 5.2 (b), for all grain refiners used, particularly in the case of Al-5%Ti-1%B and Al-1.7%Ti-1.4%B. These improvements may be explained by the reductions in the grain sizes of the as-cast alloy samples after application of the low addition levels of the grain refiners, as shown in Figure 4.25. Furthermore, the adverse effect of Sr on the grain refining efficiency of boron-bearing

master alloys observed for boron additions in the 0.02-0.1% range should also be taken into consideration.

Relatively wide scattering was also observed for elevated levels of grain refiner additions, as may be seen in Figure 5.6 (c). The increasing trend may also be observed with respect to YS, particularly in the case of Al-10%Ti and Al-1.7%Ti-1.4%B master alloys which is consistent with the refinement in grain sizes of the corresponding as-cast alloy samples.

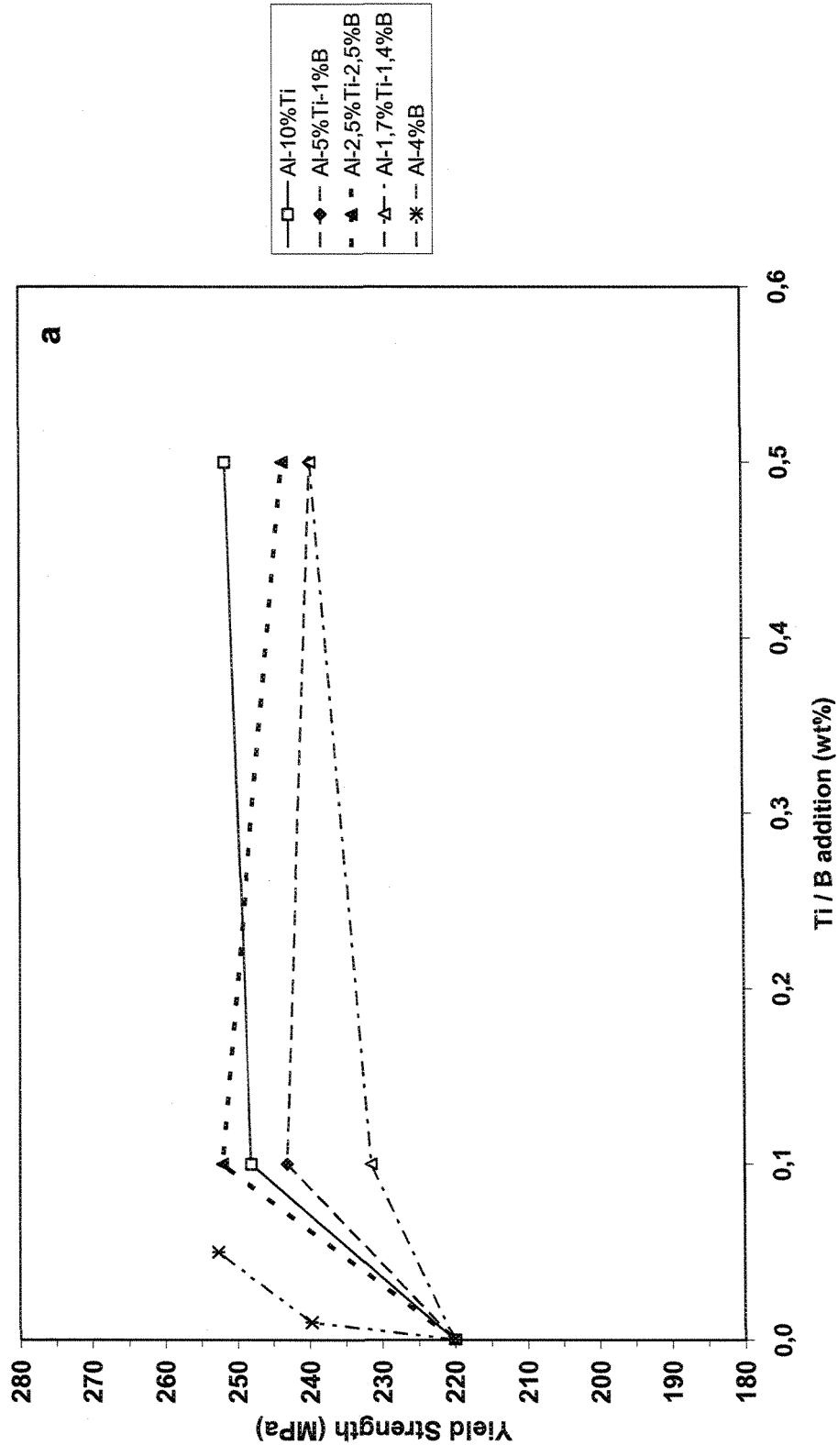


Figure 5.6 (a)

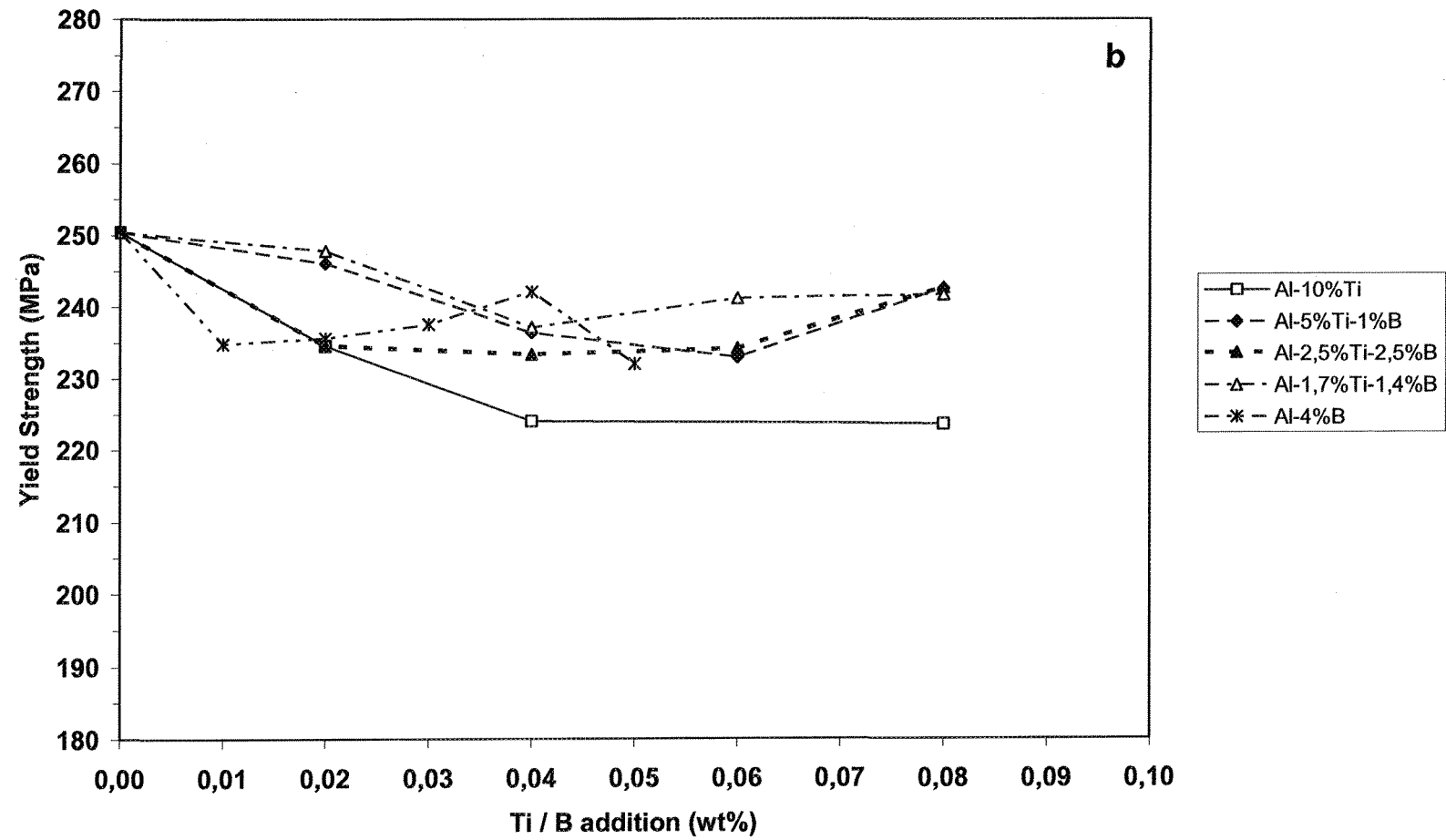
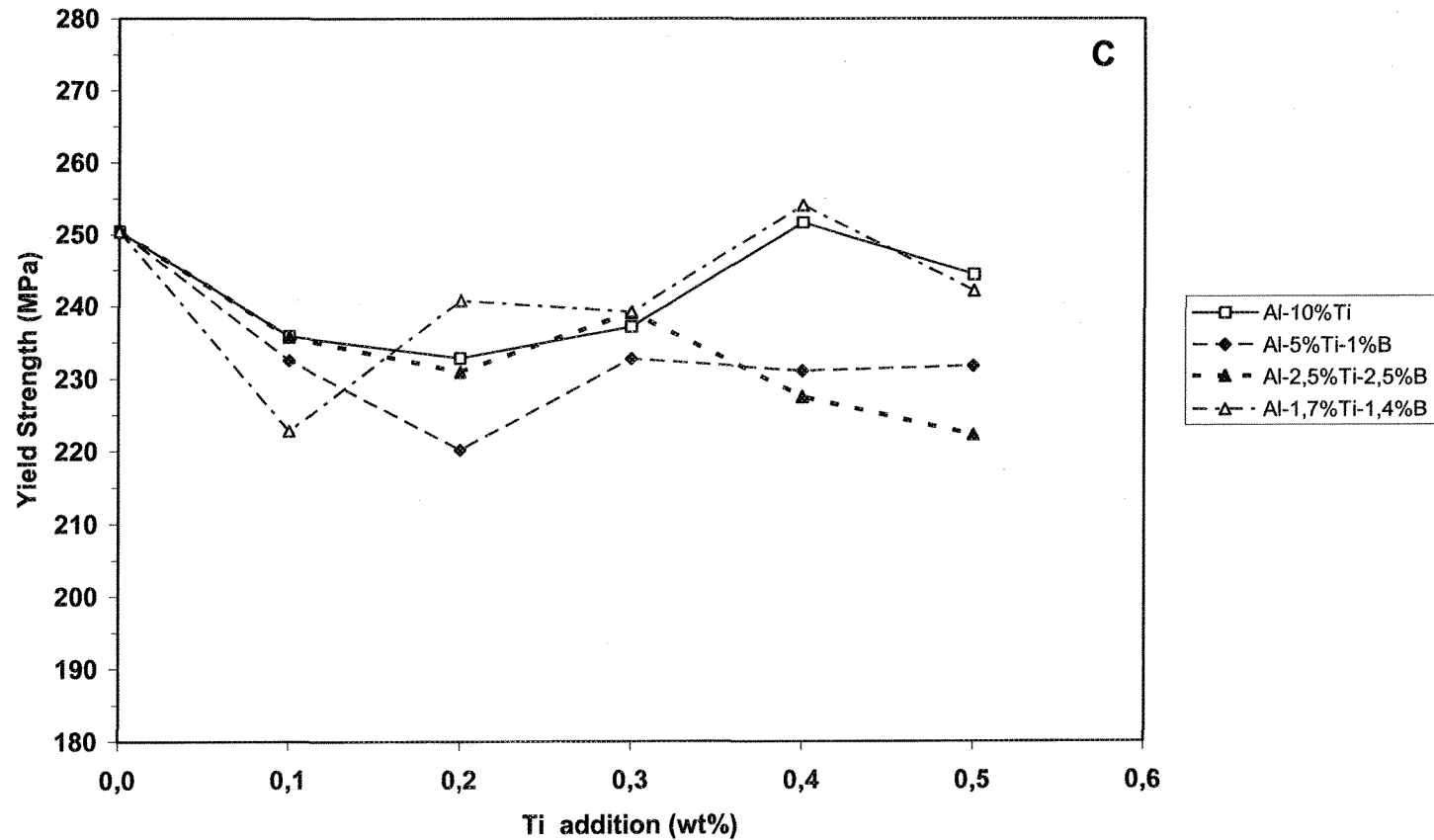


Figure 5.6 (b)



**Figure 5.6** Variation of yield strength as a function of Ti or B content in T6 tempered, Sr-modified, grain-refined A356.2 alloy: (a) modified with 30 ppm Sr addition; (b, c) modified with 200 ppm Sr addition.

### 5.3 IMPACT PROPERTIES

While tensile testing is the most commonly used method for quantifying the mechanical properties of aluminum alloys, the impact strength is of importance in certain applications and can provide a useful estimation of the ductility of an alloy under conditions of rapid loading. In this study, the impact specimens were tested unnotched in order to increase the accuracy of the measurements and to emphasize the effect of the microstructure. One important benefit to be derived from modification is improved ductility when compared to unmodified castings. Silicon particle size and shape, as well as dendritic structure, are parameters affecting the ductility of Al-Si alloys.<sup>13</sup>

#### 5.3.1 AS-CAST CONDITION

Figures 5.7 (a) to (c) show the variation in total absorbed energy of the Sr-modified as-cast A356.2 alloy as a function of Ti and B addition levels. Figure 5.7 (a) relates to the 30 ppm Sr-modified samples, and indicates that the addition of Al-5%Ti-1%B and Al-10%Ti leads to the best results. Also, a discernible drop occurs for Al-2.5%Ti-1%B after the critical threshold of 0.1% B is exceeded. As regards the microstructure of the corresponding alloy, this type of variation may be attributed mainly to the demodification of eutectic silicon particles after the addition of 0.1%B. After the addition of Al-4%B and Al-1.7%Ti-1.4%B master alloys, an unexpected drop in toughness values may be observed; such a drop is not in conformity with the percentage elongation results. The presence of iron and others intermetallics, and the differences in the type of testing (tensile vs impact),

including the difference in loading speeds, may be responsible for the abovementioned inconsistency. Moreover, magnesium silicide and iron intermetallics, particularly  $\beta$ -AlFeSi (which is present in the microstructure in the form of coarse needles) may have an impact on the mechanical properties. The loss of Sr as a result of the Sr-B interaction not only leads to the demodification of eutectic silicon particles, but may also affect the morphology of the  $\beta$ -iron intermetallics. According to Samuel *et al.*,<sup>71</sup> Sr has an adverse effect on the fragmentation and partial dissolution of the  $\beta$ -iron intermetallics in the aluminum matrix.

The samples for which Figure 5.7 (b) provides an illustration were modified using 200 ppm of Sr addition and a low addition level of the master alloy, leading to results which were relatively higher than those observed for the 30 ppm Sr-modified samples. The most impressive results from the point of view of stability and degree of toughness were recorded for Al-2.5%Ti-2.5%B. As regards Al-4%B, toughness values were less than those for Al-5%Ti-1%B, but showed a rising trend with regard to all amounts of addition, in the same manner as elongation does in corresponding alloys. The results displayed by Al-1.7%Ti-1.4%B are also close to those for Al-2.5%Ti-2.5%B, whereas those for Al-10%Ti reveal two different trends with the maximum recorded for 0.04% Ti.

The dispersion of the results obtained does not make it possible to reach any distinct conclusion. Impact strength is more sensitive to small variations in the microstructure than is elongation,<sup>72</sup> while the influence of porosity on the impact test results of Al-Si alloys is not as significant as it is on those for tensile tests.<sup>73</sup> However, the fibrous morphology of the Si-phase as a result of the addition of higher levels of strontium to the alloy appears to have a favourable effect on the impact strength.

Figure 5.7 (c) reveals that toughness values tend to disperse mainly between  $\sim 9$  and 15 joules for all master alloys at high levels of addition, even for the Al-10%Ti master alloy which does not contain boron. Thus, there is no increase in toughness values to be observed for the upper ranges of Ti-addition; whereas for lower ranges it is possible to observe an increase in total absorbed energy. Impact strength is imparted to the alloys by means of the ductile Al matrix which separates low amounts of intermetallic particles from each other at low addition levels, *i.e.* there are fewer sites for the type of stress concentration which facilitates crack initiation.

The fineness of the microstructure which may result from increased solidification rate or grain refiner addition has a beneficial effect on impact strength, *i.e.* the finer the microstructure, the higher the total absorbed energy. From Figures 5.7 (a) to (c), it is clear that by adding combinations of Ti and B, toughness values are greatly improved, but only when the full modification state is operating in the presence of the right levels of addition and type of master alloy. Figures 5.7 (a) and (c) also indicate that the lack of sufficient Sr may lead to a decline in toughness, regardless of whether this results from a low level of addition or from the lack of an available amount of this element. This fact is evident to some extent with regard to Al-1.7%Ti-1.4%B and Al-2.5%Ti-2.5%B additions. In view of the fact that no clear trends in toughness variations at high levels of addition is to be observed, it becomes evident that further trials need to be carried out with regard to this particular aspect.



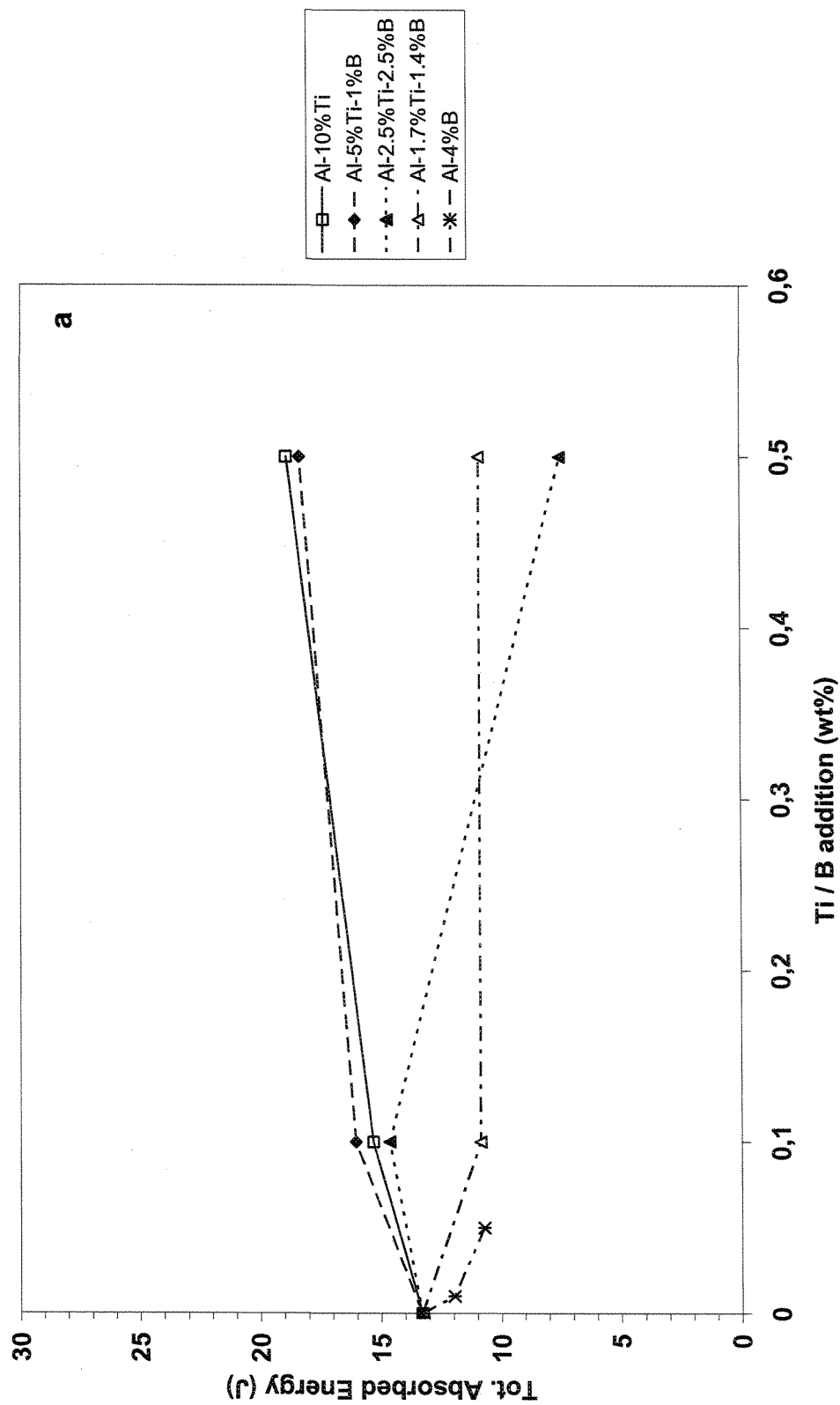


Figure 5.7 (a)

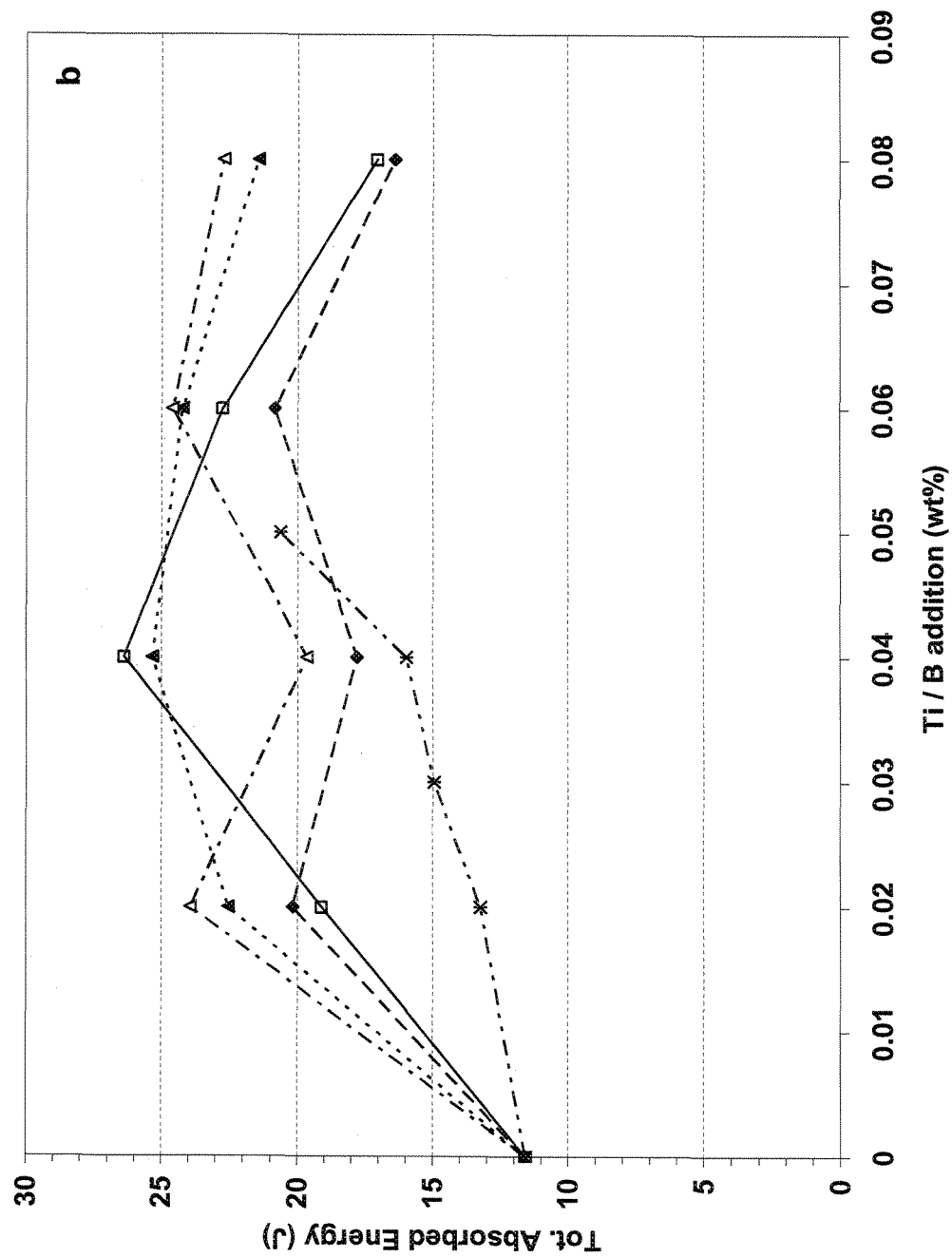
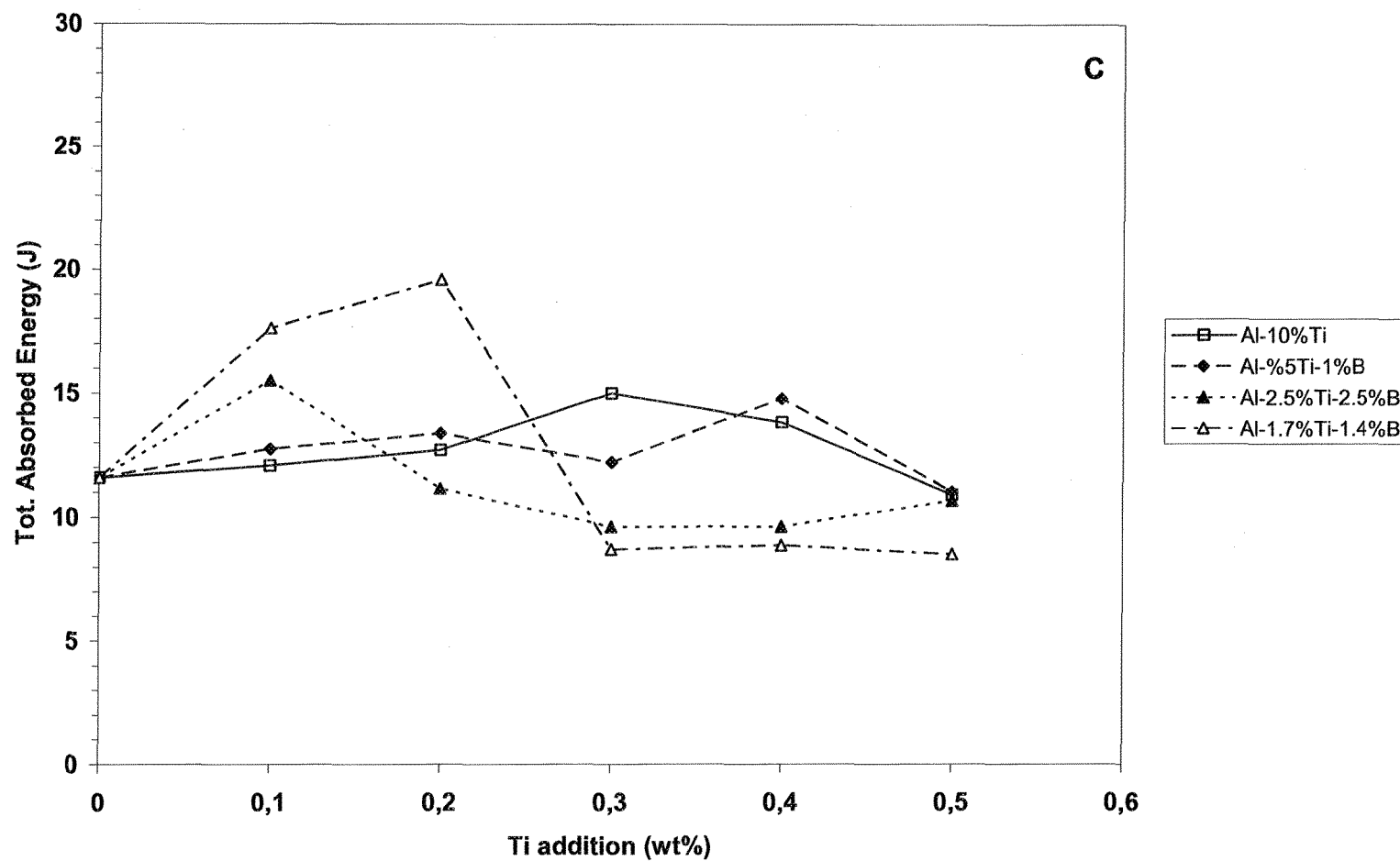


Figure 5.7 (b)



**Figure 5.7** Variation of total absorbed energy as a function of Ti or B content in as cast, Sr-modified, A356.2 alloy, (a) modified with 30 ppm Sr addition (b, c) modified with 200 ppm Sr addition.

### 5.3.2 T6-TEMPERED CONDITION

Figures 5.8(a) to (c) show the variation in total absorbed energy of the Sr-modified A356.2 alloy samples as a function of Ti and B addition levels, under T6-tempered conditions. Figure 5.8 (a), which relates to the 30 ppm Sr-modified samples, shows that T6 temper results in a considerable increase in the total absorbed energy for all master alloys. Microstructural changes such as silicon fragmentation and spheroidization may be caused by maintaining the alloy at high temperatures; these, in turn, bring about improvements in the impact properties. The downward trends in the case of Al-2.5%Ti-2.5%B and Al-4%B master alloys still remain after increases in addition levels. The degradation in the total absorbed energy values of Al-2.5%Ti-2.5%B may be related to the presence of coarse acicular silicon particles which frequently result from the interaction of Sr and B, as well as to insufficient time allowed for the solutionizing stage of the T6 temper. The toughness values of the alloys refined using Al-1.7%Ti-1.4%B and Al-5%Ti-1%B maintained their stationary state between 0.1% and 0.5 % Ti additions, whereas the difference in the toughness values of 0.1 % and 0.5 % Ti with respect to Al-10 %Ti will be observed to have increased compared to the as-cast condition.

Figure 5.8 (b) shows toughness variations in the 200 ppm Sr-modified A356.2 alloy samples for the various types of master alloy, for low levels of Ti addition. All of the impact properties of heat-treated samples are significantly higher than the corresponding values of as-cast samples. A clear rising trend may be observed for Al-4%B; whereas toughness values remain stable in Al-1.7%Ti-1.4%B after the addition of 0.02%Ti, while

for Al-2.5%Ti-2.5%B this variation is not as stable as it is for Al-1.7%Ti-1.4%B. The highest values for total absorbed energy are obtained after using Al-5%Ti-1%B and Al-10%Ti master alloys following upon the addition of 0.04 % Ti. With regard to all grain refiners, data scattering, makes it nearly impossible to obtain indisputable conclusions for each of the master alloys; it may also be stated that impact ductility improves with the addition of B or Ti.

Figure 5.8 (c) shows a noticeable decline in the toughness values of samples refined using the master alloys Al-2.5%Ti-2.5%B and Al-1.7%Ti-1.4%B. An arc-shaped variation may be observed for Al-5%Ti-1%B and shows the highest total absorbed energy value at 0.2% Ti. As may be seen in the figure, the improvements associated with the T6 temper for Al-5%Ti-1%B are considerably greater than those for the remaining master alloys.

The values provided by the figures in this chapter confirm the sensitivity of impact toughness to the microstructural variations associated with Sr addition. Both Al-1.7%Ti-1.4%B and Al-2.5%Ti-2.5%B show a decline in toughness values with the accompanying increase in the levels of addition, whereas ductility is more uniform and exhibits higher values as a result of using the master alloys Al-10%Ti and Al-5%Ti-1%B under certain conditions. There is a significant deterioration in impact properties to be observed resulting from the Sr-B interaction, and/or from a supplementary addition of master alloys in some cases. The improvements in toughness may be attributed primarily to the change in silicon particle morphology, as well as to the dissolution and fragmentation of a number of the intermetallic compounds formed during the T6 temper.

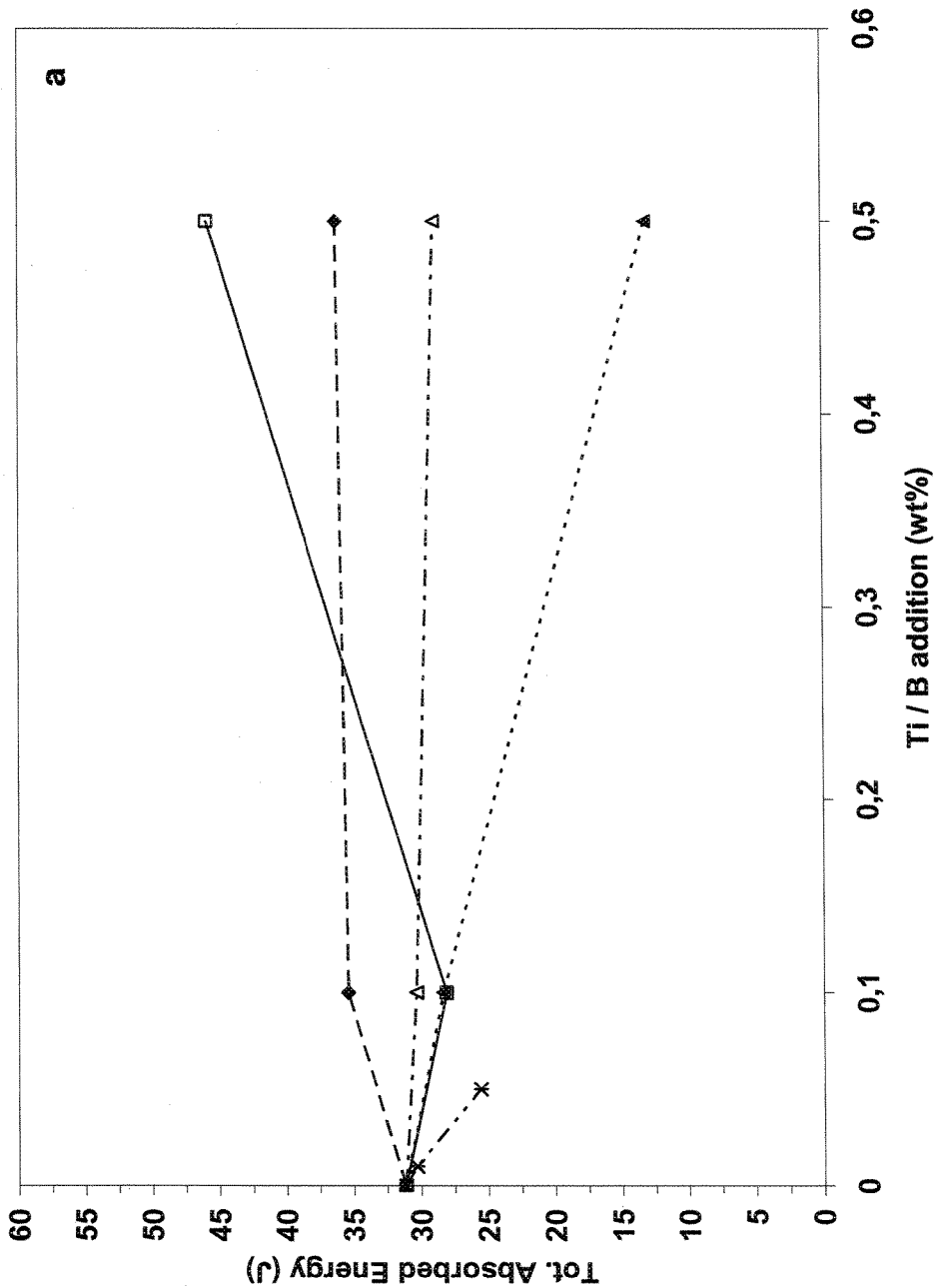


Figure 5.8 (a)

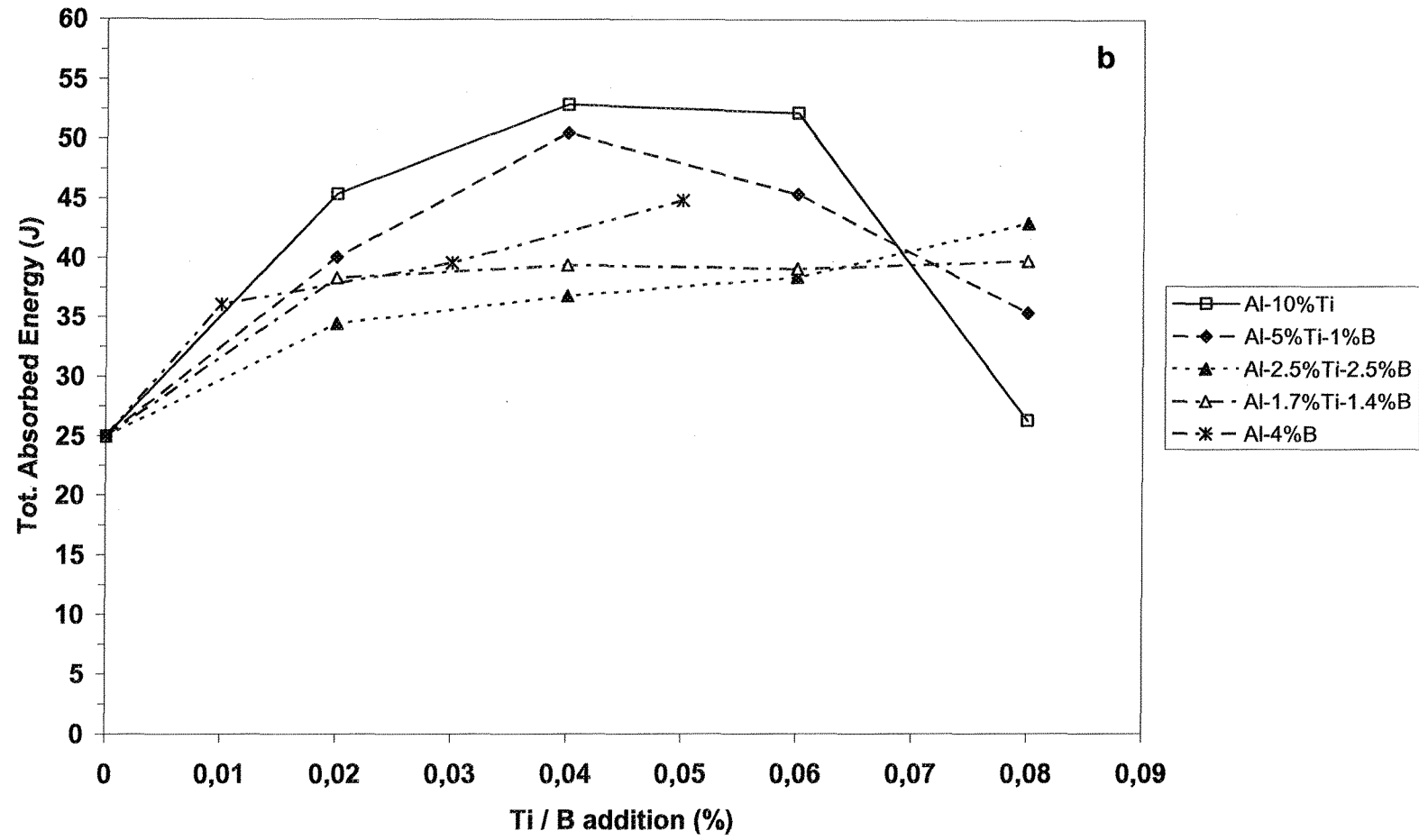
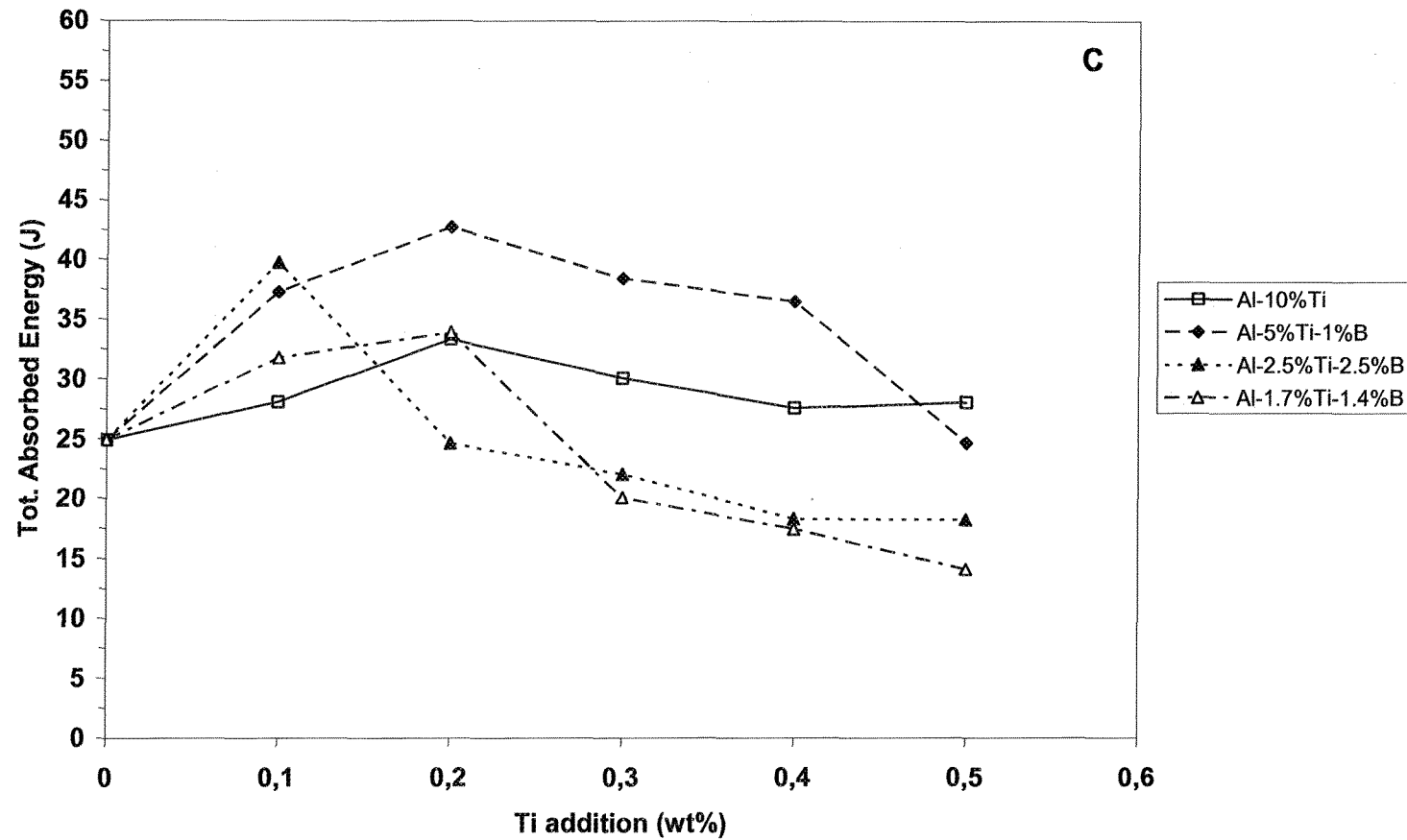


Figure 5.8 (b)



**Figure 5.8** Variation of total absorbed energy as a function of Ti or B content in T6-tempered, Sr-modified A356.2 alloy, (a) modified with 30 ppm Sr addition (b, c) modified with 200 ppm Sr addition.



It should be noted that the  $\beta$ -AlFeSi phase needles present in the microstructures of the A356.2 alloy may be responsible for a detrimental effect to be observed with regard to the mechanical properties. Strontium has been reported to decrease the nucleation sites for  $\beta$ -AlFeSi phase needles and to attenuate their deleterious effects on mechanical properties.<sup>74</sup> Thus, any given factor, such as low Sr addition or any interaction between Sr and B, which may cause a reduction in the amount of Sr available, will have a negative effect on ductility values. Furthermore, coarse silicon particles present in the samples treated with Al-2.5%Ti-2.5%B and Al-1.7%Ti-1.7%B may retard the spheroidization process due to the same Sr-B interaction. Such a delay would make it possible for coarse flakes of silicon particles to remain in the microstructure, even after T6 temper, ultimately providing further possibilities for crack propagation throughout the surrounding material.

#### **5.4 OPTIMUM GRAIN REFINING CONDITIONS**

Based on the optimum values of tensile properties, *i.e.* yield strength, ultimate tensile strength and elongation, and total absorbed energy for the 30 ppm and 200 ppm Sr-modified A356.2 alloy samples in as-cast and T6 conditions, corresponding grain refiner additions were specified as the optimum addition required for the various grain refiner used in this study. Tables 5.1 and 5.2 summarize these data for the as-cast and T6-treated alloys, respectively.

**Table 5.1** Grain refiner addition for achieving optimum properties for Sr-modified A356.2 alloy in the as-cast condition

Grain refiner type		Al-10%Ti	Al-5%Ti-1%B	Al-2.5%Ti-2.5%B	Al-1.7%Ti-1.4%B	Al-4%B
Partial Modification (30 ppm Sr)	Optimum addition (wt%)	0.1%Ti	0.1%Ti	0.1%Ti	0.1%Ti	0.05%B
	El.(%)	6.86	7.48	5.73	6.11	7.55
	UTS (MPa)	186.65	188.38	174.31	174.33	180.99
	YS(MPa)	99.35	103.60	95.77	92.07	98.55
	Toughness(J)	15.31	16.05	14.64	10.85	10.71
Full Modification (200 ppm Sr)	Optimum addition (wt%)	0.2%Ti	0.2%Ti	0.04%Ti	0.02%Ti	0.05%B
	El.(%)	8.64	9.61	8.78	9.18	9.14
	UTS (MPa)	194.35	191.03	189.46	191.91	180.83
	YS(MPa)	102.38	99.20	97.01	97.72	93.21
	Toughness(J)	12.70	13.38	25.32	23.95	20.61

**Table 5.2** Grain refiner addition for achieving optimum properties for Sr-modified A356.2 alloy in the T6-tempered condition

Grain refiner type		Al-10%Ti	Al-5%Ti-1%B	Al-2.5%Ti-2.5%B	Al-1.7%Ti-1.4%B	Al-4%B
Partial Modification (30 ppm Sr)	Optimum addition (wt%)	0.1%Ti	0.1%Ti	0.1%Ti	0.1%	0.05%B
	El. (%)	6.68	7.58	7.19	7.79	10.22
	UTS (MPa)	323.36	319.00	320.26	315.13	329.96
	YS (MPa)	248.04	243.04	252.05	231.51	250.20
	Toughness (J)	28.12	35.38	28.34	30.35	25.58
Full Modification (200 ppm Sr)	Optimum addition (wt%)	0.06%Ti	0.04%Ti	0.04%Ti	0.02%Ti	0.01%B
	El. (%)	8.97	9.67	9.74	9.66	8.89
	UTS (MPa)	314.12	322.19	319.63	323.67	313.79
	YS (MPa)	251.98	236.42	233.42	247.84	234.84
	Toughness (J)	52.16	50.48	36.79	38.30	36.06

**CHAPTER 6**  
**CONCLUSIONS**

## CHAPTER 6

### CONCLUSIONS

This study was carried out in order to determine the effects of interaction between modifiers and grain refiners in A356.2 cast aluminum alloy. The research thus involved examining the relationship between Sr and B and/or Ti in A356.2 alloy. Based on the results obtained from the research, the following conclusions may be drawn.

1. No sign of any Sr-Ti interaction was found over the range of Ti levels studied. This was confirmed by thermal analysis, mechanical testing, as well as electron probe microanalysis. Therefore, Ti addition does not have any adverse effect on the performance of Sr as a modifier in A356.2 alloy.
2. There is no significant Sr-B interaction at low addition levels of the Al-Ti-B type grain refiners up to 0.1 % B. Increase in the B-content beyond this level leads to changes in the shape and size of the eutectic silicon particles, as was observed in the microstructures of A356.2 alloy grain refined using Al-2.5%Ti-2.5%B and Al-1.7%Ti-1.4%B master alloys at B levels exceeding 0.1 %. Thus, 0.1% B addition can be considered as the starting point for the eutectic Si particles to revert to coarse flakes in such cases.

3. A quantity of Sr-rich particles appear in the case of the alloy which has been refined with the addition of 0.5%B in the form of Al-4%B, after it has undergone modification with 200 ppm of Sr; this would suggest that such particles contain B and Sr predominantly with a composition approaching  $\text{SrB}_6$ .
4. No significant variations in yield strength (YS) of the as-cast alloy are observed, regardless of the amount of Sr or grain refiner additions. The T6-tempered alloys exhibit much higher YS values compared to the as-cast alloys. Under T6 temper condition, yield strength values of 30 ppm Sr-modified alloys are observed to decrease would for the addition of Al-2.5%Ti-2.5%B and Al-1.7%Ti-1.4%B grain refiners, while a rising trend is discernible for all grain refiners additions in the 200 ppm Sr-modified alloy, particularly for additions of Al-10%Ti and Al-1.7%Ti-1.4%B.
5. The T6 temper does not lead to any improvement in the elongation of the grain refined alloys compared to the as-cast condition, except in the case when Al-4% B is used for grain refining.
6. In the T6-tempered alloys, higher tensile strength (UTS) values may be obtained through the addition of lower amounts of the master alloys, in the range of 0.02% to 0.04% Ti. Thus, it is important to select the appropriate grain refining agent in conjunction with the appropriate amount of addition to maximize the alloy strength with respect to the heat treatment used.

7. Combinations of Ti and B greatly improve the alloy toughness but only if the alloy is in a fully modified state, and the right type of master alloy and addition levels are used. The impact properties of all T6-tempered alloys are significantly higher than those obtained in the as-cast condition, regardless of the type of master alloy employed.
8. The interaction between Sr and B may also lead to a decrease in the amount of boron available for  $\text{TiB}_2$  formation and, hence, result in poor grain refining. This was evidenced by a number of grain size measurements which showed some coarsening for master alloy additions corresponding to the addition range levels of 0.02 – 0.1%B.

## **RECOMMENDATIONS FOR FUTURE RESEARCH**

With a view to advancing the state of knowledge in the field of modification of eutectic silicon in the A356.2 alloy and acquiring information in greater detail on the subject, it is to be recommended that further experiments be carried out on the following aspects of this specific research:

1. Using fractographic methods to explore and interpret the causes of fracture as they relate to the effects of the strontium-boron interaction on the tensile behaviour of the A356.2 alloy.
2. Using extended thermal analysis trials in order to carry out an in-depth exploration of the modifying effects of boron on silicon.



## REFERENCES

- <sup>1</sup> M. Warmuzek, "Aluminum-Silicon Casting Alloys, Atlas of Microfractographs", ASM International, Materials Park, OH, 2004.
- <sup>2</sup> S. Shivkumar, L. Wang, D. Apelian, "Molten metal processing of advanced cast aluminum alloys," *Journal of Metals*, Jan, 1991, pp. 26-32.
- <sup>3</sup> B. Closset, J.E Gruzleski, "Structure and properties of hypoeutectic Al-Si-Mg alloys modified with pure strontium," *Metallurgical Transactions A*, Vol. 13A, 1982, pp. 945-951.
- <sup>4</sup> S.G. Shabestari, H. Moemeni, "Effect of copper and solidification conditions on the microstructure and mechanical properties of Al-Si-Mg alloys," *Journal of Materials Processing Technology*, Vol. 147, 2004, pp. 153-154.
- <sup>5</sup> D.G. McCartney, "Grain refining of aluminum and its alloys using inoculants," *International Materials Reviews*, Vol. 34(5), 1989, pp. 247-260.
- <sup>6</sup> F. Zupanic, S. Spaic, A. Krizman, "Contribution to the ternary system Al-Ti-B Part 2 - Study of alloys in Al-AlB<sub>2</sub>-TiB<sub>2</sub> triangle," *Materials Science and Technology*, Vol. 14, 1998, p. 1203.
- <sup>7</sup> H. Li, T. Sritharan, Y.M. Lam, "Effects of processing parameters on the performance of Al grain refinement master alloys Al-Ti and Al-B in small ingots," *Journal of Materials Processing Technology*, Vol. 66, 1997, pp. 153-257.
- <sup>8</sup> C. Lee, S. Chen, "Quantities of grains of aluminum and those of TiB<sub>2</sub> and Al<sub>3</sub>Ti particles added in the grain-refining processes," *Materials Science and Engineering A*, Vol. A325, 2002, pp. 242-248.
- <sup>9</sup> K. Kashyap, T. Chandrashekar, "Effects and mechanisms of grain refinement in aluminium alloys," *Bulletin of Materials Science*, Vol. 24(4), Aug 2001, pp. 345-353.
- <sup>10</sup> G. Jones, P.J. Pearson, "Factors affecting the grain-refinement of aluminum using titanium and boron additives," *Metallurgical Transactions B*, Vol. 7B, 1976, pp. 223-234.
- <sup>11</sup> C.H. Cáceres, C. J. Davidson, J. R. Griffiths, "The deformation and fracture behaviour of an Al-Si-Mg casting alloy," *Materials Science and Engineering A*, Vol. A197, 1995, pp. 171-179.

- 
- <sup>12</sup> L. Grand, "The modification of Al-Si alloys," *La Revue de l'aluminium*, Vol. 29, 1952, p. 5.
- <sup>13</sup> J. G. Conley, J. Huang, J. Asada, K. Akiba, "Modeling the effects of cooling rate, hydrogen content, grain refiner and modifier on microporosity formation in Al A356 alloys," *Materials Science and Engineering A*, Vol. A285, 2000, p. 49.
- <sup>14</sup> B. Talaat, F. Hasse, "Solidification Mechanism of Unmodified and Strontium Modified Al-Si Alloys," *Materials Transactions, The Japan Institute of Metals (JIM)*, Vol. 41(4), 2000, pp. 507-515.
- <sup>15</sup> A. Atasoy, "The effect of twinning on the growth of silicon crystals in Al-Si eutectic alloys," *Zeitschrift für Metallkunde*, Vol. 78, 1987, pp. 177-183.
- <sup>16</sup> C.W. Meyers, A. Saigal, J.T. Berry, "Fracture Related Properties of A357-T6 Cast Alloy and Their Interrelation with Microstructure," *AFS Transactions*, Vol. 91, 1983, pp. 281-288.
- <sup>17</sup> H. Mahmoud, T. Kobayashi, "Mechanical Properties of Modified and Nonmodified Eutectic Al-Si alloys," *Journal of Japan Institute of Light Metals*, Vol. 44(1), 1994, pp. 28-34.
- <sup>18</sup> Y.J. Li, S. Brusethaug, A. Olsen, "Influence of Cu on the mechanical properties and precipitation behavior of AlSi7Mg0.5 alloy during aging treatment," *Scripta Materialia*, Vol. 54(1), 2006, pp. 99-103.
- <sup>19</sup> X. Chen, H. Geng, Y. Li, "Study on the eutectic modification level of Al-7%Si Alloy by computer aided recognition of thermal analysis cooling curves," *Materials Science and Engineering A*, Vol. A419, 2006, pp. 283-289.
- <sup>20</sup> A. Apelian, J.A. Cheng, "Al-Si Processing Variables on Grain Refinement and Eutectic Modification," *AFS Transactions*, Vol. 94, 1986, pp. 797-808.
- <sup>21</sup> L. Clapham, R.W. Smith, "The Mechanism of the Partial Modification of Al-Si Eutectic Alloys," *Journal of Crystal Growth*, Vol. 79, 1986, pp. 866-873.
- <sup>22</sup> H. Liao, Y. Sun, "Correlation between mechanical properties and amount of dendritic  $\alpha$ -Al phase in as-cast near-eutectic Al-11.6% Si alloys modified with strontium," *Journal of Materials Science*, Vol. 37, 2002, pp. 3489-3495.
- <sup>23</sup> H. Liao, G. Sun, "Mutual poisoning effect between Sr and B in Al-Si casting alloys," *Scripta Materialia*, Vol. 48, 2003, pp. 1035-1039.

- 
- <sup>24</sup> D. Apelian, G.K. Sigworth, K.R. Whaler, "Assessment of grain refinement analysis," *AFS Transactions*, Vol. 92, 1984, pp. 297-307.
- <sup>25</sup> J. Charbonnier, J. Morice, R. Portalier; "L'analyse thermique appliquée en fonderie au contrôle des alliages d'aluminium avant coulée," *Hommes et Fonderie*, Nov. 1975, pp. 29-36.
- <sup>26</sup> N. Tenekedjiev, J.E. Gruzleski, "Thermal Analysis of Strontium Treated Hypoeutectic and Eutectic Aluminum-Silicon Casting Alloys," *AFS Transactions*, Vol. 99, 1991, pp. 1-6.
- <sup>27</sup> N. Tenekedjiev, H. Mulazimoglu, B. Closset, J. Gruzleski, *Microstructures and Thermal Analysis of Strontium-Treated Aluminum-Silicon Alloys*, American Foundrymen's Society, Inc., Des Plaines, Illinois, USA 1995.
- <sup>28</sup> V. Rauta, "The Experimental Study over the Modification of Aluminum-Silicon Cast Alloys," in *Conference on High Quality Aluminum Castings*, May 13-14, 1993, Otaniemi, Finland, 1993.
- <sup>29</sup> A. J. Cornish, "The influence of Boron on the Mechanism of Grain Refinement in Dilute Aluminium-Titanium Alloys," *Metals Science*, Vol. 9, 1975, pp. 477-484.
- <sup>30</sup> A.T. Joenoes, J.E. Gruzleski, "Magnesium Effects on the Microstructure of unmodified and modified Al-Si alloys," *Cast Metals*, Vol. 4(2), 1991, pp. 62-71.
- <sup>31</sup> P.S. Mohanty, R. Guthrie, J.E. Gruzleski, "Studies on the fading behavior of Al-Ti-B Master alloys and Grain Refinement Mechanisms Using LiMCA," *Light Metals 1995*, The Mining, Minerals and Materials Society, Warrendale, PA, 1995, pp. 859-867.
- <sup>32</sup> M. Johnsson, "A Critical Survey of the Grain Refining Mechanisms of Aluminum," *Chemical Communications*, No. 5, 1993.
- <sup>33</sup> A.L. Greer, A.M. Bunn, A. Tronche, P.V. Evans, D.J. Bristow, "Modelling of inoculation of metallic melts: Application to grain refinement of aluminum by Al-Ti-B," *Acta Materiala*, Vol. 48, 2000, pp. 2823-2835.
- <sup>34</sup> Y.C. Lee, A.K. Dahle, D.H. StJohn, J.E.C. Hutt, "The effect of grain refinement and silicon content on grain formation in hypoeutectic Al-Si alloys," *Materials Science and Engineering A*, Vol. A 259, 1999, pp. 43-52.
- <sup>35</sup> M. Vader, J. Noordegraaf, P.C. van Wiggeren, "Aluminum Master Alloys with Reduced Intermetallic Phase Sizes Open up Windows for New Applications," *Kawecki-Billiton Metaal Industrie* 8.V.

- 
- <sup>36</sup> G.K. Sigworth, M.M. Guzowski, "Grain refining of hypoeutectic Al-Si casting alloys," *AFS Transactions*, Vol. 92, 1985, pp. 907-912.
- <sup>37</sup> P.A. Tondel, "Grain refinement of hypoeutectic Al-Si foundry alloys", Ph.D. Thesis, University of Trondheim, 1994, pp. 39-44.
- <sup>38</sup> P.S. Mohanty, J.E. Gruzleski, "Grain refinement mechanisms of hypoeutectic Al-Si alloys," *Acta Materialia*, Vol. 44(9), 1996, pp. 3749-3760.
- <sup>39</sup> A.K. Prasada Rao, K. Das, B.S. Murty, M. Chakraborty, "Microstructural and wear behavior of hypoeutectic Al-Si alloy (LM25) grain refined and modified with Al-Ti-C-Sr master alloy," *Wear*, Vol. 261, Issue 2, July 2006, pp. 133-139.
- <sup>40</sup> P. L. Schaffer, L. Arnberg, A. K. Dahle, "Segregation of particles and its influence on the morphology of the eutectic silicon phase in Al-7 wt. % Si alloys," *Scripta Materialia*, Vol. 54, 2006, pp. 677-682.
- <sup>41</sup> T. Gudmundsson, T.I. Sigfusson, D.G. McCartney, E. Wuilloud, P. Fisher, "Trace element distribution in Al-Ti-B master alloys," *Light Metals 1995*, The Mining, Minerals and Materials Society, Warrendale, PA, 1995, pp 851-854.
- <sup>42</sup> L. Ying Pio, S. Sulaiman, A. Hamouda, M. Ahmad, "Grain refinement of LM6 Al-Si alloy sand castings to enhance mechanical properties," *Journal of Materials Processing Technology*, Vol. 162-163, 2005, pp. 435-441.
- <sup>43</sup> A. Taylor, H. Wang, D. H. St-John, F. Bainbridge, "Anomalous Grain Coarsening Behavior in Grain-Refined Aluminum Alloys Cast Using Low Superheat," *Light Metals 2001*, The Mining, Minerals and Materials Society, Warrendale, PA, 2001, pp. 935-941.
- <sup>44</sup> J. A. Spittle, J. M. Keeble, "The grain refinement of Al-7Si alloys with boron containing refiners," *Light Metals 1999*, The Mining, Minerals and Materials Society, Warrendale, PA, 1999, pp. 673-677.
- <sup>45</sup> E. Bondhus, T. Sagstad, N. Dahle, "Grain refinement of hypoeutectic Al-Si foundry alloys with TiBloy," *Light Metals*, 1999, pp. 693-697.
- <sup>46</sup> N. Roy, A.M. Samuel, F.H. Samuel, "Porosity Formation in Al-9wt pct Si- 3wt pct Cu Alloy Systems: Metallographic Observations," *Metallurgical and Materials Transactions A*, Vol. 27A, Feb. 1996, pp. 415-429.

- 
- <sup>47</sup> M. Easton, D. StJohn, "Grain refinement of aluminum alloys: Part II. Confirmation of, and a mechanism for the solute paradigm," *Metallurgical and Materials Transactions A*, Vol. 30A, 1999, pp. 1613-1623.
- <sup>48</sup> M.M. Guzowski, G.K. Sigworth, D.A. Sentner, "The role of boron in the grain refinement of aluminum with titanium," *Metallurgical and Materials Transactions A*, Vol. 18A, 1987, pp. 603-619.
- <sup>49</sup> J. A. Marcantonio, L. F. Mondolfo, "Grain refinement in aluminum alloyed with titanium and boron," *Metallurgical Transactions*, 2 1971, pp. 465-471.
- <sup>50</sup> L. Lu, A.K. Dahle, "Effects of combined additions of Sr and Al-Ti-B grain refiners in hypoeutectic Al-Si foundry alloys," *Materials Science and Engineering A*, Vol. A435, 2006, pp. 288-296.
- <sup>51</sup> W. Schneider, P. Cooper, T. Quested, A. Greer, "A comparison of the family of Al-Ti-B refiners and their ability to achieve a fully equiaxed grain structure in DC casting," *Light Metals 2003*, The Mining, Minerals and Materials Society, Warrendale, PA, 2003, pp. 953-959.
- <sup>52</sup> ICDD, JCPDS—International centre for diffraction data, PCPDFWIN Version 2.02, 1999.
- <sup>53</sup> A. A. Abdel-Hamid, "Effect of other elements on the grain refinement of Al by Ti and B," *Zeitschrift für Metallkunde*, Vol. 80, 1989, pp. 566-569.
- <sup>54</sup> J.Z. Yi, P.D. Lee, T.C. Lindley, T. Fukui, "Statistical modeling of microstructure and defect population effects on the fatigue performance of cast A356-T6 automotive components," *Materials Science and Engineering A*, Vol. A432, 2006, pp. 59-68.
- <sup>55</sup> Q.G. Wang, C.H. Cáceres, "The Fracture Mode in Al-Si-Mg Casting Alloys," *Materials Science and Engineering A*, Vol. A241(1), 1998, pp. 72-82.
- <sup>56</sup> S. Shivkumar, L. Wang, R. Lavigne, "Quantitative Evaluation of Pore Characteristics in Cast Al Alloys," *Light Metals 1993*, The Mining, Minerals and Materials Society, Warrendale, PA, 1993, pp. 829-838.
- <sup>57</sup> N.D. Alexopoulos, Sp.G. Pantelakis, "Quality evaluation of A357 cast aluminum alloy specimens subjected to different artificial aging treatment," *Materials and Design*, Vol. 25, 2004, pp. 419-430.

- 
- <sup>58</sup> M. Johnsson, L. Bäckerud, G.K. Sigworth, "Study of the Mechanism of Grain-refinement of Aluminum after Additions of Ti-containing and B-containing Master Alloys," *Metallurgical Transactions A*, Vol. 24A, 1993, pp. 481-491.
- <sup>59</sup> Z. Poniewierski, "Effet du type de modification sur la microstructure de l'eutectic Al-Si," *Revue Internationale des Hautes Températures et des Réfractaires*, Vol. 14, 1977, pp. 273-260.
- <sup>60</sup> G. Guiglionda, W. J. Poole, "The role of damage on the deformation and fracture of Al-Si eutectic alloys," *Materials Science and Engineering A*, Vol. A336, Oct. 2002, pp. 159-169.
- <sup>61</sup> D.L. McLellan, "Modeling Microstructural Characteristics of Al-Si-Mg Castings. to Develop Product Assurance," *AFS Transactions*, Vol. 90, 1982, pp. 173-191.
- <sup>62</sup> J.P. Anson, J.E. Gruzleski, M. Stucky, "Effect of Strontium concentration on microporosity in A356 aluminum alloy," *AFS Transactions* Vol. 109, 2001, p. 243-258.
- <sup>63</sup> S.A. Kori, B.S. Murty, M. Chakraborty, "Development of an efficient grain refiner for Al-7%Si alloy and its modification with strontium," *Materials Science and Engineering A*, Vol. A283, 2000, pp. 94-104.
- <sup>64</sup> J.G. Li, B.Q. Zhang, L. Wang, W.Y. Yang, H.T. Ma, "Combined effect and its mechanism of Al-3wt.%Ti-4wt.%B and Al-10wt.%Sr master alloy on microstructures of Al-Si-Cu alloy," *Materials Science and Engineering A*, Vol. A328, 2002, pp. 169-176.
- <sup>65</sup> K. Nogita, A. K. Dahle, "Effects of boron on eutectic modification of hypoeutectic Al-Si alloys," *Scripta Materialia*, Vol. 48, 2003, pp. 307-313.
- <sup>66</sup> K. Nogita, S.D. McDonald, A. Dahle, "Effects of Boron-Strontium Interactions on Eutectic Modification in Al-10 %Si Alloys," *Materials Transactions*, Vol. 44(4), 2003, pp. 692-695.
- <sup>67</sup> M. D. Dighe, A. M. Gokhale, "Relationship between microstructural extremum and fracture path in a cast Al-Si-Mg alloy," *Scripta Materialia*, Vol. 37(9), 1997, p. 1435-1440.
- <sup>68</sup> J. Campbell, *Castings*, Butterworth-Heinemann, Oxford, UK, 1991.
- <sup>69</sup> D. Apelian, S. Shivkumar, G. Sigworth, "Fundamental Aspects of Heat Treatment of Cast Al-Si-Mg Alloys," *AFS Transactions*, Vol. 97, 1989, pp. 727-742.

- 
- <sup>70</sup> J.F. Hernandez-Paz, F. Paray, J.B. Gruzleski, D. Emadi, "Natural Aging and Heat Treatment of A356 Aluminum Alloy," *AFS Transactions*, Vol. 112, 2004, pp. 155-164.
- <sup>71</sup> F.H. Samuel, P. Ouellet, A.M. Samuel, H.W. Doty, "Effect of Mg and Sr Additions on the Formation of Intermetallics in Al-6 Wt Pct Si-3.5 Wt Pct Cu-(0.45) to (0.8) Wt Pct Fe 319-Type Alloys," *Metallurgical and Materials Transactions A*, Vol. 29A 1998, pp. 2871-2884.
- <sup>72</sup> M. Drouzy, S. Jacob, M. Richard, "Interpretation of Tensile Results by Means of Quality Index and Probable Yield Strength," *AFS International. Cast Metals Journal*, Vol. 5, 1980, pp. 43-50.
- <sup>73</sup> M. Tsukuda, S. Koike, M. Hurada, "The heat treatment of Al-7%Si-0.3%Mg alloy," *Journal of Japan. Institute of Light Metals*, Vol. 28(1), Jan. 1978, pp. 8-14.
- <sup>74</sup> B. Suárez-Peña, J. Asensio-Lozano, "Influence of Sr modification and Ti grain refinement on the morphology of Fe-rich precipitates in eutectic Al-Si die cast alloys," *Scripta Materialia*, Vol. 54, 2006, pp. 1543-1548.